AWARD NUMBER: W81XWH-13-1-0242

TITLE: Regulation of Mitochondria Function by TRAF3 in B Lymphocytes and B cell Malignancies

PRINCIPAL INVESTIGATOR: Ping Xie

CONTRACTING ORGANIZATION: Rutgers, the State University of New Jersey
New Brunswick, NJ 08901-8559

REPORT DATE: August 2014

TYPE OF REPORT: Annual progress report

PREPARED FOR: U.S. Army Medical Research and Materiel Command
Fort Detrick, Maryland 21702-5012

REPORT DOCUMENTATION PAGE

Form Approved
OMB No. 0704-0188

1. REPORT DATE	2. REPORT TYPE	3. DATES COVERED
August 2014	Annual	1 Aug 2013 – 31 Jul 2014

4. TITLE AND SUBTITLE

Regulation of Mitochondria Function by TRAF3 in B Lymphocytes and B-Cell Malignancies

5a. CONTRACT NUMBER

5b. GRANT NUMBER
W81XWH-13-1-0242

5c. PROGRAM ELEMENT NUMBER

6. AUTHOR(S)

Ping Xie

E-Mail: xiep@rci.rutgers.edu

5d. PROJECT NUMBER

5e. TASK NUMBER

5f. WORK UNIT NUMBER

7. PERFORMING ORGANIZATION NAME(S) AND ADDRESS(ES)

Rutgers, the State University
New Jersey 08854-8000

8. PERFORMING ORGANIZATION REPORT NUMBER

9. SPONSORING / MONITORING AGENCY NAME(S) AND ADDRESS(ES)

U.S. Army Medical Research and Materiel Command

Fort Detrick, Maryland 21702-5012

10. SPONSOR/MONITOR'S ACRONYM(S)

11. SPONSOR/MONITOR'S REPORT NUMBER(S)

12. DISTRIBUTION / AVAILABILITY STATEMENT

Approved for Public Release; Distribution Unlimited

13. SUPPLEMENTARY NOTES

14. ABSTRACT

This project aims to investigate how a new tumor suppressor gene, TRAF3, regulates mitochondria function in B lymphocytes and B cell malignancies. TRAF3 deletions and mutations occur in a variety of B cell malignancies, including B cell chronic lymphocytic leukemia (B-CLL), non-Hodgkin lymphoma (NHL, such as splenic marginal zone lymphoma and mantle cell lymphoma), multiple myeloma (MM), and Waldenström's macroglobulinemia. We found that specific deletion of TRAF3 from B lymphocytes results in remarkably prolonged survival of mature B cells, which eventually leads to development of splenic marginal zone lymphoma or B1 lymphoma in mice. In this context, understanding how TRAF3 promotes B cell apoptosis is critical for rational design of therapeutic intervention of human B cell neoplasms. In pursuing such underlying mechanisms, we have obtained an unexpected but highly interesting finding.

15. SUBJECT TERMS
TRAF3, mitochondria, apoptosis, oncogenic B cell survival, B cell malignancies

16. SECURITY CLASSIFICATION OF:			17. LIMITATION OF ABSTRACT	18. NUMBER OF PAGES	19a. NAME OF RESPONSIBLE PERSON
a. REPORT	b. ABSTRACT	c. THIS PAGE			USAMRMC
Unclassified	Unclassified	Unclassified	Unclassified	100	19b. TELEPHONE NUMBER *(include area code)*

Table of Contents

Page

Annual progress report

1. INTRODUCTION: This project aims to investigate how a new tumor suppressor gene, TRAF3, regulates mitochondria function in B lymphocytes and B cell malignancies. TRAF3 deletions and mutations occur in a variety of B cell malignancies, including B cell chronic lymphocytic leukemia (B-CLL), non-Hodgkin lymphoma (NHL, such as splenic marginal zone lymphoma and mantle cell lymphoma), multiple myeloma (MM), and Waldenström's macroglobulinemia. We found that specific deletion of TRAF3 from B lymphocytes results in remarkably prolonged survival of mature B cells, which eventually leads to development of splenic marginal zone lymphoma or B1 lymphoma in mice. In this context, understanding how TRAF3 promotes B cell apoptosis is critical for rational design of therapeutic intervention of human B cell neoplasms. In pursuing such underlying mechanisms, we have obtained an unexpected but highly interesting finding. Although it has been widely believed that in the absence of stimulation, TRAF3 protein is evenly distributed in the cytosol, we found that most cellular TRAF3 is localized at mitochondria in resting splenic B cells. This proposal thus aims to test the central hypothesis that TRAF3 directly modulates the physiology of mitochondria to induce apoptosis in B lymphocytes. We will also delineate the profile of proteins assembled in the mitochondrial TRAF3 signaling complex of B cells. Our long-term goal is to gain new insights into the complex mechanisms of B lymphomagenesis, and to identify new therapeutic targets for the treatment of B-CLL, NHL and MM.

2. KEYWORDS: TRAF3, B lymphocytes, mitochondria, B cell chronic lymphocytic leukemia, non-Hodgkin lymphoma, multiple myeloma, affinity purification, mass spectrometry-based sequencing.

3. ACCOMPLISHMENTS:

(1) What were the major goals of the project?

There are two major goals of this project:

Aim 1. **To elucidate the roles of TRAF3 in modulating mitochondrial functions**

We will perform complementary studies using a new mouse model (B-TRAF3$^{-/-}$ mice) and human patient-derived multiple myeloma cell lines with TRAF3 deletions or mutations. We will analyze a variety of mitochondrial functions, including morphology, number, membrane potential, respiration and energy production, reactive oxygen species production, mitochondria phospholipid levels, and mitochondrial gene expression. We will also employ mutagenesis to determine what structural feature(s) of TRAF3 are required for each of its mitochondria regulatory roles.

Specific tasks of Aim 1:
1a. Mitochondria membrane potential: completed.
1b. Mitochondria morphology and number: in progress.
1c. Mitochondria respiration and energy production: in progress.
1d. Mitochondria ROS production and adenine nucleotides: in progress.
1e. Mitochondrial phospholipid levels: 50% completed.
1f. Mitochondrial gene expression: 50% completed.
1g. Reconstitution with TRAF3 mutants: 30% completed.

Aim 2. To identify novel TRAF3-interacting proteins in mitochondria of B lymphocytes

Considering that TRAF3 does not contain any mitochondria targeting motif nor transmembrane domain, we hypothesize that TRAF3 is targeted to mitochondria through interactions with mitochondrial proteins. To test this, we propose to identify novel mitochondrial TRAF3-interacting proteins using biochemical affinity purification followed by mass spectrometry-based sequencing. We will perform extensive proteomic and bioinformative analyses to prioritize the identified proteins. We will next employ genetic means to explore the functions of identified proteins in the survival of normal and malignant B cells.

Specific tasks of Aim 2:
2a. Generation and testing of hTRAF3 vectors for tandem affinity purification: 100% completed.
2b. Tandem affinity purification of mitochondrial TRAF3-interacting proteins: 100% completed.
2c. Mass spectrometry-based sequencing of purified proteins: 100% completed.
2d. Proteomic bioinformatic analyses of identified proteins: 30% completed.
2e. Prioritization of identified proteins: in progress.
2f. Verification of interaction with TRAF3 by TAP or co-immunoprecipitation: in preparation.
2g. Lentiviral shRNA vector-mediated knockdown in TRAF3-/- tumor B cells: in planning.
2h. Lentiviral vector-mediated ectopic overexpression in B cells: in planning.

(2) What was accomplished under these goals?

Aim 1: **To elucidate the roles of TRAF3 in modulating mitochondrial functions**

Our newest data demonstrated that most cellular TRAF3 is not evenly distributed in the cytosol as widely believed, but localized at mitochondria in resting splenic B cells. This led us to test a new hypothesis that TRAF3 directly modulates the physiology of mitochondria to induce apoptosis in B lymphocytes. Such study will allow us to delineate the roles of TRAF3 in regulating mitochondria functions in Aim 1.

1) Mitochondrial membrane potential: Mitochondrial membrane potential change precedes mitochondria-dependent apoptosis. We measured the mitochondrial membrane potential changes in LMC and premalignant TRAF3$^{-/-}$ B cells, and found that TRAF3 deletion drastically inhibited the mitochondrial membrane permeabilization in resting splenic B cells. This supports our hypothesis, and prompts us to thoroughly examine mitochondria morphology and functions.

2) Mitochondrion morphology and number: It is known that mitochondrion morphology and number often reflects its functional state. We have purified LMC and premalignant TRAF3$^{-/-}$ splenic B cells, and fixed the cells in 0.1M cacodylate buffer with 2.5% glutaraldehyde, 4% paraformaldehyde, and 8 mM $CaCl_2$. We are currently preparing the samples for electron microscopic examination, which will be analyzed on a JOEL 1200EX electron microscope to discern potential changes in mitochondrial morphology or number caused by TRAF3 deficiency. We have also prepared total cellular DNA, nuclear genomic DNA, and mitochondrial DNA from LMC and premalignant TRAF3$^{-/-}$ splenic B cells, and are currently determining the copy number of mitochondrial DNA (ND1) relative to nuclear DNA (pcam1) using quantitative real-time PCR.

3) Mitochondrial phospholipid levels: Mitochondrial phospholipids play critical roles in regulating mitochondria functions. We have extracted total cellular lipids and mitochondrial lipids from LMC and premalignant TRAF3$^{-/-}$ splenic B cells, and have analyzed the levels of **169 lipids and phospholipids** in these samples using LC-MS/MS, including phosphatidylcholine (PC), phosphatidylethanolamine (PE) and cardiolipin (CL). We are now in the process of analyzing the MS data of 169 lipids and phospholipids.

4) Mitochondrial gene expression: Mitochondrion-specific gene expression is essential to proper mitochondrion functions. We have prepared total cellular RNA and cDNA from LMC and

premalignant TRAF3$^{-/-}$ splenic B cells, and are currently performing quantitative real-time PCR to measure the transcript levels of key mitochondrial genes, including mitofusin 1 and 2, superoxide dismutase 2 (SOD2), mitochondrial uncoupling protein 3 (UCP3), mitochondrial inner membrane protein (IMMT), and ATP synthase. We have also prepared protein lysates from purified mitochondria of LMC and premalignant TRAF3$^{-/-}$ splenic B cells, and are doing Western blot analyses to determine the protein levels of the above mitochondrial genes.

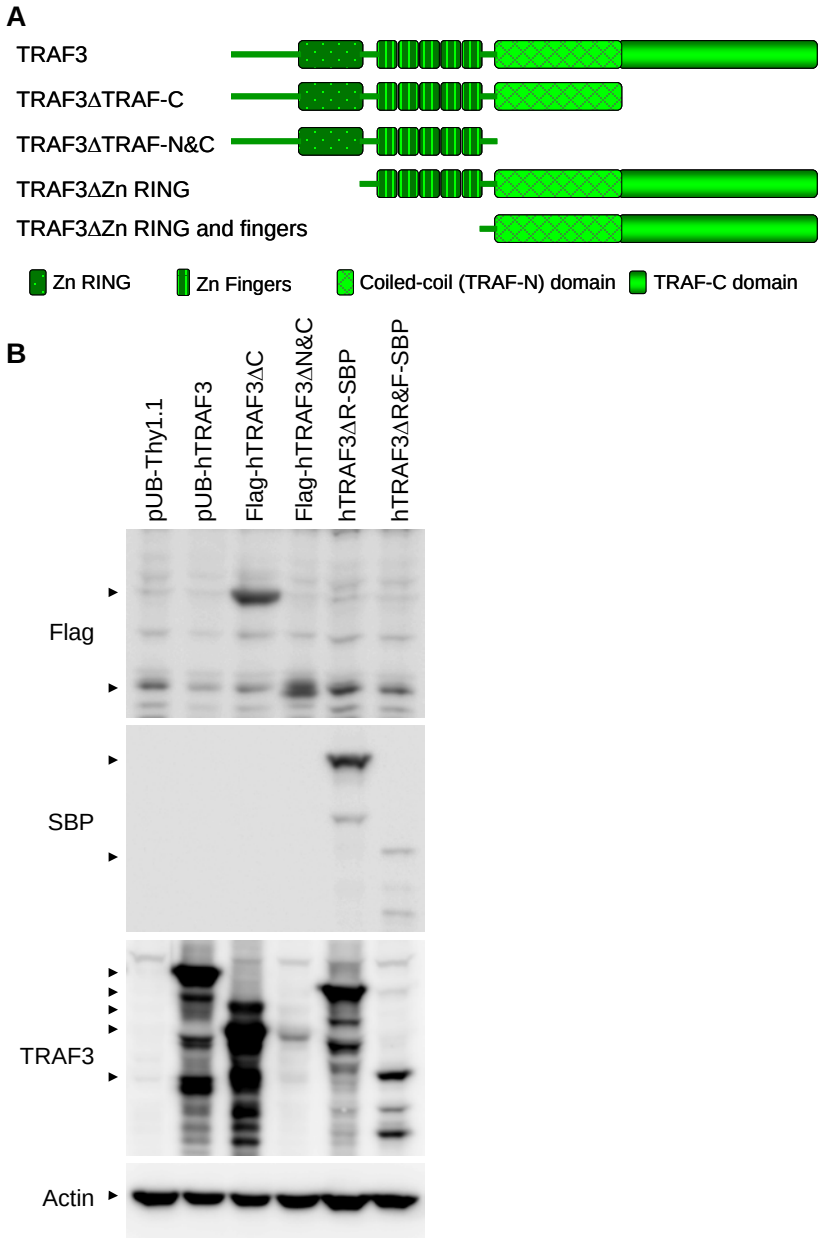

Fig. 1. **Lentiviral expression vectors of TRAF3 mutants generated in this study.** (**A**) Schematic diagram of the TRAF3 deletion mutants generated in this study. Domains of TRAF3 that are deleted are indicated. (**B**) Verification of expression of TRAF3 mutants by Western blot analysis. Human multiple myeloma 8226 cells (containing biallelic deletions of the TRAF3 gene) were transduced with lentiviral expression vectors of wild type or mutants of human TRAF3. Mutants analyzed include N-terminal Flag-tagged TRAF3ΔTRAF-C (Flag-hTRAF3ΔC), N-terminal Flag-tagged TRAF3ΔTRAF-N&C (Flag-hTRAF3ΔN&C), C-terminal SBP-tagged TRAF3ΔZinc RING (hTRAF3ΔR-SBP), and C-terminal SBP-tagged TRAF3ΔZinc RING and fingers (hTRAF3ΔR&F-SBP). Cells transduced with an empty lentiviral expression vector (pUB-Thy1.1) were used as control in these experiments. Transduction efficiency of each lentiviral vector is > 85%. Total cellular lysates were prepared on day 5 post transduction, and then analyzed by Western blot analyses. Proteins were immunoblotted for Flag, SBP, and TRAF3, followed by actin. Immunoblot of actin was used as a loading control. Please note that the N-terminal Flag-tagged TRAF3ΔTRAF-N&C (Flag-hTRAF3ΔN&C) was not detected by TRAF3 antibody, which recognizes amino acids 322-444 of human TRAF3. We also observed degradation of wild type or mutant TRAF3 in transduced human multiple myeloma 8226 cells.

5) Reconstitution with TRAF3 mutants: We have generated several lentiviral vectors to express deletion mutants of human TRAF3 that lack its different structural domains (Fig. 1A). We have used

these lentiviral vectors to transduce TRAF3-deficient human multiple myeloma cell line 8226 cells, and have verified the expression of TRAF3 mutants using Western blot analysis (Fig. 1B). We next compared the cell cycle distribution among three cell types: (1) 8226 cells transduced with a control lentiviral vector; (2) 8226 cells transduced with wild type TRAF3; (3) 8226 cells transduced with each deletion mutant. Our results demonstrate that reconstitution with wild type TRAF3 induced apoptosis and inhibited proliferation of human multiple myeloma 8226 cells. Interestingly, we found that the four TRAF3 mutants examined have completely or partially lost the apoptotic and anti-proliferative functions of TRAF3 (Fig. 2). Our results suggest that the **TRAF-C**, **TRAF-N**, **Zinc RING**, and **Zing fingers** all contribute to the tumor suppressive functions of TRAF3 in B cells. We will continue to further examine mitochondrial physiology and functions using similar reconstitution experiments to elucidate what structural features of TRAF3 are required for its mitochondria regulatory roles.

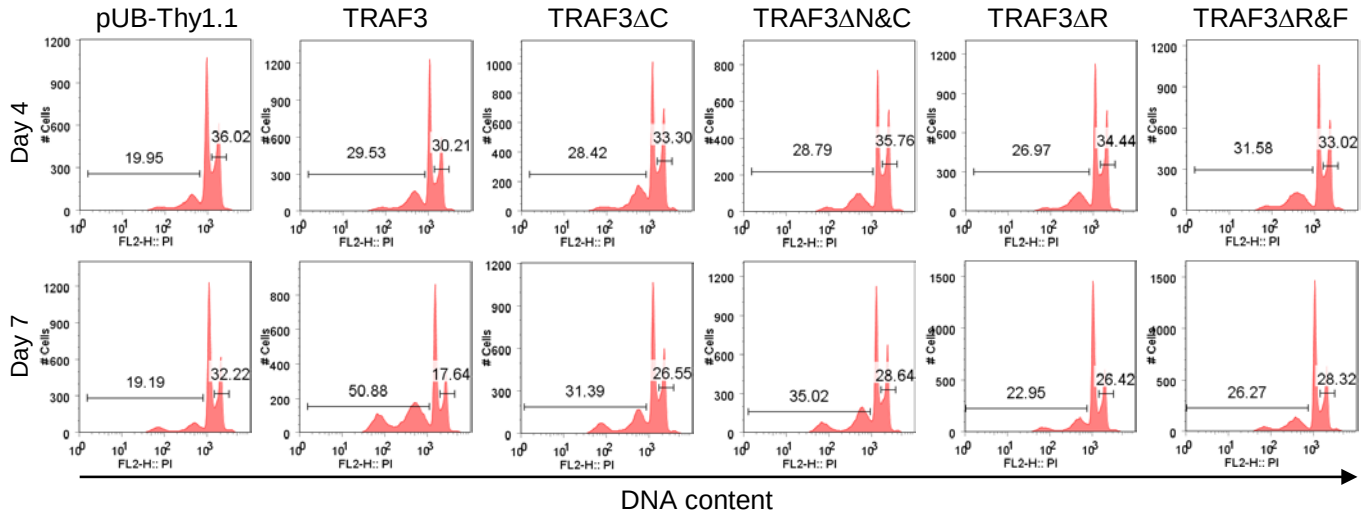

Fig. 2. **Tumor suppressive function of TRAF3 requires its TRAF-C, TRAF-N, Zinc Ring, and Zing finger domains.** Human multiple myeloma 8226 cells (containing biallelic deletions of the TRAF3 gene) were transduced with lentiviral expression vectors of wild type or mutants of human TRAF3. TRAF3 mutants analyzed include TRAF3ΔTRAF-C (TRAF3ΔC), TRAF3ΔTRAF-N&C (TRAF3ΔN&C), TRAF3ΔZinc RING (TRAF3ΔR), and TRAF3ΔZinc RING and fingers (TRAF3ΔR&F). Cells transduced with an empty lentiviral expression vector (pUB-Thy1.1) were used as control in these experiments. Transduction efficiency of each lentiviral vector is > 85%. Cell cycle distribution of transduced cells was determined on day 4 and day 7 post transduction. Cells were fixed, and then stained with propidium iodide (PI). Stained cells were subsequently analyzed on a flow cytometer. Representative FACS histograms of PI staining are shown, and percentages of apoptotic cells (DNA content < 2n; sub-G1) and proliferating cells (2n < DNA content ≤ 4n; S/G2/M) are indicated.

Aim 2: To identify novel TRAF3-interacting proteins in mitochondria of B lymphocytes

Given that TRAF3 does not contain any mitochondria targeting motif nor transmembrane domain, we hypothesize that TRAF3 is localized at mitochondria in resting splenic B cells through interaction with other mitochondrial proteins. We are testing this hypothesis in Aim 2.

1) Generation and testing of tagged hTRAF3 vectors for tandem affinity purification: We employed a newly developed TAP strategy that uses streptavidin-binding peptide (SBP, Stratagene) and 6xHis as the tandem tag. This new TAP strategy offers several advantages as compared to the conventional TAP systems. (1) The overall recovery of the dual affinity purification (>50%) is the highest of existing TAP tags. (2) The protease cleavage step in the original TAP protocol that caused yield loss is avoided, as both tags can be eluted from their respective resins under mild conditions. (3)

Both streptavidin and nickel resins are relatively inexpensive and have a high capacity. (4) The sequential purification can be performed in a single buffer system. (5) The immobilized metal affinity chromatography (IMAC) supports purification under denaturing conditions. We have generated lentiviral expression vectors of an N-terminal FLAG tag or a C-terminal SBP-6xHis tag in frame with the human TRAF3 coding sequence (pUB-Flag-hTRAF3 or pUB-hTRAF3-SBP-6xHis), respectively. We have used these vectors to transduce TRAF3-deficient human patient-derived MM cell lines (HMCLs) 8226 and LP1 cells, and our results verified that both tagged TRAF3 proteins maintain the mitochondrial localization of native TRAF3. We also tested the tandem affinity purification efficiency of pUB-hTRAF3-SBP-6xHis using transfected 293T cells, and confirmed that purification of transfected cell lysates using both streptavidin resin and nickel beads allowed high recovery rate of the SBP-6xHis-tagged TRAF3 (Fig. 3). Interestingly, however, we noticed that nickel beads also pulled down Flag-tagged TRAF3 as well as endogenous TRAF2 and TRAF6 independent of the 6xHis tag (Fig. 3). This reminds us that TRAF proteins contain Zinc binding motifs, and can therefore bind to nickel beads in the absence of histidine tag. Based on these results, we decide to discontinue the use of nickel beads, and isolate TRAF3-interacting proteins using one-step affinity purification by streptavidin resin.

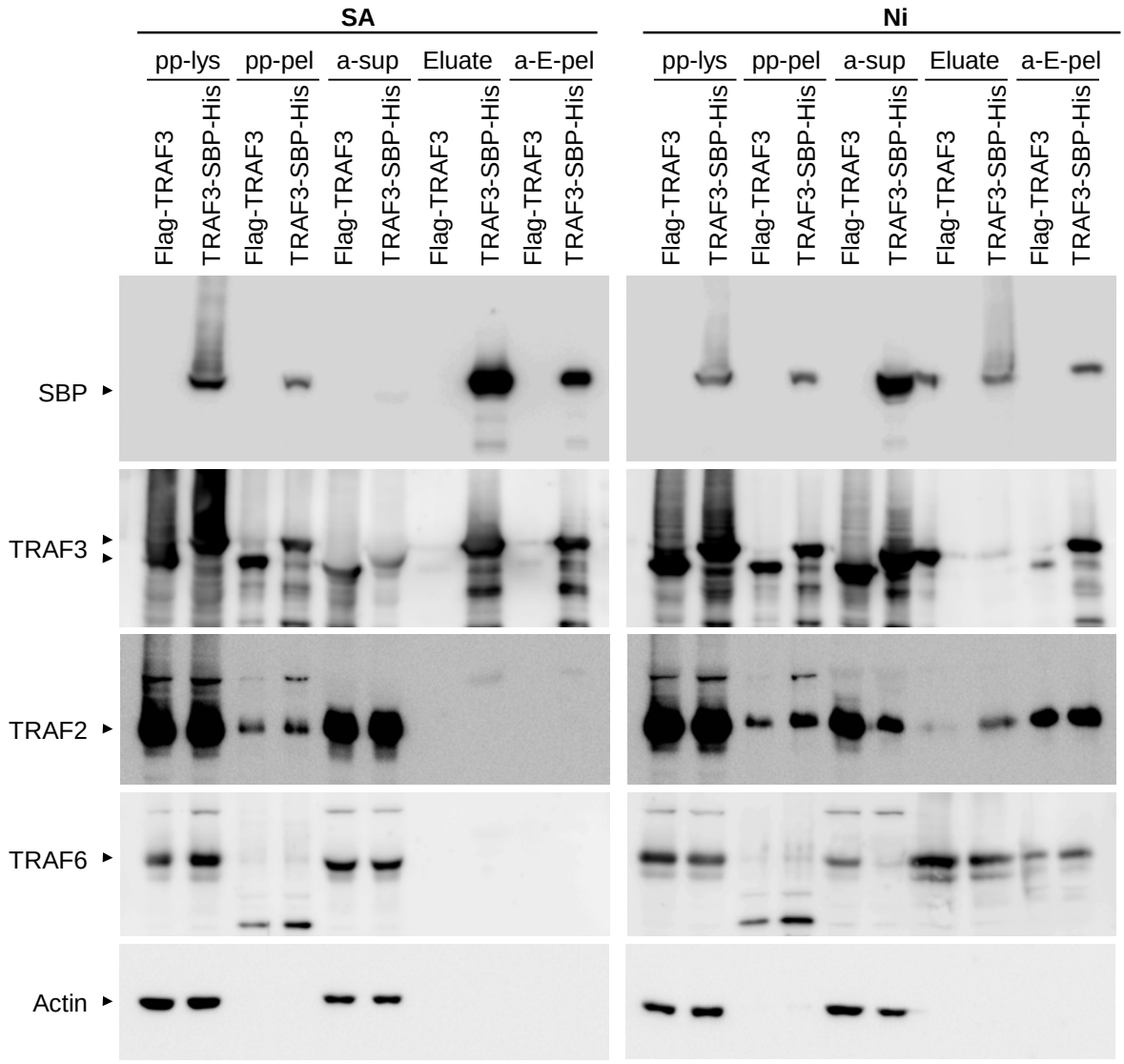

Fig. 3. **Testing of tandem affinity purification of tagged TRAF3.** 293T cells were transfected with lentiviral expression vectors of an N-terminal Flag-tagged TRAF3 (FLAG-TRAF3) or a C-terminal SBP-6xHis tagged TRAF3 (TRAF3-SBP-His). Transduction efficiency of each lentiviral vector is > 85%. Cells were harvested on day 3 post transfection, and total cellular proteins were lysed in 1% CHAPS lysis buffer. Transfected TRAF3-SBP-His were affinity purified by streptavidin-sepharose resin (SA) or nickel beads (Ni), respectively. Lysates of cells transfected with FLAG-TRAF3 that were purified by the same procedures were used as negative control in these experiments. Proteins were immunoblotted for SBP tag, TRAF3, TRAF2, and TRAF6, followed by actin. Blots of whole cell lysates before affinity purification (pp-lys) were used as the input control. Other samples examined include insoluble pellets of 1% CHAPS lysates (pp-pel), supernatant after affinity purification (immunoprecipitation) by SA or Ni (a-sup), eluates of immunoprecipitates (Eluate), and proteins that cannot be eluted and are still associated with beads after elution (a-E-pel).

2) Affinity purification of mitochondrial TRAF3-interacting proteins: We have used the validated lentiviral expression vector pUB-hTRAF3-SBP-6xHis to transduce human multiple myeloma 8226 cells (containing biallelic deletions of the TRAF3 gene). Use of these cells eliminates the affects of endogenous TRAF3. We purified mitochondria from transduced 8226 cells by biochemical fractionation, and solubilized mitochondrial proteins in 1% CHAPS lysis buffer. We then purified the SBP-6xHis-tagged TRAF3 and associated mitochondrial proteins using streptavidin resin. A small aliquot (5%) of the immunoprecipitates were used for Western blot analysis, and our results confirmed the high recovery rate of SBP-6xHis-tagged TRAF3 (Fig. 4). Cells transduced with Flag-tagged TRAF3 were subjected to the same purification procedure and used as negative control (Fig. 4). All residual streptavidin immunoprecipitates were separated on 4-16% gradient SDS-PAGE (Invitrogen) and visualized using Gel Code Blue (Pierce) staining. The gel lanes for TRAF3 complex (pUB-hTRAF3-SBP-6xHis) and negative control (pUB-Flag-hTRAF3) were each sectioned into 15 continuous slices, which were delivered to our collaborator Drs. David Perlman and Saw Kyin at Princeton University for further processing and sequencing by LC-MS/MS.

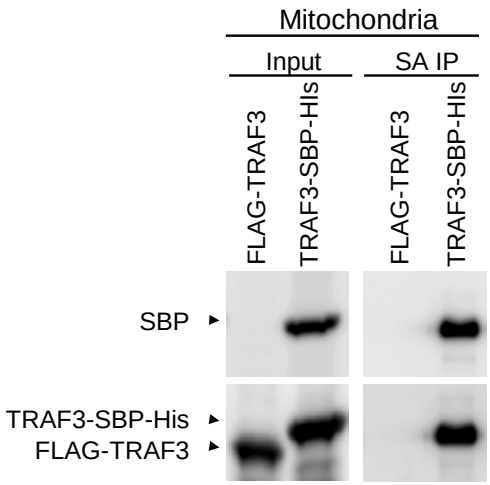

Fig. 4. Large scale affinity purification of SBP-6xHis-tagged TRAF3 from purified mitochondria of transduced human multiple myeloma cells. Human multiple myeloma 8226 cells (150×10^6 cells) were transduced with lentiviral expression vectors of N-terminal Flag-tagged TRAF3 (FLAG-TRAF3) or C-terminal SBP-6xHis tagged TRAF3 (TRAF3-SBP-His). Transduction efficiency of each lentiviral vector is > 85%. Tranduced cells were harvested on day 4 post transduction, and were fractionated to isolate mitochondria. Mitochondrial proteins were solubilized in 1% CHAPS lysis buffer, and then immunoprecipitated with streptavidin-sepharose beads. Immunoprecipitates of TRAF3-SBP-6xHis by streptavidin-sepharose beads (SA IP) from purified mitochondria were used to identify TRAF3-interacting proteins. Immunoprecipitates of FLAG-TRAF3 by streptavidin-sepharose beads were used as negative control in these experiments. Proteins were immunoblotted for SBP tag, and followed by TRAF3. Blots of mitochondrial lysates before immunoprecipitation were used as the input control.

3) Mass spectrometry-based sequencing of purified proteins: The gel slice samples were subjected to thiol reduction by TCEP, alkylation with iodoacetamide, and digestion with sequencing-grade modified trypsin. Peptides were eluted from the gel slices, desalted, and then subjected to reversed-phase nano-flow ultra high performance capillary liquid chromatography (uPLC) followed by high-resolution/ high-mass accuracy MS/MS analysis using an LC-MS platform consisting of an Eksigent Nano Ultra 2D Plus uPLC system hyphenated to a Thermo Orbi Velos mass spectrometer. The MS/MS

were set to operate in data dependent acquisition mode using a duty cycle in which the top 15 most abundant peptide ions in the full scan MS will be targeted for MS/MS sequencing. Full scan MS1 spectra were acquired at 100,000 resolving power and can be expected to maintain mass calibration to within 2-3 ppm mass accuracy. Drs. David Perlman and Saw Kyin searched the LC-MS/MS data against the human IPI and UniProt databases using the Mascot and Proteome Discoverer search engines. Protein assignments were considered highly confident using a stringent false discovery rate threshold of <1%, as estimated by reversed database searching, and requiring that ≥2 peptide spectral counts per protein be unambiguously identified. We estimated rough relative protein amounts using spectra counting values. Through these studies, we **have successfully identified 154 TRAF3 interacting proteins at mitochondria of B cells**. Among these, 4 proteins are previously known TRAF3-interacting proteins, including TRAF2, TANK, NUP62, and UBE2N. We are currently performing proteomic and bioinformatics analyses of the identified TRAF3 interacting proteins to prioritize the list for further investigation.

(3) What opportunities for training and professional development has the project provided?

This DoD award has provided critical support for the career development of the PI, Dr. Ping Xie. Supported by this grant, Dr. Xie is able to establish a new collaboration with Dr. David Perlman at Princeton University, and has learned from him a number of bioinformatic and proteomic analytical tools. Dr. Xie has given one conference talk and five seminar presentations at other institutions to promote our research program. With the support of this award, Dr. Xie has the opportunity to mentor one new postdoctoral fellow, one graduate student, and two new undergraduate students. This DoD grant also allows Dr. Xie to better integrate her educational and research efforts, including the undergraduate courses of Immunology and Immunology Lab, and the graduate course of Advanced Topics in Immunology. Taken together, this DoD award has been essential for Dr. Xie to acquire the leadership and expertise to advance her professional development at the forefront of cancer research.

Trainees of this project
Postdoctoral fellow:
Yingying Liu

Graduate students performing PhD thesis research in the lab:
Shanique Edwards

Undergraduate students performing honors thesis research in the lab:
Xin Chen
Debanjan Saha

Awards received by trainees of this project
2014 Shanique Edwards, Graduate Student, Anne B. and James B. Leathem Fellow, Rutgers University

Participation in conferences:
Xie P. TRAF3 in innate immunity and inflammation. Infectious and Inflammatory Disease Retreat, Institute of Infectious Disease of New Jersey, Newark, NJ. July 10, 2014

(4) How were the results disseminated to communities of interest?

Dr. Xie was invited to give one conference talk and five seminar presentations at other institutions to share our recent results and findings with communities of interest. In addition, our lab was opened to visitors on Rutgers University Open House day on April 5, 2014. Dr. Xie has introduced our research activities and reported our new results to visitors, including parents and high school students. The objective of such outreach activities is to promote public understanding and increasing interest in scientific research.

(5) What do you plan to do during the next reporting period to accomplish the goals?

Aim 1: **To elucidate the roles of TRAF3 in modulating mitochondrial functions**

1) Mitochondrion respiration and energy production: The primary function of mitochondria includes respiration and energy production. We will measure four key parameters of these functions, including basal respiration, ATP turnover, proton leak, and maximal respiration, using a Cell Mito Stress Test Kit (Seahorse). Using this assay, the rate of mitochondrial ATP synthesis in a defined basal state can be estimated from the decrease in respiration on inhibiting the ATP synthase with oligomycin. Maximal respiratory capacity and total reserve capacity will be measured by injecting the mitochondrial uncoupler FCCP, and Complex III inhibitor antimycin, respectively.

2) Mitochondrial reactive oxygen species (ROS) production and adenine nucleotides: Mitochondrial dysfunction may lead to increased ROS production and consequently oxidative stress, and altered TCA cycle intermediates. We will investigate the effects of TRAF3 on ROS production in mouse and human B cells. ROS levels will be determined using 29-79-dichlorodihydro-fluorescene diacetate (DCF-DA, Molecular Probes). We will also measure major TCA cycle intermediates, including ATP, ADP, and AMP, by LC-MS.

Aim 2: To identify novel TRAF3-interacting proteins in mitochondria of B lymphocytes

1) Proteomic bioinformatic analyses of identified proteins: We are performing the following proteomic bioinformatic analyses of our LC-MS/MS sequencing results. (**a**) Expression levels in mature B lymphocytes: We attempt to correlate our protein detection with the reported transcript expression levels of identified proteins in different B cell populations by surveying the public gene expression database of Immune Genome (http://www.immgen.org), including pro-B, pre-B, B1, marginal zone B, and follicular B cells. (**b**) Protein domain and motif analysis: We are analyzing the domain structure and known motifs of each identified protein using the following programs: UCSC Genome Browser (http://genome.ucsc.edu/), ExPASy PROSITE (http://prosite.expasy.org/), and MOTIF (http://www.genome.jp/tools/motif/). (**c**) Subcellular localization analysis: Potential mitochondrial localization of identified proteins are being searched in the published literature, or predicted using the UCSC Genome Browser and Ingenuity Pathways Analysis. (**d**) Survey public cancer genome and gene expression databases: We will survey available cancer genome databases to determine whether the identified genes exhibit alterations in mRNA expression or DNA copy number, or mutations in primary human B lymphomas and other cancers, and whether alterations in these genes correlate with poor prognosis in human cancer patients (http://www.oncomine.org). (**e**) Functional clustering and pathway analysis: Allocation of identified genes in functional clusters and signaling pathways are being conducted using Ingenuity Pathways Analysis software (CINJ). Together, results of these proteomic and bioinformatic analyses will provide additional information to allow us to prioritize the list of mitochondrial TRAF3-interacting proteins to pursue those most likely to be relevant to human cancer and lymphomagenesis.

2) Prioritization of identified proteins: To select the most critical TRAF3-interacting proteins for further study, we will use the following prioritization scheme: (**a**) expression of the identified gene is clearly detected or high in mature B cells, and is **not** B cell subset-specific, as prolonged survival is

observed in all mature B cell subsets, including follicular, marginal zone and B1 B cells of B-TRAF3$^{-/-}$ mice[1]; (**b**) the identified protein contains domain structure or motifs that may mediate direct interaction with TRAF3, such as the coiled-coiled domain or the "PXQXT/S" motif; (**c**) the identified protein is a known mitochondrial protein or contains a mitochondrial targeting motif; (**d**) alterations of the identified gene have been documented in human B-CLL, NHL and multiple myeloma in the published literature or in the public gene expression database of cancers (http://www.oncomine.org), including changes in mRNA expression, DNA copy number, or mutations. (**e**) for proteins within the same signaling pathway, ones that have been most consistently detected across replicates, have the highest number of unique identified peptides or LC-MS/MS spectral counting values, and have not been detected in the negative control sample will be given the highest priority.

3) Verification of interaction with TRAF3 by co-immunoprecipitation: We will verify the association of TRAF3 and identified proteins in the order of their priority score. (**a**) Affinity purification with tagged TRAF3 in transduced human B cells: We will first use the same affinity purification procedure of that used for LC-MS/MS to purify SBP-His tagged TRAF3 complex, and presence of each identified protein in the TRAF3 complex will be verified using Western blot analysis as we described. (**b**) Co-immunoprecipitation with endogenous TRAF3 in mouse splenic B cells: resting splenic B cells will be purified from B-TRAF3$^{-/-}$ and LMC mice. Endogenous TRAF3 will be immunoprecipitated from mitochondrial lysates of splenic B cells. Potential co-immunoprecipitation of TRAF3 and each identified protein will be determined by Western blot analysis. TRAF3$^{-/-}$ B cells will serve as negative control in these experiments. (**c**) Affinity purification with TRAF3 deletion mutants in transduced human B cells: We have generated four deletion mutants of TRAF3 as depicted in Fig. 1A. We have also generated lentiviral expression vectors of SBP-His tagged versions of these mutants, which will be used for the affinity purification procedure. Association of each identified protein with such TRAF3 mutants will be examined using Western blot analyses. We predict that association of the identified proteins with TRAF3 will be affected by the absence of either Zinc ring/Zinc fingers or the coiled-coil domain of TRAF3. These studies will demonstrate the association of TRAF3 and identified proteins in the same molecular complex in mitochondria of B cells, either directly or indirectly.

4) Lentiviral shRNA vector-mediated knockdown in B cells: We will use lentiviral shRNA vector-mediated gene knockdown to determine whether each identified protein is anti-apoptotic or pro-apoptotic in tumor B cells. We will use these lentiviral vectors to transduce TRAF3$^{-/-}$ B lymphoma cell lines or the human MM cell line 8226 cells. Cells transduced with a scrambled shRNA control vector will be used as control. Specific knockdown of the protein will be verified by Western blot analysis. We will determine the functional consequence of each protein knockdown on the survival, proliferation, and tumorigenicity. (**a**) Survival and apoptosis: We will monitor the survival, apoptosis, and cell cycle distribution of transduced cells using annexin V staining and PI staining, followed by FACS analysis. (**b**) Proliferation of tumor B cells: Proliferation of transduced B lymphoma cells and HMCLs will be determined by CFSE labeling, MTT assay, and growth curves. (**c**) *In vivo* tumorigenicity test: For TRAF3$^{-/-}$ B lymphoma cell lines, we will *i.p.* inject cells transduced with the shRNA vector or a scrambled shRNA control into NOD SCID recipient mice. For HMCLs, we will *s.c.* inject transduced cells into the right flank of immunodeficient NSG recipient mice (Jackson Laboratory, Stock Number 005557). Recipient mice with transplanted B lymphomas or HMCL xenografts will be monitored daily, and will be examined for the presence and severity of B lymphomas or for the size of xenografts. Together, the knockdown studies will determine whether each identified protein is necessary for the survival of TRAF3$^{-/-}$ tumor B cells, and whether it can serve as a therapeutic target in B cell neoplasms.

5) Lentiviral vector-mediated ectopic overexpression in B cells: We will generate lentiviral expression vectors to ectopically overexpress each identified protein in LMC and TRAF3$^{-/-}$ splenic B cells. Cells transduced with an empty lentiviral expression vector (pUB-Thy1.1) will be used as control

in these experiments. Transduction efficiency and verification of protein expression will be subsequently determined by FACS and Western blot analyses. Survival and apoptosis of transduced cells will be determined. Transduced cells will also be analyzed in the absence or presence of B cell stimuli (BAFF, CD40 ligand, LPS or CpG). These experiments will allow us to probe the roles of each identified TRAF3-interacting protein in regulating the survival of B lymphocytes.

4. IMPACT

What was the impact on the development of the principal discipline(s) of the project?

Aberrant B cell survival is one important pathogenic factor that leads to B cell malignancies, which comprise >50% of blood cancers. Despite recent advances, many types of B cell neoplasms remain incurable, highlighting a clear need for new therapeutic approaches. TRAF3 inactivation frequently occurs in a variety of B cell neoplasms, including B-CLL, NHL, MM and WM. Notably, TRAF3 inactivation has particular relevance to military personnel, veterans and their family members: (1) The Epstein-Barr virus (EBV)-encoded protein LMP1 sequesters over 80% of cellular TRAF3 in B cells. EBV reactivation is more common in soldiers and veterans, and is associated with increased risk of B lymphoma. (2) Infections and inflammations trigger TRAF3 degradation through signaling by the TNF-Rs (such as CD40) or Toll-like receptors (such as TLR4). Soldiers and veterans have increased risk of infections and inflammations, due to duty environment, bioterror weapons, physical injury, and stress, etc. (3) Soldiers and veterans exposed to radioactive and chemical weapons/equipment have increased risk of mutations in blood cells, including those of *TRAF3*. In this study, we have identified 150 novel TRAF3-interacting proteins in purified mitochondria of human multiple myeloma cells. Many of these TRAF3 interactors are novel regulators of B cell survival. Our ongoing study aims to further elucidate the mechanisms of how the TRAF3 and its interactors regulate mitochondrial physiology to inhibit B cell survival. We expect that our study will identify new diagnostic markers and therapeutic targets, and will thus open up new avenues for the prevention and treatment of B cell malignancies, the most common blood cancers.

What was the impact on other disciplines? Nothing to Report.

What was the impact on technology transfer? Nothing to Report.

What was the impact on society beyond science and technology?

Our lab was opened to visitors on Rutgers University Open House day on April 5, 2014. Dr. Xie has introduced our research activities and reported our new results to visitors, including parents and high school students. The objective of such outreach activities is to promote public understanding and increasing interest in scientific research.

5. CHANGES/PROBLEMS

Changes in approach and reasons for change: Nothing to report.

Actual or anticipated problems or delays and actions or plans to resolve them: Nothing to report.

Changes that had a significant impact on expenditures: Nothing to report.

Significant changes in use or care of human subjects: Nothing to report.

Significant changes in use or care of vertebrate animals: Nothing to report.

Significant changes in use or care of biohazards and/or select agents: Nothing to report.

6. PRODUCTS

(1) Publications, conference papers, and presentations

Journal publications:

1. **Xie P**. TRAF molecules in cell signaling and in human diseases. *J. Mol. Signal.* 8:7, pages 1 – 31, doi:10.1186/1750-2187-8-7, 2013. (Acknowledged this DoD grant.)
2. Edwards S, Baron J, Moore CR, Liu Y, Perlman DH, Hart RP, and **Xie P**. Mutated in colorectal cancer (MCC) is a novel oncogene in B lymphocytes. J. Hematol. & Oncol., in press. (Acknowledged this DoD grant; please see the appendix)

Books or other non-periodical, one-time publications: Nothing to Report.

Invited conference talks and presentations:

1. **Xie P.** TRAF3-mediated regulation of innate immunity and inflammation. The Child Health Institute of New Jersey, New Brunswick, NJ. Feb. 17, 2014
2. **Xie P.** Molecular mechanisms of TRAF3 in immune regulation and cancer pathogenesis. Cardiovascular Seminar Series, Department of Internal Medicine, Saha Cardiovascular Center, the University of Kentucky, Lexington, KY. July 7, 2014
3. **Xie P.** TRAF3 in innate immunity and inflammation. Infectious and Inflammatory Disease Retreat, Institute of Infectious Disease of New Jersey, Newark, NJ. July 10, 2014
4. **Xie P.** Mechanisms of TRAF3 inactivation-initiated B lymphomagenesis. Department of Systems and Computational Biology, Albert Einstein College of Medicine of Yeshiva University, Bronx, NY. July 15, 2014
5. **Xie P.** TRAF3: a tumor suppressor gene in B lymphocytes. Department of Pharmacology, the University of Illinois at Chicago, Chicago, IL. Aug. 11, 2014
6. **Xie P.** TRAF3: a regulator of innate immunity and inflammation. Department of Cell & Molecular Physiology, University of Loyola, Chicago, IL. Aug. 27, 2014

(2) Website(s) or other Internet site(s): Nothing to Report.

(3) Technologies or techniques: Nothing to Report.

(4) Inventions, patent applications, and/or licenses: Nothing to Report.

(5) Other Products:

Research materials: We have generated a number of lentiviral expression vectors of TRAF3, including wild type and mutant TRAF3 with or without tags, which allow affinity purification and structure-function study of TRAF3. We will make these DNA vectors available to other scientists upon request.

7. PARTICIPANTS & OTHER COLLABORATING ORGANIZATIONS

(1) What individuals have worked on the project?

Ping Xie, PhD, PI: No change.
David Perlman, PhD, collaborator: No change

Name: Yingying Liu, PhD
Project Role: Postdoctoral associate
Researcher Identifier (e.g. ORCID ID): 1234567
Nearest person month worked: 12
Contribution to Project: Dr. Liu has performed most experiments described in this progress report, including mitochondrial function analyses, generation of lentiviral expression vectors of TRAF3 for TAP and TRAF3 mutants, and affinity purification of mitochondrial TRAF3-interacting proteins from transduced human multiple myeloma cells.
Funding Support: this DoD grant.

Name: Shanique Edwards, PhD
Project Role: Graduate student
Researcher Identifier (e.g. ORCID ID): 1234567
Nearest person month worked: 3
Contribution to Project: Shanique has helped to test and troubleshoot the tandem affinity purification protocol to identify TRAF3-interacting proteins from purified B cell mitochondria, and has also applied this strategy to discover mitochondrial proteins interacting with a novel oncogene, MCC, that we recently identified in $TRAF3^{-/-}$ mouse B lymphomas.
Funding Support: Shanique has been supported by a Teaching Assistantship.

(2) Has there been a change in the active other support of the PD/PI(s) or senior/key personnel since the last reporting period?

Nothing to Report.

(3) What other organizations were involved as partners?

Partner Organization Name: Princeton University
Location of Organization: Princeton Collaborative Proteomics & Mass Spectrometry Center, Lewis-Sigler Institute of Integrative Genomics, Princeton University, Princeton, NJ 08544

Partner's contribution to the project:
Facilities: performed protein sequencing by LC-MS/MS at Princeton University.
Collaboration: Dr. David Perlman analyzed LC-MS/MS data.

8. SPECIAL REPORTING REQUIREMENTS

COLLABORATIVE AWARDS: Not applicable.

QUAD CHARTS: Not applicable.

9. APPENDICES: A research article in press is attached.

Research article in press in Journal of Hematology & Oncology

Mutated in colorectal cancer (MCC) is a novel oncogene in B lymphocytes

Shanique K.E. Edwards[1,2], Jacqueline Baron[1], Carissa R. Moore[1], Yan Liu[1], David H. Perlman[3], Ronald P. Hart[1,4,5], and Ping Xie[1,5]

[1]Department of Cell Biology and Neuroscience, [2]Graduate Program in Molecular Biosciences, and [4]W.M. Keck Center for Collaborative Neuroscience, Rutgers University, Piscataway, New Jersey 08854

[3]Princeton Collaborative Proteomics & Mass Spectrometry Center, Lewis-Sigler Institute of Integrative Genomics, Princeton University, Princeton, NJ 08544

[5]Member, Rutgers Cancer Institute of New Jersey

Email addresses for all authors:

Shanique K.E. Edwards: sedward3@rci.rutgers.edu

Jacqueline Baron: jackiebaron7@gmail.com

Carissa R. Moore: CMoore@Streck.com

Yan Liu: yanx@rci.rutgers.edu

David H. Perlman: perlmand@Princeton.EDU

Ronald P. Hart: rhart@rutgers.edu

Ping Xie: xiep@rci.rutgers.edu

Address correspondence to: Dr. Ping Xie, Department of Cell Biology and Neuroscience, Rutgers University, 604 Allison Road, Nelson Labs Room B336, Piscataway, New Jersey 08854. Phone: (732) 445-0802; Fax: (732) 445-1794; E-mail: xiep@rci.rutgers.edu

Abstract

Background: Identification of novel genetic risk factors is imperative for a better understanding of B lymphomagenesis and for the development of novel therapeutic strategies. TRAF3, a critical regulator of B cell survival, was recently recognized as a tumor suppressor gene in B lymphocytes. The present study aimed to identify novel oncogenes involved in malignant transformation of TRAF3-deficient B cells.

Methods: We used microarray analysis to identify genes differentially expressed in TRAF3$^{-/-}$ mouse splenic B lymphomas. We employed lentiviral vector-mediated knockdown or overexpression to manipulate gene expression in human multiple myeloma (MM) cell lines. We analyzed cell apoptosis and proliferation using flow cytometry, and performed biochemical studies to investigate signaling mechanisms. To delineate protein-protein interactions, we applied affinity purification followed by mass spectrometry-based sequencing.

Results: We identified *mutated in colorectal cancer* (*MCC*) as a gene strikingly up-regulated in TRAF3-deficient mouse B lymphomas and human MM cell lines. Aberrant up-regulation of *MCC* also occurs in a variety of primary human B cell malignancies, including non-Hodgkin lymphoma (NHL) and MM. In contrast, *MCC* expression was not detected in normal or premalignant TRAF3$^{-/-}$ B cells even after treatment with B cell stimuli, suggesting that aberrant up-regulation of *MCC* is specifically associated with malignant transformation of B cells. In elucidating the functional roles of MCC in malignant B cells, we found that lentiviral shRNA vector-mediated knockdown of MCC induced apoptosis and inhibited proliferation in human MM cells. Experiments of knockdown and overexpression of MCC allowed us to identify

several downstream targets of MCC in human MM cells, including phospho-ERK, c-Myc, p27, cyclin B1, Mcl-1, caspases 8 and 3. Furthermore, we identified 365 proteins (including 326 novel MCC-interactors) in the MCC interactome, among which PARP1 and PHB2 were two hubs of MCC signaling pathways in human MM cells.

Conclusions: Our results indicate that in sharp contrast to its tumor suppressive role in colorectal cancer, MCC functions as an oncogene in B cells. Our findings suggest that MCC may serve as a diagnostic marker and therapeutic target in B cell malignancies, including NHL and MM.

Keywords:

MCC, TRAF3, B lymphoma, multiple myeloma, PARP1, PHB2

Background

B cell neoplasms account for over 90% of lymphoid tumors worldwide, and comprise >50% of blood cancers. Despite recent advances in treatment, many types of human B cell lymphomas remain incurable, highlighting a clear need for new preventative and therapeutic strategies [1, 2]. Increasing evidence indicates the importance of genetic determinants in B lymphomagenesis [3-5]. Identification and validation of new genetic risk factors are imperative for a better understanding of B cell malignant transformation and for the development of new therapeutic strategies. Recent studies from our laboratory and others have identified TRAF3, a critical determinant of B cell survival, as a tumor suppressor gene in B lymphocytes. TRAF3 is a member of the tumor necrosis factor receptor (TNF-R)-associated factor (TRAF) family (TRAF1-6) of cytoplasmic adaptor proteins [6]. All TRAF proteins have the distinctive feature of a C-terminal TRAF domain, which mediates the interaction with TRAF-binding motifs of receptors of the TNF-R superfamily [6, 7]. Homozygous deletions and inactivating mutations of the TRAF3 gene have been identified in non-Hodgkin lymphoma (NHL), including splenic marginal zone lymphoma (MZL), B cell chronic lymphocytic leukemia (B-CLL) and mantle cell lymphoma (MCL), as well as multiple myeloma (MM) and Waldenström's macroglobulinemia (WM) [8-11].

By generating and characterizing a mouse model that has the *Traf3* gene specifically deleted in B lymphocytes (B-TRAF3$^{-/-}$ mice), we recently reported that TRAF3 deletion leads to spontaneous development of MZL and B1 lymphoma in mice [12, 13]. Interestingly however, B lymphoma development in B-TRAF3$^{-/-}$ mice exhibits a long latency (approximately 9 months), indicating that TRAF3 inactivation and its

aberrant signaling pathways are not sufficient to induce B lymphomagenesis and that additional oncogenic pathways are necessary for B lymphoma development. Although TRAF3 deletions or mutations exist in human patients with NHL and MM, it is not known whether TRAF3 inactivation is the primary or secondary oncogenic mutation in human samples. Thus, B-TRAF3$^{-/-}$ mice offer the unique advantage to identify secondary oncogenic pathways that drive B lymphomagenesis in the context of TRAF3 inactivation. To identify such secondary oncogenic alterations that mediate the malignant transformation of TRAF3$^{-/-}$ B cells, we performed a transcriptome microarray analysis using TRAF3$^{-/-}$ mouse splenic B lymphomas. Surprisingly, our microarray analysis identified *mutated in colorectal cancer* (*MCC*), a tumor suppressor gene of colorectal cancer, as a strikingly up-regulated gene in B lymphomas spontaneously developed in different individual B-TRAF3$^{-/-}$ mice.

The *MCC* gene was discovered in 1991 through its linkage to the region showing loss of heterozygosity (LOH) in familial adenomatous polyposis (FAP) [14-17]. Subsequent studies revealed that the *adenomatous polyposis coli* (*APC*) gene and not *MCC* is responsible for FAP. The APC gene is mutated somatically in 60–80% of sporadic colorectal cancers (CRCs), whereas somatic mutation of MCC is relatively rare, 3–7%, in sporadic CRCs [14-18]. However, it was subsequently reported that the MCC gene is silenced through promoter methylation in approximately 50% of primary sporadic CRCs and 80% of serrated polyps, suggesting that the silencing of MCC is important in early colon carcinogenesis via the serrated neoplasia pathway [19-22]. Furthermore, loss-of-function mutations, LOH, or decreased expression of the *MCC* gene are also detected in a number of other human cancers, including lung cancer [17, 23], gastric carcinoma

[24], esophageal cancer [25], and hepatocellular carcinoma [26, 27]. In addition, an SNP of the MCC gene (rs11283943) is significantly associated with increased risk of breast cancer [28]. Although an inactivating *MCC* mutation in mice alone failed to induce any evident CRCs, the homozygous mice displayed a slightly higher proliferation rate of the epithelial crypt cells [29, 30]. Interestingly, an unbiased genetic screening of a mouse model of CRC implicated *MCC* mutation as a key event in colorectal carcinogenesis [18]. Consistent with the genetic evidence, functional studies revealed that MCC blocks cell cycle progression in NIH3T3 fibroblasts and CRCs [31, 32], inhibits cell proliferation and migration in CRCs [20, 32-34], and is required for DNA damage response in CRCs [35]. MCC appears to specifically target and negatively regulate the oncogenic NF-κB and β-catenin pathways in CRCs and hepatocellular carcinoma [20, 27, 32, 36]. Mutation studies have revealed that the N-terminal domain (130-278 aa) of MCC is required for repressing the Wnt/β-catenin signaling pathway [20] and that the PDZ-binding motif at the extreme C-terminus of MCC mediates its interaction with Scrib-Myosin IIB to regulate cytoskeletal reorganization and cell migration in CRCs [34]. Collectively, the above genetic and functional evidence indicates that *MCC* functions as a tumor suppressor gene in CRCs by inhibiting cycle cell progression and migration, and by promoting DNA damage-induced cell cycle arrest in colorectal epithelial cells.

It has been shown that during development, MCC is expressed in diverse tissues derived from all three embryonic germ layers, including the developing gut and central nervous system [29]. In adults, MCC is expressed in the surface epithelium of the colon and villi of the small intestines as well as other tissues, including the cerebellar cortex, kidney, pancreas, and liver [31, 37]. However, expression of MCC was not reported in

lymphocytes, and the function of MCC in lymphocytes or lymphomas has not been explored. In the present study, we aimed to address this gap in knowledge.

Our unexpected finding that *MCC* was strikingly up-regulated in TRAF3$^{-/-}$ mouse B lymphomas prompted us to further examine *MCC* expression in human B cell neoplasms. Our results demonstrated high levels of aberrant *MCC* expression in 6 human patient-derived MM cell lines with TRAF3 deletions or relevant mutations. We also surveyed the public gene expression database of microarray data of human cancers (http://www.oncomine.org), and learned that *MCC* was also aberrantly and significantly elevated in a variety of primary human B cell malignancies. These include primary effusion lymphoma (PEL), centroblastic lymphoma (CBL), diffuse large B-cell lymphoma (DLBCL), Burkitt's lymphoma (BL), and MM [38-41]. However, expression of the transcript and protein of MCC was not detected in wild type B cells or premalignant TRAF3$^{-/-}$ B cells, even after treatment with a variety of B cell stimuli, including CD40, BCR, LPS, and CpG. These results suggest that aberrant MCC expression is associated specifically with B cell tumorigenesis. We next investigated the functions of MCC in malignant B cell survival and proliferation, and found that lentiviral shRNA vector-mediated knockdown of MCC induced apoptosis and inhibited proliferation in human patient-derived MM cell lines. Furthermore, we identified MCC signaling pathways and interacting partners in malignant B cells. Our results thus provide novel mechanistic insights into how MCC promotes malignant B cell survival and proliferation. Taken together, our findings indicate that in sharp contrast to its tumor suppressive function in CRCs and other human carcinomas, MCC is oncogenic in B lymphocytes.

Results

Transcriptome microarray analysis of TRAF3$^{-/-}$ mouse B lymphomas

TRAF3$^{-/-}$ B cells purified from young B-TRAF3$^{-/-}$ mice exhibit prolonged survival but do not proliferate autonomously [12], and therefore are premalignant B cells. Consistent with this, no B lymphoma development was observed in B-TRAF3$^{-/-}$ mice younger than 9 month old [13]. The long latency of B lymphoma development observed in B-TRAF3$^{-/-}$ mice suggests that TRAF3 inactivation and its downstream signaling pathways are not sufficient and that additional oncogenic alterations are required to induce B lymphomagenesis. To identify such secondary oncogenic alterations, to provide new insights into the molecular mechanisms of B cell malignant transformation, and to discover new therapeutic targets for the treatment of B cell malignancies, we performed global gene expression profiling of TRAF3$^{-/-}$ mouse B lymphomas by transcriptome microarray analysis. We used RNA samples of 3 representative TRAF3$^{-/-}$ splenic B lymphomas (mouse ID: 6983-2, 7041-10, and 7060-8), in which B lymphomas are >70% of B cells, as assessed by FACS analysis of B cell populations and Southern blot analysis of IgH gene rearrangements [13]. Results of the microarray analysis have identified 160 up-regulated genes and 244 down-regulated genes in TRAF3$^{-/-}$ B lymphomas as compared to LMC spleens (cut-off fold of changes: 2-fold up or down, $p < 0.05$; Supplementary Table 1) (NCBI GEO accession number: GSE48818). Selective examples of these identified genes are shown in the heatmap (Fig. 1A). Functional clustering and pathway analyses by Ingenuity (http://www.ingenuity.com) revealed that genes differentially expressed in TRAF3$^{-/-}$ B lymphomas include transcription factors, cell

surface receptors, enzymes, cell cycle regulators, protein translation regulators, lipid metabolism regulators, and novel genes with unknown functions.

From the genes identified by the microarray analysis, we selected 12 genes up-regulated in TRAF3$^{-/-}$ B lymphomas for further verification by quantitative real time PCR using TaqMan gene expression assay kits. Our data verified the mRNA up-regulation of the 12 genes examined, including *Diras2*, *MCC*, *Tbc1d9*, *Ccbp2*, *Btbd14a*, *Sema7a*, *Twsg1*, *Ppap2b*, *TCF4*, *Tnfrsf19*, *Zcwpw1*, and *Abca3* (Fig. 1B). Striking up-regulation of these transcripts was verified in the three splenic B lymphoma samples used for microarray analyses (mouse ID: 6983-2, 7041-10, and 7060-8), and also confirmed in three additional splenic B lymphomas (mouse ID: 7140-7, 7140-3 and 5-5) as well as ascites from two cases (mouse ID: 7060-8 and 7140-3; Fig. 1B). Thus, up-regulation of these 12 genes is recurrent in B lymphomas spontaneously developed in different individual B-TRAF3$^{-/-}$ mice.

We next surveyed public gene expression databases of human cancers (http://www.oncomine.org) [42] and searched the literature to investigate whether the genes identified in our microarray analyses exhibit alterations in mRNA expression, DNA copy number variation, or mutations in primary human B lymphomas and other cancers. Interestingly, we found that among the up-regulated genes identified in our microarray analysis, *MCC* is most consistently up-regulated in a variety of primary human B cell malignancies, including PEL, CBL, DLBCL, BL, and MM [38-41]. It has been previously shown that *MCC* functions as a tumor suppressor gene in CRCs and hepatocellular carcinoma [20, 27, 31-35]. However, the functional roles of MCC in lymphocytes or lymphomas remain unknown. In this context, we selected to further

explore the expression and function of MCC in B lymphocytes and B cell malignancies in the present study.

Striking up-regulation of MCC in TRAF3$^{-/-}$ mouse B lymphomas but not in premalignant TRAF3$^{-/-}$ B lymphocytes

We first verified the up-regulation of *MCC* in splenic B lymphomas and ascites spontaneously developed in 8 different individual B-TRAF3$^{-/-}$ mice at the protein level using Western blot analysis (Fig. 2A). In contrast, MCC protein expression was not detected in LMC splenic B cells (Fig. 2A). We also compared the transcript expression of *MCC* in different mature B cell subsets or B cells of different developmental stages by surveying the public gene expression database of Mouse Immune Genome (http://www.immgen.org). Mature B cell subsets examined include follicular, marginal zone, germinal center, and B1 B cells, and developing B cells examined include common lymphoid progenitor, pre-pro-B, pro-B, pre-B, newly-formed B, and transitional (T1, T2 and T3) B cells. The data in Mouse Immune Genome indicate that the *MCC* transcript is barely detected in any mature B cell subsets or developing B cells of any developmental stages. It has been previously shown that the expression of MCC is gradually up-regulated during differentiation of PC12 cells induced by NGF [37]. We thus investigated the potential up-regulation of *MCC* during the proliferation, differentiation, and activation of B lymphocytes induced by a variety of B cell stimuli. We purified splenic B cells from LMC or tumor-free young B-TRAF3$^{-/-}$ mice (age: 10-12 weeks; premalignant TRAF3$^{-/-}$ splenic B cells), and then stimulated the cells with various B cell stimuli. These include agonistic anti-CD40 Abs, LPS (TLR4 agonist), B cell receptor (BCR)

crosslinking Abs, and CpG2084 (TLR9 agonist), alone or in combination. TLR4 and TLR9 were examined as a representative of plasma membrane- and endosome- localized members of the TLR family, respectively [43]. We found that the transcript of *MCC* was neither up-regulated nor detected in LMC or premalignant TRAF3$^{-/-}$ splenic B cells after treatment with any of the stimuli examined (Fig. 2B). In contrast, the expression of *Zcwpw1*, another gene identified by our microarray analysis, was robustly up-regulated in LMC or premalignant TRAF3$^{-/-}$ splenic B cells after treatment with LPS alone, LPS in combination with CD40, or CpG in combination with CD40. This indicates that expression of *Zcwpw1* is induced during the proliferation and activation of B lymphocytes. However, unlike *Zcwpw1*, the expression of *MCC* is only up-regulated and detected in TRAF3$^{-/-}$ B lymphomas, suggesting that MCC up-regulation is selectively associated with B cell malignant transformation.

We next cloned the full-length coding sequence of the MCC transcripts from primary splenic B lymphomas of 4 different individual B-TRAF3$^{-/-}$ mice (mouse ID: 6983-2, 7060-8, 105-8, and 115-6) by reverse transcription and PCR. Our sequencing results demonstrated that the *MCC* gene expressed in TRAF3$^{-/-}$ B lymphomas is predicted to encode a protein of 828 amino acids and does not contain any mutations. In an effort to understand how *MCC* is up-regulated in TRAF3$^{-/-}$ B lymphomas, we first determined the copy number of the MCC gene in primary splenic B lymphomas of 8 different individual B-TRAF3$^{-/-}$ mice using Taqman Copy Number Assay Kit. Our results revealed that the copy number of the MCC gene was not changed in TRAF3$^{-/-}$ mouse B lymphomas as compared to that observed in LMC splenocytes (Fig. 2C). We next investigated the involvement of epigenetic alterations in MCC up-regulation by performing chromatin

immunoprecipitation (ChIP) analyses. We used antibodies specific for a repressive histone mark (trimethylated Lys 27 of histone 3, H3K27Me3) and an activating histone mark (acetylated Lys 9/14 of histone 3, H3K9/14Ac), respectively. We chose to examine these two epigenetic modifications based on previous evidence that alterations of H3K27Me3 and H3K9/14Ac frequently occur in human B lymphomas and MM [44-51]. Our results showed that the activating H3K9/14 acetylation of the promoter region of the *MCC* gene was not obviously changed in TRAF3$^{-/-}$ B lymphoma cells as compared to LMC or premalignant TRAF3$^{-/-}$ splenic B cells (Fig. 2D). In contrast, the repressive H3K27 trimethylation of the *MCC* promoter region was almost completely abolished in TRAF3$^{-/-}$ B lymphoma cells, and also modestly decreased in premalignant TRAF3$^{-/-}$ splenic B cells (Fig. 2D). Such changes in H3K27 trimethylation was not observed in the promoter region of *Diras2* (Fig. 2D), another gene strikingly up-regulated in TRAF3$^{-/-}$ B lymphomas identified in our study. The trimethylation of H3K27 that is almost completely abolished in the *MCC* promoter region in TRAF3$^{-/-}$ B lymphomas is intriguing, considering that the expression levels and activity of EZH2 of the polycomb repressive complex 2 (PRC2) catalyzing H3K27Me3 are often elevated in human B lymphomas and MM [45-47]. This unexpected decrease of the repressive H3K27Me3 of the *MCC* promoter region may be caused by increased activity of the H3K27 demethylase UTX or altered recognition of the *MCC* promoter by PRC2 in TRAF3$^{-/-}$ B lymphoma cells. Altered recognition of the *MCC* promoter by PRC2 might be brought about by changes in DNA methylation of this region, accessory proteins of the PRC2 complex, or expression of EZH2-binding non-coding RNA surrounding the MCC gene locus in TRAF3$^{-/-}$ B lymphomas [47, 52-54]. Regardless of the exact mechanisms, our

results suggest that alterations in epigenetic modifications (such as H3K27Me3) of the *MCC* promoter region contribute at least partially to the up-regulation of MCC observed in TRAF3$^{-/-}$ B lymphomas.

Aberrant up-regulation of MCC in human patient-derived MM cell lines with TRAF3 deletions or relevant mutations

To confirm the clinical relevance of our study, we examined *MCC* expression in 6 human patient-derived MM cell lines with TRAF3 deletions or relevant mutations. These include: two cell lines with TRAF3 bi-allelic deletions (KMS11 and 8226), two cell lines with TRAF3 frameshift mutations (LP1 and U266), and two cell lines with cIAP1/2 bi-allelic deletions (KMS28PE and KMS20). Similar to TRAF3 inactivation, bi-allelic deletions of cIAP1/2 also lead to constitutive activation of the non-canonical NF-κB pathway, NF-κB2 (p52/RelB) [9]. We found that MCC is aberrantly up-regulated in all examined human MM cell lines at both the transcript and protein levels (Fig. 3A and 3B). Robust expression of MCC was also detected in an EBV-transformed B lymphoblastoid cell line C3688 [55], which also exhibits constitutive NF-κB2 activation. In contrast, MCC expression was not detected in normal human blood B lymphocytes. It should be noted that MM is the tumor of terminally differentiated B cells, plasma cells. By directly comparing with purified normal plasma cells, microarray analyses by Zhan *et al.* have previously identified aberrant up-regulation of the *MCC* transcript in MM patient samples [39, 40]. Similarly, microarray analyses by Basso *et al*. have demonstrated aberrant up-regulation of the *MCC* transcript in patient samples of B lymphomas (PEL, CBL, BL and DLBCL) as compared with normal B cells of different activation stages, including naive

pre-germinal center B cells, centroblasts, centrocytes, and memory B cells [38]. Together, the above evidence indicates that *MCC* is aberrantly up-regulated only in malignant B cells and neoplastic plasma cells, but not in their normal counterparts.

We then cloned the full-length coding sequence of the MCC transcripts from LP1 and KMS11 cells by reverse transcription and PCR. Sequencing results of the PCR products of MCC transcripts demonstrated that the coding cDNAs of the MCC gene cloned from human MM cells are predicted to encode a protein of 829 amino acids and contain no mutations. Our results thus demonstrated that MCC is aberrantly expressed in both mouse and human transformed B cells, but not expressed in normal B lymphocytes.

Subcellular localization of MCC and its regulation in human MM cells during ER stress responses

Subcellular localization of a protein provides important clues about its potential function. It has been previously shown that MCC is localized in the cytosol as well as in the nucleus, and is also associated with the plasma membrane and membrane organelles in epithelial cells [20, 31, 33, 37]. To elucidate where MCC exerts its roles in malignant B cells, we examined the subcellular localization of MCC using a biochemical fractionation method. To investigate whether MCC protein level is regulated in response to apoptosis induction and ER stress, we employed two ER stress inducers, DTT (a chemical that reduces disulfides to thiols and thus affects protein folding or conformation) and thapsigargin (an inhibitor of ER Ca^{2+} transport). We prepared the cytosol, microsomes (rich in ER), mitochondria and nuclei fractions from human MM cells in the absence or presence of treatment with DTT or thapsigargin. Our results

revealed that MCC protein was primarily localized in the mitochondria, but also detectable in the ER, cytosol and nucleus in human MM cells (Fig. 3C). Interestingly, we noticed that the two ER stress inducers, DTT and thapsigargin, markedly inhibited the protein levels of MCC, but did not change the subcellular localization of MCC in human MM cells (Fig. 3C). The ER stress responses induced by DTT and thapsigargin were evident as demonstrated by the cleavage of the cellular inhibitor of apoptosis, cIAP2, and the induction of apoptosis in human MM cells (Fig. 3C and data not shown). Yang *et al.* have previously shown that cIAP2 is cleaved by the mitochondrial serine protease Omi/HtrA2 during apoptosis [56]. Given the predominant mitochondrial localization of MCC, it is likely that the ER stress-induced decrease of MCC protein levels may be mediated through selective mitochondrial autophagy or proteasome-dependent degradation [57-59]. Together, our data demonstrated that MCC exhibits a primary mitochondrial localization in human MM cells, and that MCC protein levels are down-regulated by ER stress and apoptosis induction in malignant B cells. These results suggest that MCC may play a role in regulating malignant B cell survival and proliferation.

Lentiviral shRNA vector-mediated knockdown of MCC induced apoptosis and inhibited proliferation in human MM cells

Previous studies have shown that MCC blocks cell cycle progression and inhibits cell proliferation in fibroblasts and CRCs [20, 31, 32, 35]. To explore the functional roles of MCC in regulating malignant B cell survival and proliferation, we employed genetic means to manipulate the expression levels of MCC in human MM cells, including lentiviral vector-mediated overexpression and knockdown of MCC, respectively. In

contrast to the cell cycle blocking and proliferation inhibitory effects of MCC overexpression reported in fibroblasts and CRCs [20, 31, 32, 35], we found that overexpression of MCC in human MM cell line 8226 cells, which express endogenous MCC at relatively modest levels, did not affect cell cycle progression, cell proliferation, or cell survival at all (data not shown). It has been previously shown that the expression level of ectopically transfected MCC was strongly reduced in CRCs after several passages, suggesting selection against MCC expression in CRC cultures [35]. However, we observed that overexpression of MCC was maintained in human MM 8226 cells after >10 passages. Together, the results of our overexpression studies argue against a negative role for MCC in the survival or proliferation of malignant B cells.

We next screened four lentiviral shRNA vectors specific for human *MCC* using the human MM cell line LP1 cells. Cells transduced with a scrambled shRNA vector were used as control in these experiments. Our results of Western blot analysis showed that the MCC shRNA 1332 knocked down the protein levels of MCC by ~85% reduction, while the MCC shRNA 2689 decreased MCC levels by ~70% reduction in LP1 cells (Fig. 4A). We subsequently used these MCC shRNA lentiviruses to transduce human MM cell lines LP1 and KMS11 cells. We found that both MCC shRNAs 1332 and 2689 inhibited growth and induced apoptosis in human MM cells, as demonstrated by growth curve determination, trypan blue or PI staining of dead cells, and annexin V staining of apoptotic cells (Fig. 4B and 4C). Interestingly, MCC shRNA 1332 that resulted in a greater decrease in MCC protein level was also most effective at inducing apoptosis in human MM cells. In contrast, MCC shRNAs 1388 and 2284, which did not markedly knock down MCC protein level, did not drastically induce apoptosis in human MM cells

(Fig. 4). We further determined whether knockdown of MCC inhibits the proliferation of human MM cells by performing cell cycle analysis and proliferation dye labeling experiments. Results of cell cycle analysis demonstrated that transduction of MCC shRNA 1332 or 2689 resulted in a dramatic decrease in the proliferating cell population (S/G2/M phase: $2n < \text{DNA content} \leq 4n$) and an increase in the apoptotic cell population (DNA content < 2n) in human MM cells (Fig. 5A). As observed for apoptosis induction, MCC shRNA 1332 was also more potent than shRNA 2689 in decreasing the proliferating cell population of human MM cells (Fig. 5A). Our results of the proliferation dye labeling experiments further confirmed that knockdown of MCC by shRNA 1332 remarkably inhibited the proliferation of human MM cells. This was demonstrated both by the reduction of GFP+ shRNA 1332-transduced cells and by the slower dilution of the proliferation dye in shRNA 1332-transduced cells as compared to scrambled shRNA-transduced cells or untransduced cells after culture for 4 days (Fig. 5B). Taken together, our results demonstrate that MCC plays a positive role and is required for the survival and proliferation in human MM cells, indicating that MCC acts as an oncogene in B lymphocytes.

MCC signaling pathways in human MM cells

To understand the mechanisms of MCC shRNA-mediated induction of apoptosis and inhibition of proliferation in human MM cells, we investigated the involvement of known MCC targets. In light of the previous evidence that MCC specifically targets and negatively regulates the oncogenic NF-κB and β-catenin pathways in CRCs and hepatocellular carcinoma [20, 27, 32, 36], we determined the effects of MCC knockdown

on the levels of these two pathways in human MM cells, including IκBα, IκBβ, RelA, phospho-β-catenin and β-catenin [20, 27, 32, 36]. Our results showed that knockdown or overexpression of MCC did not change any of the proteins of the NF-κB and β-catenin pathways in human MM cells (Fig. 6). We further examined another known MCC target involved in DNA damage response in CRCs, phospho-histone H3 (P-HH3) [35], which is a marker of mitosis. Contrary to what was observed in CRCs [35], we found that knockdown of MCC markedly decreased the level of P-HH3 in human MM cells, confirming the proliferation-promoting function of MCC in malignant B cells.

We then measured the levels or activation of a number of regulators of cell apoptosis and proliferation, including caspases, the Bcl-2 family proteins, and cyclins. Our results demonstrated that knockdown of MCC led to activation of both caspases 8 and 3, as evidenced by their cleavage into active caspase fragments (Fig. 6). Interestingly, knockdown of MCC decreased the level of Mcl1 (an anti-apoptotic protein of the Bcl2 family), while overexpression of MCC increased the level of Mcl1 in human MM cells (Fig. 6). However, MCC knockdown or overexpression did not affect the protein levels of other members of the Bcl2 family, including Bcl-xL, Bcl2, Bim, Bad, Bid and Bik (Fig. 6). Among the cell cycle regulators examined, knockdown of MCC caused specific down-regulation of the protein levels of cyclin B1 and cyclin A, while overexpression of MCC increased the level of cyclin B1 in human MM cells (Fig. 6). Knockdown of MCC also led to specific up-regulation of the protein level of the cell cycle inhibitor p27, which was modestly down-regulated by overexpression of MCC in human MM cells (Fig. 6). In contrast, MCC knockdown did not change other cell cycle regulators examined, including cyclin D1, cyclin D2, p21, E2F1, and p53 (Fig. 6). Our findings suggest that MCC

inhibits apoptosis and induces proliferation by inhibiting cleavage of caspases 8 and 3, up-regulating Mcl1 and cyclin B1, and down-regulating p27 in human MM cells.

To further understand the mechanisms of MCC-mediated regulation of cell survival and proliferation, we sought to investigate key signaling pathways that are known to play important roles in regulating B cell survival and proliferation, including the activation of p38, ERK, JNK, Akt and c-Myc [60]. Our results showed that knockdown of MCC led to specific decreases in the phosphorylation level of ERK1/2 and the protein level of c-Myc (a downstream target of ERK), while overexpression of MCC exhibited the opposite effect in human MM cells (Fig. 6). In contrast, knockdown or overexpression of MCC did not change the activation of p38, JNK and Akt in human MM cells (Fig. 6). These results indicate that ERK-c-Myc is a key signaling pathway underlying the oncogenic roles of MCC in malignant B cells.

MCC interacting proteins in human MM cells

To gain further insights into the molecular mechanisms underlying the oncogenic roles of MCC in B cells, we set out to identify MCC interacting proteins in human MM cells. To facilitate co-immunoprecipitation studies, we constructed two lentiviral expression vectors of tagged human MCC, including pUB-FLAG-hMCC and pUB-hMCC-SBP-6xHis, which express an N-terminal FLAG tagged or a C-terminal SBP-6xHis tagged MCC, respectively. We used these vectors to transduce human patient-derived MM cell line 8226 cells, which express endogenous MCC at relatively modest levels. Our flow cytometric data demonstrated that the lentiviral transduction efficiency by pUB-FLAG-hMCC and pUB-hMCC-SBP-6xHis was > 85% in 8226 cells (data not

shown). Transduced FLAG-hMCC and hMCC-SBP-6xHis were immunoprecipitated from whole cell lysates using anti-FLAG-agarose or streptavidin-sepharose beads, respectively. We first examined a number of previously known MCC interacting proteins identified in CRCs or 293T cells, including β-catenin, Mst3, VCP, PP2A, DFFA, VHL, VDAC, scribble, and myosin IIb [20, 32-34, 61]. However, none of these proteins were detected in co-immunoprecipitates with either FLAG-MCC or MCC-SBP-6xHis in human MM cells. Thus, our findings suggest that MCC inhibits apoptosis and promotes proliferation likely through interaction with novel, previously unknown partners in malignant B cells.

To delineate the novel MCC-interactome in human MM cells, we turned to employ an unbiased strategy, affinity purification followed by mass spectrometry-based sequencing. Considering the primary mitochondrial localization of MCC in human MM cells, immunoprecipitates of hMCC-SBP-6xHis by streptavidin-sepharose beads from both whole cell lysates and purified mitochondria of 8226 cells were analyzed by high resolution LC-MS/MS, respectively. In these experiments, immunoprecipitates of FLAG-hMCC by streptavidin-sepharose beads were used as negative control. Using this strategy, we identified 365 proteins in the MCC-interactome of human MM cells: 333 MCC interacting proteins in whole cell lysates, and 207 MCC interactors in mitochondria (Fig. 7A, and Supplementary Table 2). Among these, 175 MCC interactors were identified in both whole cell lysates and purified mitochondria of human MM cells. However, only 39 (out of 365, 10.7%) proteins of our study were also previously identified as MCC interacting proteins in CRCs or 293T cell (Fig. 7A, and

Supplementary Table 2) [20, 32-34, 36, 61]. Thus, most of the proteins identified in our study are novel MCC-interacting partners.

We next performed disease association analyses using Ingenuity (http://www.ingenuity.com), and cancer is identified as the top disease associated with the MCC-interactome identified in our study. Results of Ingenuity analyses showed that 195 of the 333 (58.5%) MCC interactors in whole cell lysates and 91 of the 207 (43.96%) MCC interactors in mitochondria are associated with cancer. Functional annotation and clustering analyses by Ingenuity revealed that mitochondrial MCC interactors are mainly regulators of cell death and survival (81 of 207, 39.1%)(Fig. 7B). Similarly, MCC interactors in whole cell lysates are mainly regulators of cell death and survival (123 of 333, 36.9%) or cellular growth and proliferation (120 of 333, 36%)(Fig. 7C). Other MCC interactors include regulators of DNA replication and repair, molecular transport, and protein trafficking (Fig. 7B and 7C). Together, the MCC-interactome identified in our study is consistent with the prominent roles of MCC in promoting survival and proliferation in human MM cells (Figs. 4 and 5).

There are two isoforms of *MCC* encoding proteins that differ at their extreme N-terminus due to alternative promoter usage, isoform 1 (828 amino acids in mouse and 829 amino acids in human) and isoform 2 (1019 amino acids). The *MCC* that we cloned from LP1 cells and used to generate FLAG-hMCC and hMCC-SBP-6xHis is isoform 1 (829 aa). Interestingly, our LC-MS/MS data identified 6 unique peptides of the isoform 2 of MCC (1019 aa) in the immunoprecipitates of hMCC-SBP-6xHis in both whole cell lysates and purified mitochondria (Supplementary Fig. 1 and Supplementary Table 2).

These results demonstrate that the two isoforms of MCC form hetero-dimers or hetero-oligomers in human MM cells.

From the top 10 MCC-interactors identified in both whole cell lysates and purified mitochondria of human MM cells, we selected to further verify the interaction of MCC with two important regulators of cell survival and proliferation, PARP1 and prohibitin-2 (PHB2, Fig. 7D and 7E) [62-65], by co-immunoprecipitation and Western blot analyses. Our results confirmed the interactions of MCC with PARP1 and PHB2 in both whole cell lysates and purified mitochondria of human MM cells (Fig. 8A, and 8B). We further performed an interaction network analysis using the top 100 MCC-interactors of human MM cells (60 proteins identified in both whole cell lysates and mitochondria, 10 proteins identified in mitochondria only, and 30 proteins identified in whole cell lysates only) and the STRING analysis tool (http://www.string-db.org) [66], which builds protein interaction networks based on known and predicted protein-protein interactions. As shown in Fig. 8C, 61 proteins of the top 100 MCC-interactors form an interaction network centered upon PARP1 and PHB2. Interestingly, PARP1 and PHB2 have also been previously shown to directly or indirectly interact with and/or regulate MCC targets identified by knockdown and overexpression of MCC studies in human MM cells (Fig. 6), including ERK, c-Myc, p27, cyclin B1, Mcl-1, caspase 8, and caspase 3 [62-65]. Taken together, our findings indicate that MCC promotes cellular survival and proliferation by associating with and modulating the interaction network centered at PARP1 and PHB2 in malignant B cells.

Discussion

The late onset and long latency of lymphoma development observed in B-TRAF3$^{-/-}$ mice suggest that secondary oncogenic hits are required to promote B cell transformation. In the present study, we identified *MCC* as a gene strikingly up-regulated in TRAF3$^{-/-}$ mouse B lymphomas and human MM cell lines. Aberrant expression of *MCC* has also been documented in primary human B cell malignancies, including PEL, CBL, DLBCL, BL, and MM [38-41]. In contrast, *MCC* expression was not detected in normal or premalignant TRAF3$^{-/-}$ B cells even after treatment with B cell stimuli, suggesting that aberrant expression of *MCC* is specifically associated with malignant transformation of B cells. In elucidating the function of MCC in malignant B cells, we found that lentiviral shRNA-mediated knockdown of MCC induced apoptosis and inhibited proliferation in human MM cells. Experiments of knockdown and overexpression of MCC allowed us to identify downstream targets of MCC in human MM cells, including ERK, c-Myc, p27, cyclin B1, Mcl-1, caspase 8, and caspase 3. Furthermore, we delineated the profile of proteins assembled in the MCC signaling complex in whole cells or mitochondria by employing affinity purification followed by mass spectrometry-based sequencing. Our results indicate that MCC associates with the interaction network centered upon PARP1 and PHB2 to promote cellular survival and proliferation in malignant B cells. Collectively, our findings indicate that MCC functions as an oncogene in B cells.

Paradoxically, in contrary to the up-regulation of *MCC* in B cell neoplasms, the *MCC* gene is frequently deleted, mutated, or silenced in other human cancers, including colorectal cancer [14-17, 19, 20, 22], lung cancer [17, 23], gastric carcinoma [24],

esophageal cancer [25], and hepatocellular carcinoma [26, 27]. Functional evidence and signaling pathway studies indicate that *MCC* acts as a tumor suppressor gene by inhibiting the oncogenic NF-κB and β-catenin pathways in CRCs and hepatocellular carcinoma [20, 27, 31-36]. We also previously observed regulation of β-catenin by Sox5, another gene identified in our microarray analysis, in human MM cells [67]. However, NF-κB and β-catenin levels were not altered by knockdown or overexpression of MCC in human MM cells. Thus, MCC plays distinct roles via different signaling mechanisms in B cell malignancies versus other human cancers.

It has been shown that in CRCs, MCC mainly localizes in the cytoplasm, and is induced to shuttle into the nucleus in response to DNA damage [35]. Interestingly, we found that MCC is primarily localized at mitochondria, but also detectable in the ER, cytosol and nucleus in human MM cells. MCC does not contain any mitochondrial targeting motifs or transmembrane domains. Through delineation of the mitochondrial MCC-interactome, we identified a number of mitochondrial proteins that are associated with MCC in human MM cells, including PHB2, prohibitin (PHB), ECHA, VDAC3, ADT1, ADT2, and ADT3. All of these mitochondrial proteins are known as critical regulators of cell survival and apoptosis (http://www.ingenuity.com). Therefore, MCC is primarily localized at mitochondria to promote cellular survival by interacting with multiple mitochondrial proteins in malignant B cells.

Most proteins (326 out of 365, 89.3%) of the MCC-interactome identified in our study are novel, previously unknown MCC-interacting partners. Among these, PARP1 is the top novel MCC-interactor identified in both mitochondrial and whole cell lysates of human MM cells. PARP1, the most abundant member of the polyADP-ribose

polymerases (PARP) family, catalyzes post-translational modification of proteins by polyADP-ribosylation. This modification affects protein-protein and protein-DNA interactions. In additional to its pivotal role in DNA repair, PARP1 also critically regulates transcription, cell survival, and proliferation [62, 63]. PARP1 can act in both a pro- and anti-tumor manner depending on the context [62]. In this study, we identified PARP1 as a signaling hub of the MCC-interactome in human MM cells (Fig. 8C). PARP1 is known to interact with numerous MCC interactors identified in our study, including CDK1, MCM4, XRCC6, RFC1, CCT2, SSRP1, TOP2B, HIST1H1C, and SUPT16H (http://www.string-db.org). Interestingly, PARP1 has been shown to directly or indirectly regulate the activation or expression of multiple MCC targets identified by our knockdown and overexpression experiments, including caspase 8, ERK, c-Myc, p27, cyclin B1, and Mcl1 (Fig. 6). Indeed, PARP1 can induce the PARylation of caspase-8, thereby inactivating caspase-8 and inhibiting caspase-mediated apoptotic signaling [62]. PARP1 directly interacts with phosphorylated ERK2 to mediate cell proliferation, whereas PARP1 inhibition causes loss of ERK2 stimulation [62, 63]. PARP1 also down-regulates the expression of MKP-1, which dephosphorylates ERK [62]. Through modifications of chromatin or interactions with gene specific promoters/transcription factors, PARP1 regulates in total 3.5% of the transcriptome, including increasing the expression of c-Myc [62, 63] and repressing the expression of p27 [68]. Furthermore, PARP1 can indirectly regulate the degradation and anti-apoptotic function of Mcl1 through interaction with CDK1/cyclin B1 [69, 70]. Therefore, PARP1 is a novel MCC-interactor that plays a central role in mediating the oncogenic effects of MCC in malignant B cells.

Thirty-nine proteins of the MCC-interactome identified in our study are previously known as MCC-interacting proteins in CRCs or 293T cells. Among these, PHB2 is the top known MCC-interactor identified in both mitochondrial and whole cell lysates of human MM cells. PHB2, a ubiquitously expressed pleiotropic protein, is mainly localized in mitochondria by forming heteromeric complex with PHB, but also present in the cytosol, nucleus and plasma membrane [64, 65, 71]. PHB2 plays crucial roles in regulating mitochondrial function, cell survival, proliferation, stress response, and development [64, 65, 71]. PHB2 is expressed at higher levels in proliferating cells, including neoplastic tissues [64, 65, 71]. Silencing or abrogation of PHB2 induces apoptosis and reduces proliferation in a variety of cancer cells [64, 65, 71]. Here we identified PHB2 as another hub of the MCC interaction network in human MM cells (Fig. 8C). Previous studies have demonstrated the association between PHB2 and multiple MCC-interactors identified in our study, including PHB, CSNK1D (CK1δ), CSNK1E (CK1ε), ATP5B, NUMA1, and SLC25A6 (http://www.string-db.org) [65, 72]. PHB2 has also been shown to directly or indirectly regulate the activity or expression of multiple MCC targets identified in our study, including caspase 3, ERK, c-Myc, p27, and cyclin B1 (Fig. 6). For example, over-expression of PHB2 inhibits caspase 3 activation and cell apoptosis, whereas down-regulation of PHB2 is associated with increased caspase 3 expression and cell apoptosis [64, 65, 71]. PHB and PHB2 interact with c-Raf to induce the phosphorylation of ERK1/2 via MEK1 [65]. Through activation of ERK1/2, PHB2 may also indirectly regulate the expression levels of downstream targets of the ERK pathway, including c-Myc, p27 and cyclin B1 [65, 71, 73, 74]. The c-Myc up-regulation mediated by MCC-PHB2 or MCC-PARP1 via ERK signaling pathway in MM cells is

functionally analogous to that induced by canonical Wnt-β-catenin signal activation observed in epithelial cells [75, 76]. Thus, similar to PARP1, PHB2 and PHB are likely to play essential roles in mediating the oncogenic effects of MCC in malignant B cells.

Interestingly, preclinical evidence indicates that both PARP1 and PHB2/PHB are excellent therapeutic targets in cancer [62, 65]. In preclinical studies, PARP inhibitors (such as olaparib) exhibit potent tumoricidal activities on breast cancer, ovarian cancer, pancreatic cancer, prostate cancer, Ewing's sarcoma, small cell lung carcinoma, and neuroblastoma, among others. The therapeutic effects of olaparib on BRCA-mutated breast cancer have been confirmed in early phase clinical trials with only mild adverse side effects [62]. Notably, PHB ligands (such as flavaglines and capsaicin) display robust cytotoxicity on cancer cells, but have cytoprotective activities on normal cells (e.g. neurons and cardiomyocytes), particularly against oxidative stress [65]. PHB and PHB2 were recently identified as the direct targets of flavaglines (e.g., rocaglamide, rocaglaol and silvestrol), natural products isolated from medicinal plants that show significant anticancer effects but no sign of toxicity in mice [65]. Capsaicin, a component of hot chili peppers, binds to PHB2, and this binding induces apoptosis in human myeloid leukemia cells [65]. Both flavaglines and capsaicin regulate subcellular localization of PHB2 [77-79]. Flavaglines specifically inhibit PHB1/2-c-Raf interaction and prevent PHB1/2-c-Raf membrane localization [79], while capsaicin induces the translocation of PHB2 from mitochondria to the nucleus [77, 78]. Such specific targeting mechanisms of PHB ligands suggest that they may exert robust synergistic effects with conventional chemotherapies that target different signaling pathways, including DNA damage response, proteasome, the Bcl-2 family, and NF-κB activation. In this regard, flavaglines have been shown to

enhance the efficacy of doxorubicin in mouse lymphoma models [65]. Therefore, identification of PARP1 and PHB2/PHB as hubs of the signaling pathways of MCC in human MM cells implicates potential use of PARP inhibitors and PHB ligands in the treatment of B cell malignancies involving aberrant expression of MCC.

Conclusions

In the present study, we have identified MCC as a novel oncogene in B lymphocytes and provided insights into its signaling mechanisms in human MM cells. In the unique cellular context of malignant B cells, MCC forms an interaction network centered at PARP1 and PHB2 to promote cellular survival and proliferation by up-regulating ERK activation, c-Myc, Mcl1, and cyclin B1, and by down-regulating p27 and suppressing cleavage of caspases 8 and 3. The lack of expression of MCC in normal or premalignant B cells but ubiquitous up-regulation of MCC in primary human B cell malignances suggests that MCC may be a useful diagnostic marker for B cell neoplasms. Our finding that knockdown of MCC induced apoptosis and inhibited proliferation in human MM cells suggests that MCC may also serve as a therapeutic target in B cell malignancies. Furthermore, the central role of PARP1 and PHB2 in the MCC interaction network of human MM cells implies that PARP1 inhibitors and PHB ligands may have therapeutic application in B cell neoplasms, including NHL and MM.

Methods

Mice, cell lines, and reagents

Mice and disease monitoring were as previously described [12, 13]. Human patient-derived MM cell lines were generously provided by Dr. Leif Bergsagel (Mayo Clinic,

Scottsdale, AZ), including 8226, KMS11, LP1, U266, KMS28PE, and KMS20. The EBV-transformed human B lymphoblastoid cell line C3688 was provided by Dr. Lori Covey (Rutgers University, Piscataway, NJ). All human B cell lines were cultured as described [80]. Most antibodies and reagents used in this study were as previously described [13, 67, 80]. Mouse monoclonal Abs to MCC were purchased from Santa Cruz Biotechnology (Santa Cruz, CA). DTT, thapsigargin, and lentiviral shRNA constructs for human MCC were purchased from Sigma-Aldrich Corp. (St. Louis, MO). The plasmid pENTR1A-NTAP-A containing the SBP tag sequence was purchased from Addgene (Cambridge, MA). PARP1 Abs were from eBioscience (San Diego, CA), and PHB2 Abs were purchased from Bethyl Laboratories Inc (Montgomery, TX). Additional polyclonal rabbit Abs were from Cell Signaling Technology (Beverly, MA).

Transcriptome microarray analysis

Total RNA was extracted from splenocytes of LMC (mouse ID: 6983-6, 7041-9, and 7060-5) and tumor-bearing B-TRAF3$^{-/-}$ mice (mouse ID: 6983-2, 7041-10, and 7060-8) using TRIzol reagent (Invitrogen, Carlsbad, CA) following the manufacturer's instructions. RNA quality was assessed on an RNA Nano Chip using an Agilent 2100 Bioanalyzer (Agilent Technologies, Palo Alto, CA). The mRNA was amplified with a TotalPrep RNA amplification kit with a T7-oligo(dT) primer according to the manufacturer's instructions (Ambion), and microarray analysis was carried out with the Illumina Sentrix MouseRef-8 24K Array at the Burnham Institute (La Jolla, CA). Results were extracted with Illumina GenomeStudio v2011.1, background corrected and variance stabilized in R/Bioconductor using the lumi package [81, 82] and modeled in the limma package [83]. Microarray data are available from NIH GEO Accession GSE48818.

Taqman assays of the transcript expression of identified genes

Complementary DNA (cDNA) was prepared from RNA using High Capacity cDNA Reverse Transcription Kit (Applied Biosystems, Carlsbad, CA). Quantitative real-time PCR of specific genes was performed using corresponding TaqMan Gene Assay kit (Applied Biosystems) as previously described [84]. Briefly, real-time PCR was performed using TaqMan primers and probes (FAM-labeled) specific for mouse *MCC, Diras2, Tbc1d9, Ccbp2, Btbd14a, Sema7a, Twsg1, Ppap2b, TCF4, Tnfrsf19, Zcwpw1, Abca3*, or human *MCC*. Each reaction also included the probe (VIC-labeled) and primers for mouse or human β-actin mRNA, which served as an endogenous control. Relative mRNA expression levels of each gene were analyzed using the Sequencing Detection Software (Applied Biosystems) and the comparative Ct method (ΔΔCt) as previously described [84].

Splenic B cell purification and stimulation

Splenic B cells were purified using anti-mouse CD43-coated magnetic beads and a MACS separator (Miltenyi Biotec Inc.) following the manufacturer's protocols as previously described [12, 84]. The purity of isolated populations was monitored by FACS analysis, and cell preparations of >95% purity were used for protein extraction. Purified B cells were cultured *ex vivo* in the absence or presence of B cell stimuli for 6, 24 or 48 hours as described previously [12, 84]. B cell stimuli examined include 2 μg/ml anti-CD40, 20 μg/ml LPS, 1 μg/ml anti-BCR, and 100 nM CpG2084, alone or in combination. Total cellular RNA was prepared at 6 or 24 hours after stimulation.

Taqman copy number assay of the mouse MCC gene

Genomic DNA was prepared from splenocytes of LMC and tumor-bearing B-TRAF3$^{-/-}$ mice as previously described [13]. Quantitative real-time PCR of the mouse MCC gene was performed using the TaqMan Copy Number Assay kit (assay ID: Mm00490037_cn; Applied Biosystems) following the manufacturer's protocols. Briefly, real-time PCR was performed using the TaqMan primers and probe (FAM-labeled) specific for the mouse MCC gene. Each reaction also included the probe (VIC-labeled) and primers specific for the mouse Trfc gene (TaqMan Copy Number Reference Assay, Applied Biosystems), which served as reference control. Relative copy numbers of the MCC gene in genomic DNA samples were analyzed using the Sequencing Detection Software (Applied Biosystems) and the comparative Ct method (ΔΔCt) following the manufacturer's protocols.

Chromatin immunoprecipitation assay

Chromatin immunoprecipitation (ChIP) assays were performed essentially as described previously [85, 86]. Briefly, 20 x 10^6 cell equivalents of fragmented chromatins (containing DNA fragments < 400 bp) were immunoprecipitated with Ig isotype control or antibodies specific for histone modifications. We used the following histone antibodies in the ChIP experiments: H3K27me3 (Millipore, Billerica, MA) and H3K9/14ac (Diagenode, Denville, NJ). Immunoprecipitated DNA were purified, and then analyzed by quantitative real time PCR using primers specific for the promoter region of the mouse *MCC* or *Diras2* gene. Primer used are: mMCC-U519F (5'- CAG GGA GGT TGG AGA GGA -3') and mMCC-U446R (5'- AAA CAT GCC CTG CCC TTG -3'); mDiras2-U559F (5'- GCA CAT GTG ACT ACT ATT G -3') and mDiras2-U480R (5'- AAT CTC

TCC TCC CAC AAG -3'). The enrichments of each gene promoter immunoprecipitated by histone marks were quantitated relative to the input DNA [86].

Cloning of the full-length cDNA of the *MCC* gene from TRAF3$^{-/-}$ mouse B lymphomas and human MM cell lines

Total cellular RNA was prepared from B lymphomas spontaneously developed in four individual B-TRAF3$^{-/-}$ mice (mouse ID: 6983-2, 7060-8, 105-8, and 115-6), and the corresponding cDNA samples were used as templates to clone the mouse MCC coding sequences using primers mMCC-F (5'- ATG AAT TCT GGA GTT GCG GTG -3') and mMCC-R (5'- TTA GAG TGA CGT TTC GTT GGT G -3'). Similarly, human MCC coding sequences were cloned from human MM cell lines LP1 and KMS11 cells using reverse transcription PCR. Primers used for the cloning of human MCC are hMCC-F (5'- TGC ATC ATG AAT TCC GGA GT -3'), and hMCC-R (5'- TTA AAG CGA AGT TTC ATT GGT GTG -3'). The high fidelity polymerase Pfu UltraII (Santa Clara, CA) was used in these PCR reactions. Sequences of the cloned mouse and human MCC were determined at GenScript (Piscataway, NJ).

Generation of lentiviral MCC expression and shRNA vectors

The coding cDNA sequence of *MCC* cloned from the human MM cell line LP1 cells was subcloned into the lentiviral expression vector pUB-eGFP-Thy1.1 [87] (generously provided by Dr. Zhibin Chen, the University of Miami, Miami, FL) by replacing the eGFP coding sequence with the MCC coding sequence. To facilitate immunoprecipitation experiments, we engineered an N-terminal FLAG tag or a C-terminal SBP-6xHis tag [88] in frame with the MCC coding sequence, respectively. We subsequently generated two lentiviral expression vectors of tagged hMCC, including

pUB-FLAG-hMCC and pUB-hMCC-SBP-6xHis. Lentiviral shRNA vectors specific for human *MCC* (including hMCC shRNA 1332, 1388, 2284 and 2689; all in Torc1 vectors) or a scrambled shRNA vector were purchased from Sigma. To facilitate FACS analysis and cell sorting, we engineered an eGFP-expressing version of all the shRNA vectors by replacing the puromycin resistance gene of Torc1 with the eGFP coding sequence. Each lentiviral expression or shRNA vector was verified by DNA sequencing.

Lentiviral packaging and transduction of human MM cells

Lentiviruses of MCC shRNA vectors and a scrambled shRNA vector were packaged following the manufacturer's protocol (Sigma) as previously described [13, 89]. Lentiviruses of MCC expression vectors were packaged and titered as previously described [67, 80, 87]. Human MM cells were transduced with the packaged lentiviruses at a MOI of 1:5 (cell:virus) in the presence of 8 μg/ml polybrene [13, 87, 89]. Transduction efficiency of cells was analyzed by flow cytometry on day 3 post transduction. All shRNA vectors contain an eGFP expression cassette, and were directly analyzed using a flow cytometer. All pUB lentiviral expression vectors have an expression cassette of the marker Thy1.1, and thus allow the transduced cells to be analyzed by Thy1.1 immunofluorescence staining followed by flow cytometry. Transduced cells were subsequently sorted or directly analyzed for apoptosis, cell cycle distribution, proliferation, and protein expression.

Growth curve determination, annexin V staining of apoptotic cells, cell cycle distribution, and cell proliferation analyses

For MCC knockdown studies, on day 4 post-transduction, successfully transduced cells were sorted for GFP+ shRNA expressing populations, and then plated in 6-well

plates for growth curve determination, annexin V staining, or cell cycle analysis. For growth curve determination, live and dead cells were differentiated using trypan blue staining, and counted using a hemacytometer. For analysis of apoptosis, cells were stained with annexin V and PI according to the manufacturer's protocol (Invitrogen), and analyzed by flow cytometry as previously described [13]. For cell cycle analysis, cells were fixed with ice-cold 70% ethanol. Cell cycle distribution was subsequently determined by propidium iodide (PI) staining followed by flow cytometry as previously described [12, 90]. For cell proliferation analysis, cells were labeled with a cell proliferation dye eFluor® 670 (eBioscience) and dilution of the proliferation dye was analyzed by flow cytometry following the manufacturer's protocol.

Total protein lysates, fractionation of cytosol, mitochondria and microsomes (rich in ER), and immunoblot analysis

For total protein lysates, cell pellets were lysed in 200 μl of 2X SDS sample buffer (0.0625 M Tris, pH6.8, 1% SDS, 15% glycerol, 2% β-mercaptoethanol and 0.005% bromophenol blue), sonicated for 30 pulses, and boiled for 10 minutes.

For biochemical fractionation, human MM cells (30×10^6 cells/condition) were cultured in the absence or presence of 250 μM DTT or 0.5 μM thapsigargin for 24 hours. Cytosol, mitochondria and microsomes (rich in ER) were fractionated from cells as previously described [91-93]. Briefly, cells were washed with ice-cold PBS, swelled in 700 μl of Mitochondria Isolation Buffer (250 mM sucrose, 10 mM HEPES, pH7.5, 10 mM KCl, 1 mM EDTA, and 0.1 mM EGTA with protease and phosphatase inhibitors) on ice for 10 minutes, and then homogenized in a Dounce homogenizer. Cell lysis was checked by trypan blue uptake, and homogenization stopped when 90% of cells were

broken. Nuclei were pelleted by centrifugation at 1,000 g for 10 minutes at 4^{o}C. The cleared lysates were then centrifuged at 10,000g for 25 minutes at 4°C to obtain the pellets of mitochondria. The supernatants were further centrifuged at 100,000 g for 2 hours to separate the pellets of microsomes (rich in ER) from cytosolic proteins (S100 fraction). One-fifth volume of 5X SDS sample buffer was added into each S100 fraction. The pellets of nuclei, mitochondria and microsomes (rich in ER) were lysed and sonicated in 300 μl of 2X SDS sample buffer, respectively. All protein samples were subsequently boiled for 10 minutes.

Total protein lysates, or cytosolic, ER, mitochondrial and nuclear proteins were separated by SDS-PAGE. Immunoblot analyses were performed using specific antibodies as previously described [67, 80]. Images of immunoblots were acquired using a low-light imaging system (LAS-4000 mini, FUJIFILM Medical Systems USA, Inc., Stamford, CT).

Co-immunoprecipitation assay in whole cell lysates

Human MM cell line 8226 cells (5 x 10^7 cells/condition) transduced with pUB-FLAG-hMCC or pUB-hMCC-SBP-6xHis were lysed and sonicated in the CHAPS lysis buffer [94] (1% CHAPS, 20 mM Tris, pH 7.4, 150 mM NaCl, 50 mM β-glycerophosphate, and 5% glycerol with freshly added 1 mM DTT and EDTA-free Mini-complete protease inhibitor cocktail). The insoluble pellets were removed by centrifugation at 10,000g for 20 minutes at 4°C. The CHAPS lysates were subsequently immunoprecipitated with anti-FLAG-agarose beads (Sigma; for FLAG-hMCC), or streptavidin-sepharose beads (Pierce, Rockford, IL; for hMCC-SBP-6xHis), separately. Immunoprecipitates were washed 5 times with the Wash Buffer (0.5% CHAPS, 20 mM

Tris, pH 7.4, 150 mM NaCl, 50 mM β-glycerophosphate, and 2.5% glycerol with freshly added 1 mM DTT and EDTA-free Mini-complete protease inhibitor cocktail). Immunoprecipitated proteins were resuspended in 2x SDS sample buffer, boiled for 10 minutes, and then separated on SDS-PAGE for mass spectrometry or immunoblot analyses.

Co-immunoprecipitation assay in mitochondrial lysates

Human MM cell line 8226 cells (1.5×10^8 cells/condition) transduced with pUB-FLAG-hMCC or pUB-hMCC-SBP-6xHis were used for cytosol, mitochondria and ER fractionation as described above. Mitochondrial pellets were lysed and sonicated in the CHAPS lysis buffer [94], and cleared by centrifugation at 10,000g for 20 minutes at 4°C. The mitochondrial lysates were subsequently immunoprecipitated with streptavidin-sepharose beads (Pierce, Rockford, IL; for hMCC-SBP-6xHis). Immunoprecipitates were washed 5 times with the Wash Buffer, resuspended in 2x SDS sample buffer, boiled for 10 minutes, and then separated on SDS-PAGE for mass spectrometry or immunoblot analyses.

Mass spectrometry based-sequencing

Whole cell lysates or mitochondrial lysates immunoprecipitated with streptavidin-sepharose beads were used for LC-MS/MS. The entire gel lanes for hMCC-SBP-6xHis complex and negative control (FLAG-hMCC) were each sectioned into 15 continuous slices. The gel slice samples were subjected to thiol reduction by TCEP, alkylation with iodoacetamide, and digestion with sequencing-grade modified trypsin [95, 96]. Peptides were eluted from the gel slices, desalted, and then subjected to reversed-phase nano-flow ultra high performance capillary liquid chromatography (uPLC) followed by high-

resolution/high-mass accuracy MS/MS analysis using an LC-MS platform consisting of an Eksigent Nano Ultra 2D Plus uPLC system hyphenated to a Thermo Orbi Velos mass spectrometer. The MS/MS was set to operate in data dependent acquisition mode using a duty cycle in which the top 15 most abundant peptide ions in the full scan MS were targeted for MS/MS sequencing. Full scan MS1 spectra were acquired at 100,000 resolving power and maintained mass calibration to within 2-3 ppm mass accuracy. LC-MS/MS data were searched against the human IPI and UniProt databases using the Mascot and Proteome Discoverer search engines [95, 96]. Protein assignments were considered highly confident using a stringent false discovery rate threshold of <1%, as estimated by reversed database searching, and requiring that ≥2 peptides per protein be unambiguously identified. Rough relative protein amounts were estimated using spectra counting values.

Statistics

Statistical analyses were performed using the Prism software (GraphPad, La Jolla, CA). Statistical significance was assessed by Student *t* test. *P* values less than 0.05 are considered significant.

List of abbreviations used:

MCC: mutated in colorectal cancer

TRAF3: tumor necrosis factor receptor (TNF-R)-associated factor 3

B-TRAF3$^{-/-}$: B cell-specific TRAF3-deficient

NHL: non-Hodgkin lymphoma

MM: multiple myeloma

MZL: splenic marginal zone lymphoma

B-CLL: B cell chronic lymphocytic leukemia

MCL: mantle cell lymphoma

WM: Waldenström's macroglobulinemia

LOH: loss of heterozygosity

FAP: familial adenomatous polyposis

CRCs: colorectal cancers

PEL: primary effusion lymphoma

CBL: centroblastic lymphoma

DLBCL: diffuse large B-cell lymphoma

BL: Burkitt's lymphoma

NF-κB: nuclear factor κ light chain enhancer of activated B cells

BCR: B cell receptor

LPS: lipopolysaccharides

shRNA: short hairpin RNA

ChIP: chromatin immunoprecipitation

H3K27Me3: trimethylated lysine 27 of histone 3

H3K9/14Ac: acetylated lysine 9/14 of histone 3

DTT: dithiothreitol

ERK: extracellular signal-regulated kinase

JNK: c-Jun N-terminal kinase

SBP: streptavidin-binding peptide

SA: streptavidin

LC-MS/MS: liquid chromatography-mass spectrometry/mass spectrometry

uPLC: high performance capillary liquid chromatography

PARP1: Poly [ADP-ribose] polymerase 1

PHB2: prohibitin-2

PHB: prohibitin

PI: propidium iodide

FACS: fluorescence-activated cell sorting

PCR: polymerase chain reaction

Competing interests

The authors declare that they have no potential conflicts of interest.

Authors' contributions:

SE designed and performed experiments, analyzed data, and wrote the manuscript; JB, CM and YL carried out experiments, analyzed data, and revised the manuscript; DP performed LC-MS/MS sequencing, analyzed data, and revised the manuscript; RH analyzed microarray data and revised the manuscript; PX supervised and designed this study, analyzed data, and wrote the manuscript. All authors read and approved this manuscript.

Acknowledgements

This study was supported by the National Institutes of Health grant CA158402 (P. Xie), the Department of Defense grant W81XWH-13-1-0242 (P. Xie), a Faculty Research Grant (P. Xie), and in part by a grant from NCI (1RC1CA147187, to R. Hart) and an Aresty Research Grant (J. Baron). The FACS analyses described in this paper were supported by the Flow Cytometry Core Facility of the Cancer Institute of New Jersey (P30CA072720).

We would like to express our gratitude to Dr. P. Leif Bergsagel for providing us the human multiple myeloma cell lines used in this study, and to Dr. Lori R. Covey for critical review of this manuscript as well as for providing C3688 cells and normal human blood B cells for our study. We would also like to thank Sukhdeep Grewal, Benjamin Kreider, Punit Arora, Anand Desai, and Ashima Choudhary for technical assistance on this study.

References

1. Morton LM, Wang SS, Devesa SS, Hartge P, Weisenburger DD, Linet MS: **Lymphoma incidence patterns by WHO subtype in the United States, 1992-2001**. *Blood* 2006, **107**:265-276.
2. Ruddon R: **The Epidemiology of Human Cancer**. *In Book: Cancer Biology Edited by Ruddon, RW Fourth edition Oxford University Press* 2007:Pages: 62-116.
3. Skibola CF, Curry JD, Nieters A: **Genetic susceptibility to lymphoma**. *Haematologica* 2007, **92**:960-969.
4. Peled JU, Kuang FL, Iglesias-Ussel MD, Roa S, Kalis SL, Goodman MF, Scharff MD: **The biochemistry of somatic hypermutation**. *Annu Rev Immunol* 2008, **26**:481-511.
5. Pasqualucci L, Bhagat G, Jankovic M, Compagno M, Smith P, Muramatsu M, Honjo T, Morse HC, 3rd, Nussenzweig MC, Dalla-Favera R: **AID is required for germinal center-derived lymphomagenesis**. *Nat Genet* 2008, **40**:108-112.
6. Xie P: **TRAF molecules in cell signaling and in human diseases**. *J Mol Signal* 2013, **8**:7.
7. Boucher LM, Marengere LE, Lu Y, Thukral S, Mak TW: **Binding sites of cytoplasmic effectors TRAF1, 2, and 3 on CD30 and other members of the TNF receptor superfamily**. *Biochem Biophys Res Commun* 1997, **233**:592-600.
8. Nagel I, Bug S, Tonnies H, Ammerpohl O, Richter J, Vater I, Callet-Bauchu E, Calasanz MJ, Martinez-Climent JA, Bastard C *et al*: **Biallelic inactivation of TRAF3 in a subset of B-cell lymphomas with interstitial del(14)(q24.1q32.33)**. *Leukemia* 2009, **23**:2153-2155.
9. Keats JJ, Fonseca R, Chesi M, Schop R, Baker A, Chng WJ, Van Wier S, Tiedemann R, Shi CX, Sebag M *et al*: **Promiscuous mutations activate the noncanonical NF-kappaB pathway in multiple myeloma**. *Cancer Cell* 2007, **12**:131-144.
10. Annunziata CM, Davis RE, Demchenko Y, Bellamy W, Gabrea A, Zhan F, Lenz G, Hanamura I, Wright G, Xiao W *et al*: **Frequent engagement of the classical and alternative NF-kappaB pathways by diverse genetic abnormalities in multiple myeloma**. *Cancer Cell* 2007, **12**:115-130.
11. Braggio E, Keats JJ, Leleu X, Van Wier S, Jimenez-Zepeda VH, Valdez R, Schop RF, Price-Troska T, Henderson K, Sacco A *et al*: **Identification of copy number abnormalities and inactivating mutations in two negative regulators of nuclear factor-kappaB signaling pathways in Waldenstrom's macroglobulinemia**. *Cancer Res* 2009, **69**:3579-3588.
12. Xie P, Stunz LL, Larison KD, Yang B, Bishop GA: **Tumor necrosis factor receptor-associated factor 3 is a critical regulator of B cell homeostasis in secondary lymphoid organs**. *Immunity* 2007, **27**:253-267.
13. Moore CR, Liu Y, Shao CS, Covey LR, Morse HC, 3rd,, Xie P: **Specific deletion of TRAF3 in B lymphocytes leads to B lymphoma development in mice**. *Leukemia* 2012, **26**:1122-1127.
14. Kinzler KW, Nilbert MC, Vogelstein B, Bryan TM, Levy DB, Smith KJ, Preisinger AC, Hamilton SR, Hedge P, Markham A *et al*: **Identification of a gene located at chromosome 5q21 that is mutated in colorectal cancers**. *Science* 1991, **251**:1366-1370.

15. Nishisho I, Nakamura Y, Miyoshi Y, Miki Y, Ando H, Horii A, Koyama K, Utsunomiya J, Baba S, Hedge P: **Mutations of chromosome 5q21 genes in FAP and colorectal cancer patients**. *Science* 1991, **253**:665-669.
16. Groden J, Thliveris A, Samowitz W, Carlson M, Gelbert L, Albertsen H, Joslyn G, Stevens J, Spirio L, Robertson M *et al*: **Identification and characterization of the familial adenomatous polyposis coli gene**. *Cell* 1991, **66**:589-600.
17. Ashton-Rickardt PG, Wyllie AH, Bird CC, Dunlop MG, Steel CM, Morris RG, Piris J, Romanowski P, Wood R, White R *et al*: **MCC, a candidate familial polyposis gene in 5q.21, shows frequent allele loss in colorectal and lung cancer**. *Oncogene* 1991, **6**:1881-1886.
18. Starr TK, Allaei R, Silverstein KA, Staggs RA, Sarver AL, Bergemann TL, Gupta M, O'Sullivan MG, Matise I, Dupuy AJ *et al*: **A transposon-based genetic screen in mice identifies genes altered in colorectal cancer**. *Science* 2009, **323**:1747-1750.
19. Kohonen-Corish MR, Sigglekow ND, Susanto J, Chapuis PH, Bokey EL, Dent OF, Chan C, Lin BP, Seng TJ, Laird PW *et al*: **Promoter methylation of the mutated in colorectal cancer gene is a frequent early event in colorectal cancer**. *Oncogene* 2007, **26**:4435-4441.
20. Fukuyama R, Niculaita R, Ng KP, Obusez E, Sanchez J, Kalady M, Aung PP, Casey G, Sizemore N: **Mutated in colorectal cancer, a putative tumor suppressor for serrated colorectal cancer, selectively represses beta-catenin-dependent transcription**. *Oncogene* 2008, **27**:6044-6055.
21. Fu X, Li L, Peng Y: **Wnt signalling pathway in the serrated neoplastic pathway of the colorectum: possible roles and epigenetic regulatory mechanisms**. *J Clin Pathol* 2012, **65**:675-679.
22. Li L, Fu X, Zhang W, Xiao L, Qiu Y, Peng Y, Shi L, Chen X, Zhou X, Deng M: **Wnt signaling pathway is activated in right colon serrated polyps correlating to specific molecular form of beta-catenin**. *Hum Pathol* 2013, **44**:1079-1088.
23. D'Amico D, Carbone DP, Johnson BE, Meltzer SJ, Minna JD: **Polymorphic sites within the MCC and APC loci reveal very frequent loss of heterozygosity in human small cell lung cancer**. *Cancer Res* 1992, **52**:1996-1999.
24. Sud R, Talbot IC, Delhanty JD: **Infrequent alterations of the APC and MCC genes in gastric cancers from British patients**. *Br J Cancer* 1996, **74**:1104-1108.
25. Huang Y, Boynton RF, Blount PL, Silverstein RJ, Yin J, Tong Y, McDaniel TK, Newkirk C, Resau JH, Sridhara R *et al*: **Loss of heterozygosity involves multiple tumor suppressor genes in human esophageal cancers**. *Cancer Res* 1992, **52**:6525-6530.
26. Guichard C, Amaddeo G, Imbeaud S, Ladeiro Y, Pelletier L, Maad IB, Calderaro J, Bioulac-Sage P, Letexier M, Degos F *et al*: **Integrated analysis of somatic mutations and focal copy-number changes identifies key genes and pathways in hepatocellular carcinoma**. *Nat Genet* 2012, **44**:694-698.
27. Shukla R, Upton KR, Munoz-Lopez M, Gerhardt DJ, Fisher ME, Nguyen T, Brennan PM, Baillie JK, Collino A, Ghisletti S *et al*: **Endogenous retrotransposition activates oncogenic pathways in hepatocellular carcinoma**. *Cell* 2013, **153**:101-111.

28. Mukherjee N, Bhattacharya N, Sinha S, Alam N, Chakravarti R, Roychoudhury S, Panda CK: **Association of APC and MCC polymorphisms with increased breast cancer risk in an Indian population**. *Int J Biol Markers* 2011, **26**:43-49.
29. Young T, Poobalan Y, Ali Y, Siew Tein W, Sadasivam A, Ee Kim T, Erica Tay P, Dunn NR: **Mutated in colorectal cancer (Mcc), a candidate tumor suppressor, is dynamically expressed during mouse embryogenesis**. *Dev Dyn* 2011, **240**:2166-2174.
30. Heyer J, Yang K, Lipkin M, Edelmann W, Kucherlapati R: **Mouse models for colorectal cancer**. *Oncogene* 1999, **18**:5325-5333.
31. Matsumine A, Senda T, Baeg GH, Roy BC, Nakamura Y, Noda M, Toyoshima K, Akiyama T: **MCC, a cytoplasmic protein that blocks cell cycle progression from the G0/G1 to S phase**. *J Biol Chem* 1996, **271**:10341-10346.
32. Sigglekow ND, Pangon L, Brummer T, Molloy M, Hawkins NJ, Ward RL, Musgrove EA, Kohonen-Corish MR: **Mutated in colorectal cancer protein modulates the NFkappaB pathway**. *Anticancer Res* 2012, **32**:73-79.
33. Arnaud C, Sebbagh M, Nola S, Audebert S, Bidaut G, Hermant A, Gayet O, Dusetti NJ, Ollendorff V, Santoni MJ *et al*: **MCC, a new interacting protein for Scrib, is required for cell migration in epithelial cells**. *FEBS Lett* 2009, **583**:2326-2332.
34. Pangon L, Van Kralingen C, Abas M, Daly RJ, Musgrove EA, Kohonen-Corish MR: **The PDZ-binding motif of MCC is phosphorylated at position -1 and controls lamellipodia formation in colon epithelial cells**. *Biochim Biophys Acta* 2012, **1823**:1058-1067.
35. Pangon L, Sigglekow ND, Larance M, Al-Sohaily S, Mladenova DN, Selinger CI, Musgrove EA, Kohonen-Corish MR: **The "Mutated in Colorectal Cancer" Protein Is a Novel Target of the UV-Induced DNA Damage Checkpoint**. *Genes Cancer* 2010, **1**:917-926.
36. Bouwmeester T, Bauch A, Ruffner H, Angrand PO, Bergamini G, Croughton K, Cruciat C, Eberhard D, Gagneur J, Ghidelli S *et al*: **A physical and functional map of the human TNF-alpha/NF-kappa B signal transduction pathway**. *Nat Cell Biol* 2004, **6**:97-105.
37. Senda T, Matsumine A, Yanai H, Akiyama T: **Localization of MCC (mutated in colorectal cancer) in various tissues of mice and its involvement in cell differentiation**. *J Histochem Cytochem* 1999, **47**:1149-1158.
38. Basso K, Margolin AA, Stolovitzky G, Klein U, Dalla-Favera R, Califano A: **Reverse engineering of regulatory networks in human B cells**. *Nat Genet* 2005, **37**:382-390.
39. Zhan F, Hardin J, Kordsmeier B, Bumm K, Zheng M, Tian E, Sanderson R, Yang Y, Wilson C, Zangari M *et al*: **Global gene expression profiling of multiple myeloma, monoclonal gammopathy of undetermined significance, and normal bone marrow plasma cells**. *Blood* 2002, **99**:1745-1757.
40. Zhan F, Tian E, Bumm K, Smith R, Barlogie B, Shaughnessy J, Jr.: **Gene expression profiling of human plasma cell differentiation and classification of multiple myeloma based on similarities to distinct stages of late-stage B-cell development**. *Blood* 2003, **101**:1128-1140.
41. Zhan F, Barlogie B, Arzoumanian V, Huang Y, Williams DR, Hollmig K, Pineda-Roman M, Tricot G, van Rhee F, Zangari M *et al*: **Gene-expression signature of**

benign monoclonal gammopathy evident in multiple myeloma is linked to good prognosis. *Blood* 2007, **109**:1692-1700.
42. Bric A, Miething C, Bialucha CU, Scuoppo C, Zender L, Krasnitz A, Xuan Z, Zuber J, Wigler M, Hicks J *et al*: **Functional identification of tumor-suppressor genes through an in vivo RNA interference screen in a mouse lymphoma model**. *Cancer Cell* 2009, **16**:324-335.
43. Kumar H, Kawai T, Akira S: **Toll-like receptors and innate immunity**. *Biochem Biophys Res Commun* 2009, **388**:621-625.
44. Morin RD, Johnson NA, Severson TM, Mungall AJ, An J, Goya R, Paul JE, Boyle M, Woolcock BW, Kuchenbauer F *et al*: **Somatic mutations altering EZH2 (Tyr641) in follicular and diffuse large B-cell lymphomas of germinal-center origin**. *Nat Genet* 2010, **42**:181-185.
45. McCabe MT, Ott HM, Ganji G, Korenchuk S, Thompson C, Van Aller GS, Liu Y, Graves AP, Della Pietra A, 3rd, Diaz E *et al*: **EZH2 inhibition as a therapeutic strategy for lymphoma with EZH2-activating mutations**. *Nature* 2012, **492**:108-112.
46. Kalushkova A, Fryknas M, Lemaire M, Fristedt C, Agarwal P, Eriksson M, Deleu S, Atadja P, Osterborg A, Nilsson K *et al*: **Polycomb target genes are silenced in multiple myeloma**. *PLoS One* 2010, **5**:e11483.
47. Ezponda T, Licht JD: **Molecular Pathways: Deregulation of Histone 3 Lysine 27 Methylation in Cancer-Different Paths, Same Destination**. *Clin Cancer Res* 2014.
48. Figueroa ME, Reimers M, Thompson RF, Ye K, Li Y, Selzer RR, Fridriksson J, Paietta E, Wiernik P, Green RD *et al*: **An integrative genomic and epigenomic approach for the study of transcriptional regulation**. *PLoS One* 2008, **3**:e1882.
49. Scuto A, Kirschbaum M, Kowolik C, Kretzner L, Juhasz A, Atadja P, Pullarkat V, Bhatia R, Forman S, Yen Y *et al*: **The novel histone deacetylase inhibitor, LBH589, induces expression of DNA damage response genes and apoptosis in Ph- acute lymphoblastic leukemia cells**. *Blood* 2008, **111**:5093-5100.
50. Escoubet-Lozach L, Lin IL, Jensen-Pergakes K, Brady HA, Gandhi AK, Schafer PH, Muller GW, Worland PJ, Chan KW, Verhelle D: **Pomalidomide and lenalidomide induce p21 WAF-1 expression in both lymphoma and multiple myeloma through a LSD1-mediated epigenetic mechanism**. *Cancer Res* 2009, **69**:7347-7356.
51. Krejci J, Harnicarova A, Streitova D, Hajek R, Pour L, Kozubek S, Bartova E: **Epigenetics of multiple myeloma after treatment with cytostatics and gamma radiation**. *Leuk Res* 2009, **33**:1490-1498.
52. Zhao X, Zhang W, Wang L, Zhao WL: **Genetic methylation and lymphoid malignancies: biomarkers of tumor progression and targeted therapy**. *Biomark Res* 2013, **1**:24.
53. Goff LA, Rinn JL: **Poly-combing the genome for RNA**. *Nat Struct Mol Biol* 2013, **20**:1344-1346.
54. da Rocha ST, Boeva V, Escamilla-Del-Arenal M, Ancelin K, Granier C, Matias NR, Sanulli S, Chow J, Schulz E, Picard C *et al*: **Jarid2 Is Implicated in the Initial Xist-Induced Targeting of PRC2 to the Inactive X Chromosome**. *Mol Cell* 2014, **53**:301-316.

55. Lu KT, Dryer RL, Song C, Covey LR: **Maintenance of the CD40-related immunodeficient response in hyper-IgM B cells immortalized with a LMP1-regulated mini-EBV**. *J Leukoc Biol* 2005, **78**:620-629.
56. Yang QH, Church-Hajduk R, Ren J, Newton ML, Du C: **Omi/HtrA2 catalytic cleavage of inhibitor of apoptosis (IAP) irreversibly inactivates IAPs and facilitates caspase activity in apoptosis**. *Genes Dev* 2003, **17**:1487-1496.
57. Ciechanover A: **Intracellular protein degradation: from a vague idea through the lysosome and the ubiquitin-proteasome system and onto human diseases and drug targeting**. *Bioorg Med Chem* 2013, **21**:3400-3410.
58. Flick K, Kaiser P: **Protein degradation and the stress response**. *Semin Cell Dev Biol* 2012, **23**:515-522.
59. Klionsky DJ, Schulman BA: **Dynamic regulation of macroautophagy by distinctive ubiquitin-like proteins**. *Nat Struct Mol Biol* 2014, **21**:336-345.
60. Smith SM, Anastasi J, Cohen KS, Godley LA: **The impact of MYC expression in lymphoma biology: beyond Burkitt lymphoma**. *Blood Cells Mol Dis* 2010, **45**:317-323.
61. Ewing RM, Chu P, Elisma F, Li H, Taylor P, Climie S, McBroom-Cerajewski L, Robinson MD, O'Connor L, Li M *et al*: **Large-scale mapping of human protein-protein interactions by mass spectrometry**. *Mol Syst Biol* 2007, **3**:89.
62. Weaver AN, Yang ES: **Beyond DNA Repair: Additional Functions of PARP-1 in Cancer**. *Front Oncol* 2013, **3**:290.
63. Cohen-Armon M: **PARP-1 activation in the ERK signaling pathway**. *Trends Pharmacol Sci* 2007, **28**:556-560.
64. Artal-Sanz M, Tavernarakis N: **Prohibitin and mitochondrial biology**. *Trends Endocrinol Metab* 2009, **20**:394-401.
65. Thuaud F, Ribeiro N, Nebigil CG, Desaubry L: **Prohibitin ligands in cell death and survival: mode of action and therapeutic potential**. *Chem Biol* 2013, **20**:316-331.
66. Szklarczyk D, Franceschini A, Kuhn M, Simonovic M, Roth A, Minguez P, Doerks T, Stark M, Muller J, Bork P *et al*: **The STRING database in 2011: functional interaction networks of proteins, globally integrated and scored**. *Nucleic Acids Res* 2011, **39**:D561-568.
67. Edwards SK, Desai A, Liu Y, Moore CR, Xie P: **Expression and function of a novel isoform of Sox5 in malignant B cells**. *Leuk Res* 2014, **38**:393-401.
68. Sakamaki J, Daitoku H, Yoshimochi K, Miwa M, Fukamizu A: **Regulation of FOXO1-mediated transcription and cell proliferation by PARP-1**. *Biochem Biophys Res Commun* 2009, **382**:497-502.
69. Harley ME, Allan LA, Sanderson HS, Clarke PR: **Phosphorylation of Mcl-1 by CDK1-cyclin B1 initiates its Cdc20-dependent destruction during mitotic arrest**. *EMBO J* 2010, **29**:2407-2420.
70. Sakurikar N, Eichhorn JM, Chambers TC: **Cyclin-dependent kinase-1 (Cdk1)/cyclin B1 dictates cell fate after mitotic arrest via phosphoregulation of antiapoptotic Bcl-2 proteins**. *J Biol Chem* 2012, **287**:39193-39204.
71. Zhou TB, Qin YH: **Signaling pathways of prohibitin and its role in diseases**. *J Recept Signal Transduct Res* 2013, **33**:28-36.

72. Kategaya LS, Hilliard A, Zhang L, Asara JM, Ptacek LJ, Fu YH: **Casein kinase 1 proteomics reveal prohibitin 2 function in molecular clock**. *PLoS One* 2012, **7**:e31987.
73. Marampon F, Ciccarelli C, Zani BM: **Down-regulation of c-Myc following MEK/ERK inhibition halts the expression of malignant phenotype in rhabdomyosarcoma and in non muscle-derived human tumors**. *Mol Cancer* 2006, **5**:31.
74. Dangi S, Chen FM, Shapiro P: **Activation of extracellular signal-regulated kinase (ERK) in G2 phase delays mitotic entry through p21CIP1**. *Cell Prolif* 2006, **39**:261-279.
75. Yoshida GJ, Saya H: **Inversed relationship between CD44 variant and c-Myc due to oxidative stress-induced canonical Wnt activation**. *Biochem Biophys Res Commun* 2014, **443**:622-627.
76. Willert K, Jones KA: **Wnt signaling: is the party in the nucleus?** *Genes Dev* 2006, **20**:1394-1404.
77. Kuramori C, Azuma M, Kume K, Kaneko Y, Inoue A, Yamaguchi Y, Kabe Y, Hosoya T, Kizaki M, Suematsu M *et al*: **Capsaicin binds to prohibitin 2 and displaces it from the mitochondria to the nucleus**. *Biochem Biophys Res Commun* 2009, **379**:519-525.
78. Osman C, Merkwirth C, Langer T: **Prohibitins and the functional compartmentalization of mitochondrial membranes**. *J Cell Sci* 2009, **122**:3823-3830.
79. Li-Weber M: **Molecular mechanisms and anti-cancer aspects of the medicinal phytochemicals rocaglamides (=flavaglines)**. *Int J Cancer* 2014.
80. Edwards SK, Moore CR, Liu Y, Grewal S, Covey LR, Xie P: **N-benzyladriamycin-14-valerate (AD 198) exhibits potent anti-tumor activity on TRAF3-deficient mouse B lymphoma and human multiple myeloma**. *BMC Cancer* 2013, **13**:481.
81. Du P, Kibbe WA, Lin SM: **nuID: a universal naming scheme of oligonucleotides for illumina, affymetrix, and other microarrays**. *Biol Direct* 2007, **2**:16.
82. Du P, Kibbe WA, Lin SM: **lumi: a pipeline for processing Illumina microarray**. *Bioinformatics* 2008, **24**:1547-1548.
83. Smyth G: **Limma: linear models for microarray data.**, vol. Bioinformatics and Computational Biology Solutions using R and Bioconductor. : New York: Springer; 2005.
84. Xie P, Poovassery J, Stunz LL, Smith SM, Schultz ML, Carlin LE, Bishop GA: **Enhanced Toll-like receptor (TLR) responses of TNFR-associated factor 3 (TRAF3)-deficient B lymphocytes**. *J Leukoc Biol* 2011, **90**:1149-1157.
85. Urist M, Tanaka T, Poyurovsky MV, Prives C: **p73 induction after DNA damage is regulated by checkpoint kinases Chk1 and Chk2**. *Genes Dev* 2004, **18**:3041-3054.
86. Li J, Chen J, Ricupero CL, Hart RP, Schwartz MS, Kusnecov A, Herrup K: **Nuclear accumulation of HDAC4 in ATM deficiency promotes neurodegeneration in ataxia telangiectasia**. *Nat Med* 2012, **18**:783-790.
87. Zhou S, Kurt-Jones EA, Cerny AM, Chan M, Bronson RT, Finberg RW: **MyD88 intrinsically regulates CD4 T-cell responses**. *J Virol* 2009, **83**:1625-1634.
88. Li Y, Franklin S, Zhang MJ, Vondriska TM: **Highly efficient purification of protein complexes from mammalian cells using a novel streptavidin-binding peptide and**

hexahistidine tandem tag system: application to Bruton's tyrosine kinase. *Protein Sci* 2010, **20**:140-149.
89. Porter JF, Vavassori S, Covey LR: **A polypyrimidine tract-binding protein-dependent pathway of mRNA stability initiates with CpG activation of primary B cells**. *J Immunol* 2008, **181**:3336-3345.
90. Xie P, Kraus ZJ, Stunz LL, Liu Y, Bishop GA: **TNF Receptor-Associated Factor 3 Is Required for T Cell-Mediated Immunity and TCR/CD28 Signaling**. *J Immunol* 2011, **186**:143-155.
91. Wan Q, Kuang E, Dong W, Zhou S, Xu H, Qi Y, Liu Y: **Reticulon 3 mediates Bcl-2 accumulation in mitochondria in response to endoplasmic reticulum stress**. *Apoptosis* 2007, **12**:319-328.
92. Simmen T, Aslan JE, Blagoveshchenskaya AD, Thomas L, Wan L, Xiang Y, Feliciangeli SF, Hung CH, Crump CM, Thomas G: **PACS-2 controls endoplasmic reticulum-mitochondria communication and Bid-mediated apoptosis**. *Embo J* 2005, **24**:717-729.
93. Darios F, Corti O, Lucking CB, Hampe C, Muriel MP, Abbas N, Gu WJ, Hirsch EC, Rooney T, Ruberg M *et al*: **Parkin prevents mitochondrial swelling and cytochrome c release in mitochondria-dependent cell death**. *Hum Mol Genet* 2003, **12**:517-526.
94. Vento MT, Zazzu V, Loffreda A, Cross JR, Downward J, Stoppelli MP, Iaccarino I: **Praf2 is a novel Bcl-xL/Bcl-2 interacting protein with the ability to modulate survival of cancer cells**. *PLoS One* 2011, **5**:e15636.
95. Khan Z, Amini S, Bloom JS, Ruse C, Caudy AA, Kruglyak L, Singh M, Perlman DH, Tavazoie S: **Accurate proteome-wide protein quantification from high-resolution 15N mass spectra**. *Genome Biol* 2011, **12**:R122.
96. Ying W, Perlman DH, Li L, Theberge R, Costello CE, McComb ME: **Highly efficient and selective enrichment of peptide subsets combining fluorous chemistry with reversed-phase chromatography**. *Rapid Commun Mass Spectrom* 2009, **23**:4019-4030.

Figure legends

Figure 1. Representative genes differentially expressed in TRAF3$^{-/-}$ mouse B lymphomas identified by the transcriptome microarray analysis. (**A**) Heatmap of representative microarray data**.** The mRNA expression profiles of splenocytes from 3 pairs of LMC and tumor-bearing B-TRAF3$^{-/-}$ mice were analyzed by microarray analysis. cRNA was hybridized to the Illumina Sentrix MouseRef-8 24K Array (Illumina). Genes shown in the heatmap are selected from 160 up-regulated and 244 down-regulated genes: red indicates overexpression, blue indicates underexpression, and black indicates median expression. Values under the color key indicates Log2 (fold of change). Dendrogram on top of the heatmap shows the relatedness between samples as determined by hierarchical clustering. (**B**) Verification of transcript up-regulation of genes identified by the microarray analysis using quantitative real time PCR. Total cellular RNA was prepared from splenocytes of LMC mice, or splenic B lymphomas (spl) and ascites (asc) of diseased B-TRAF3$^{-/-}$ mice, and cDNA was synthesized by reverse transcription. Real time PCR was performed using TaqMan primers and probes (FAM-labeled) specific for mouse *Diras2*, *MCC*, *Tbc1d9*, *Ccbp2*, *Btbd14a*, *Sema7a*, *Twsg1*, *Ppap2b*, *TCF4*, *Tnfrsf19*, *Zcwpw1*, and *Abca3*. Each reaction also included the probe (VIC-labeled) and primers for mouse β-actin mRNA, which served as endogenous control. Relative mRNA expression levels of each gene were analyzed using the Sequencing Detection Software (Applied Biosystems) and the comparative Ct (ΔΔCt) method. Graphs depict the results of two experiments with duplicate reactions in each experiment (mean ± S.D.), and mouse ID of each sample is indicated in the graphs.

Figure 2. Striking up-regulation of MCC in TRAF3$^{-/-}$ mouse B lymphomas but not in premalignant TRAF3$^{-/-}$ B lymphocytes. (**A**) Western blot analysis of the MCC protein. Total cellular proteins were prepared from purified LMC splenic B cells or splenic B lymphomas (spl) or ascites (asc) of different individual B-TRAF3$^{-/-}$ mice. Proteins were immunoblotted for MCC, followed by actin. (**B**) Regulation of the expression of *MCC* and *Zcwpw1* in response to B cell stimuli. Splenic B cells were purified from 10- to 12- week-old LMC and tumor-free B-TRAF3$^{-/-}$ mice. Purified B cells were cultured *ex vivo* in the absence or presence of stimuli of B cell proliferation, differentiation and activation for 6 or 24 hours. B cell stimuli examined include: 2 μg/ml anti-CD40, 20 μg/ml LPS, 1 μg/ml anti-BCR, and 100 nM CpG2084, alone or in combination. RNA samples of primary TRAF3$^{-/-}$ mouse B lymphomas (mouse ID: 7060-8) were used as positive control of the *MCC* and *Zcwpw1* transcripts in the experiments. Taqman assays of *MCC* and *Zcwpw1* were performed as described in Figure 1. Graphs depict the results of three independent experiments with duplicate reactions in each experiment (mean ± S.D.). (**C**) Normal copy number of the *MCC* gene in TRAF3$^{-/-}$ mouse B lymphomas. Copy number of the mouse *MCC* gene in genomic DNA samples prepared from LMC splenocytes or TRAF3$^{-/-}$ B lymphomas was determined using the TaqMan Copy Number Assay kit. Mouse ID was indicated in the figure. Graphs depict the results of three experiments with duplicate reactions in each experiment (mean ± S.D.). (**D**) Histone modifications of the promoter region of the *MCC* and *Diras2* genes. Chromatin was prepared from splenic B cells purified from 10- to 12- week-old LMC and tumor-free B-TRAF3$^{-/-}$ mice (young TRAF3-/-), or TRAF3$^{-/-}$ B lymphomas. Fragmented chromatin was immunoprecipitated using antibodies specific for histone marks

(H3K27me3 or H3K9/14ac) or non-specific rabbit Ig. Immunorecipitated DNA was quantified by quantitative real time PCR using primer pairs specific for the promoter region of the *MCC* and *Diras2* genes, respectively. Quantity of immunoprecipitated DNA is presented as percentage of input DNA in graphs. The graphs depict the results of three independent experiments with duplicate reactions in each experiment (mean ± S.D.). **P* < 0.05, and ***P* < 0.0001 by Student's *t* test.

Figure 3. Aberrant expression and subcellular localization of MCC in human MM cells. (**A**) Taqman assay of the *MCC* transcript. Total cellular RNA was prepared from normal human blood B lymphocytes (Normal B), an EBV-transformed B lymphoblastoid cell line C3688, or human MM cell lines with TRAF3 deletions or relevant mutations. The human MM cell lines include KMS11, 8226, LP1, U266, KMS28PE, and KMS20. Real-time PCR was performed using TaqMan primers and probes (FAM-labeled) specific for human *MCC*. Each reaction also included the probe (VIC-labeled) and primers for human β-actin mRNA, which served as an endogenous control. Relative mRNA expression levels of the *MCC* gene were analyzed using the Sequencing Detection Software (Applied Biosystems) and the comparative Ct (ΔΔCt) method. Graphs depict the results of three independent experiments with duplicate reactions in each experiment (mean ± S.D.). (**B**) Western blot analysis of the MCC protein. Total cellular proteins were prepared from normal B lymphocytes, C3688 cells, or human MM cell lines with TRAF3 deletions or relevant mutations. Proteins were immunoblotted for MCC, followed by TRAF3 and actin. Data shown are representative of 3 experiments. (**C**) Subcellular localization of MCC and its regulation during ER stress responses. LP1 cells were cultured in the absence (control) or presence of ER stress inducers DTT or thapsigargin

(Thg). After treatment for 24 hours, cytosol (S100), ER, mitochondria (mito) and nuclei (Nuc) were biochemically fractionated from cells, and an aliquot of cells was used for total protein lysates (Total). Proteins in each fraction or total lysates were immunoblotted for MCC, Rhbdf1 (an ER protein), cIAP1, cIAP2, cyclin D2, COX IV (a mitochondrial protein), and actin. Results shown are representative of 3 independent experiments.

Figure 4. Lentiviral shRNA vector-mediated knockdown of MCC induced apoptosis in human MM cells. The human MM cell line LP1 cells were transduced with lentiviruses expressing MCC shRNAs (including 1332, 1388, 2284 or 2689) or a scrambled shRNA (Scr). (**A**) Knockdown of the MCC protein determined by immunoblot analysis. Total cellular proteins were prepared from LP1 cells successfully transduced with a scrambled shRNA (Scr), or MCC shRNA 1332, 1388, 2284 or 2689 on day 5 post-transduction. Proteins were immunoblotted for MCC, followed by actin. Immunoblot of actin was used as a loading control. Results shown are representative of 3 independent experiments, and similar results were obtained in the human MM cell line KMS11 cells. (**B**) Growth curves of live cells and percentage of live versus dead cells determined by Trypan blue-stained cell counting. On day 4 post-transduction, successfully transduced LP1 cells were cultured in a 6-well plate for growth curve determination. Live and dead cells were counted daily for 4 days using Trypan blue staining and a hemocytometer. The graphs depict the results of 3 independent experiments (mean ± S.D.). (**C**) Representative FACS profiles of transduced cells analyzed by annexin V and PI staining. On day 6 post-transduction, transduced LP1 cells were stained with annexin V and PI, and then analyzed by a flow cytometer. In the FACS profiles, apoptotic cells were identified as annexin V+ PI-, dead cells were annexin V+ PI+, and live cells were annexin V- PI-.

Data shown are representative of 3 independent experiments, and similar results were obtained in the human MM cell line KMS11 cells.

Figure 5. Knockdown of MCC induced apoptosis and inhibited proliferation in human MM cells. (**A**) Cell cycle distribution analyzed by PI staining and flow cytometry. The human MM cell line LP1 cells were transduced with lentiviruses expressing MCC shRNAs (1332 or 2689) or a scrambled shRNA (Scr). Successfully transduced (GFP+) cells were sorted by a FACS sorter on day 4 post-transduction. Top panel shows the FACS histograms of cells right after sorting (Day 0), and bottom panel shows the FACS histograms of sorted cells after cultured for 24 hours (Day 1). Gated populations in the FACS histograms indicate apoptotic cells (DNA content < 2n) or proliferating cells (2n < DNA content ≤ 4n). Results shown are representative of 3 independent experiments, and similar results were also obtained in the human MM cell line KMS11 cells. (**B**) Cell proliferation analyzed by dilution of the proliferation dye (eFluor 670)-labeling and flow cytometry. On day 4 post transduction, LP1 cells transduced with MCC shRNA 1332 (1332) or a scrambled shRNA (Scr) were labeled with a proliferation dye eFluor 670, which binds to any cellular protein containing primary amines. As cells divide, the dye is distributed equally between daughter cells that can be measured as successive halving or dilution of the fluorescence intensity of the dye. Day 0 FACS profiles and overlay histograms show the eFluor 670 signals of freshly labeled cells, while those of Day 2 and Day 4 show diluted eFluor 670 signals of cells after cultured for 2 and 4 days, respectively. Inhibited proliferation of MCC shRNA 1332-transduced cells was demonstrated by the hampered dilution of the proliferation dye as compared to those observed in both the untransduced (GFP-) cells and the scrambled

shRNA (Scr)-transduced cells. Results shown are representative of 3 independent experiments with duplicate samples in each experiment.

Figure 6. MCC signaling pathways in human MM cells. The human MM cell line LP1 cells, which express high levels of endogenous MCC, were transduced with lentiviruses expressing MCC shRNA 1332 or a scrambled shRNA (SCR). Another human MM cell line 8226 cells, which express modest levels of endogenous MCC, were transduced with lentiviruses expressing hMCC (pUB-hMCC) or Thy1.1 only (pUB-Thy1.1). Total cellular lysates were prepared and immunoblotted for known targets of MCC and regulators of apoptosis or cell cycle. Known target proteins of MCC examined include phosphorylated β-catenin (P-β-catenin), β-catenin, IκBα, IκBβ, RelA, and phosphorylated histone H3 (P-HH3). Regulators of apoptosis examined include caspase 8, caspase 3, Bcl-xL, Bcl2, Mcl1, Bim, P-Bad, Bad, Bid, and Bik. Regulators of cell cycle examined include cyclin D1, cyclin D2, cyclin B1, cyclin A, p21, p27, E2F1, p53, phosphorylated-p38 (P-p38), p38, P-ERK, ERK, P-JNK, JNK, P-Akt, Akt, and c-Myc. The MCC blot was used as a control for MCC shRNA 1332 or pUB-hMCC transduction, and the actin blot was used as a loading control. Proteins that are changed by knockdown of MCC are highlighted in blue, and those that are changed by both knockdown and overexpression of MCC are highlighted in red. Results shown are representative of 3 independent experiments.

Figure 7. The MCC-interactome in human MM cells identified by affinity purification followed by LC-MS/MS. The human MM cell line 8226 cells were transduced with lentiviruses expressing hMCC-SBP-6xHis or FLAG-hMCC. Immunoprecipitates of hMCC-SBP-6xHis by streptavidin-sepharose beads from whole

cell lysates and purified mitochondria of 8226 cells were analyzed by high resolution LC-MS/MS, respectively. Immunoprecipitates of FLAG-hMCC by streptavidin-sepharose beads were used as negative control in these experiments. (**A**) Venn diagram of MCC-interactors identified in the present study and previous studies. The diagram depicts the number of previously known MCC-interactors or MCC-interactors identified in whole cell lysates or mitochondria of human MM cells in our study, as well as the overlap between each category. (**B** and **C**) Functional clustering and annotation of MCC-interactors identified in whole cell lysates (B) or mitochondria (C) of human MM cells. The number of proteins of each functional cluster is shown. (**D**) Representative mass spectral profile of a peptide of PHB2 identified by LC-MS/MS. The deduced peptide sequence is shown. (**E**) Schematic diagram of peptide sequences of PHB2 identified by LC-MS/MS. The peptide sequences detected by LC-MS/MS are highlighted in green color.

Figure 8. PARP1 and PHB2 are two hubs of the MCC interaction network in human MM cells. The human MM cell line 8226 cells were transduced with pUB-hMCC-SBP-6xHis or pUB-FLAG-hMCC. Immunoprecipitation was performed as described in Figure 7. (**A** and **B**) Immunoblot analyses of proteins pulled down by streptavidin-sepharose beads (SA IP) from whole cell lysates (A) or purified mitochondria (B). Proteins were immunoblotted for PARP1, PHB2, SBP, and followed by MCC. Blots of an aliquot of whole cell or mitochondrial lysates before immunoprecipitation were used as the input control. (**C**) The MCC interaction network in human MM cells**.** We performed an interaction network analysis using the top 100 MCC-interactors and the STRING analysis tool (http://www.string-db.org). The top 100 MCC-

interactors identified in our study and used for the interaction network analysis include 60 proteins identified in both whole cell lysates and mitochondria, 10 proteins identified in mitochondria only, and 30 proteins identified in whole cell lysates only. Sixty-one proteins of the top 100 MCC-interactors of human MM cells form an interaction network centered at PARP1 and PHB2.

Figure 1

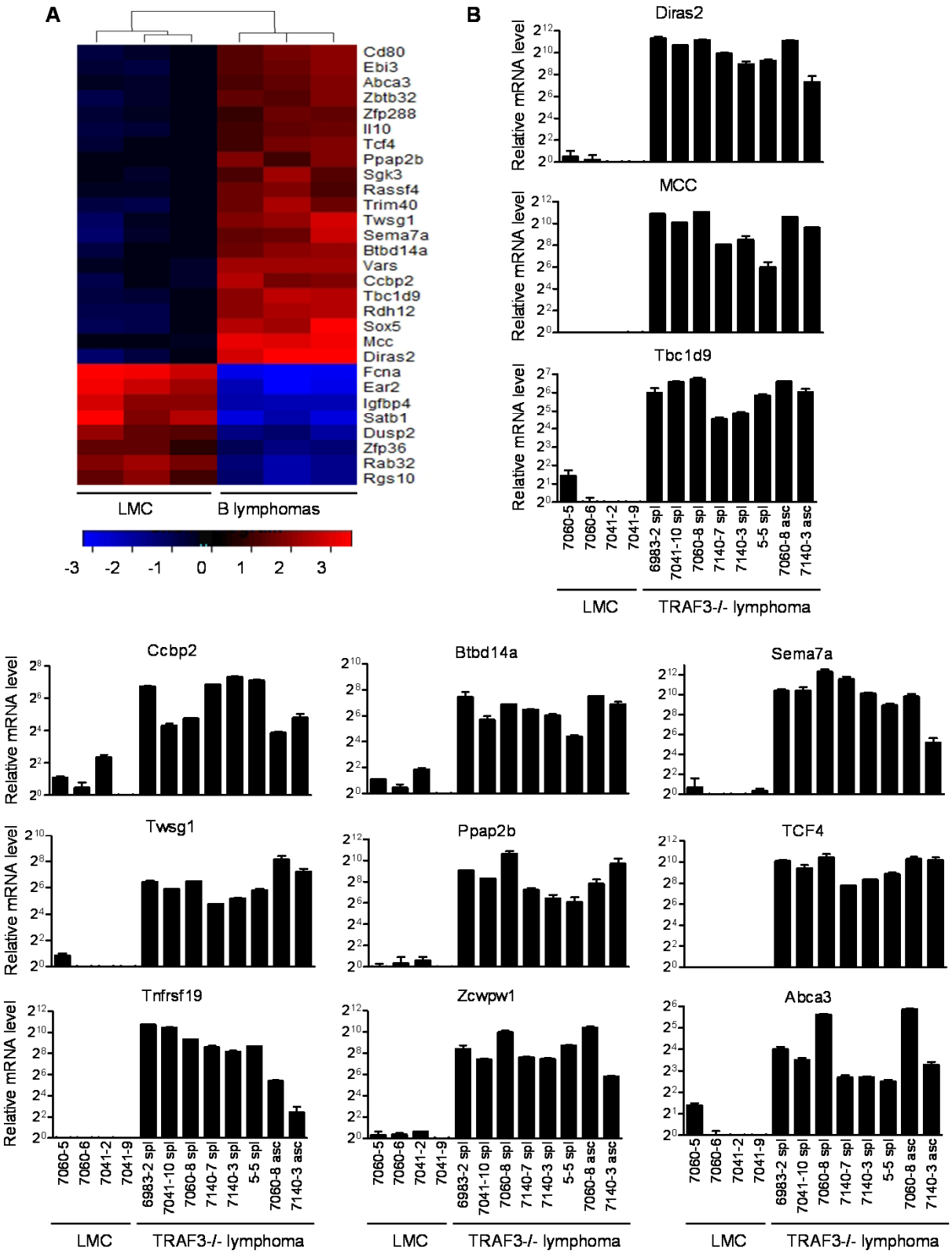
A
Cd80
Ebi3
Abca3
Zbtb32
Zfp288
Il10
Tcf4
Ppap2b
Sgk3
Rassf4
Trim40
Twsg1
Sema7a
Btbd14a
Vars
Ccbp2
Tbc1d9
Rdh12
Sox5
Mcc
Diras2
Fcna
Ear2
Igfbp4
Satb1
Dusp2
Zfp36
Rab32
Rgs10
LMC
B lymphomas
-3 -2 -1 0 1 2 3
B
Diras2
MCC
Tbc1d9
Relative mRNA level
7060-5
7060-6
7041-2
7041-9
6983-2 spl
7041-10 spl
7060-8 spl
7140-7 spl
7140-3 spl
5-5 spl
7060-8 asc
7140-3 asc
LMC
TRAF3-/- lymphoma
Ccbp2
Btbd14a
Sema7a
Twsg1
Ppap2b
TCF4
Tnfrsf19
Zcwpw1
Abca3

Figure 2

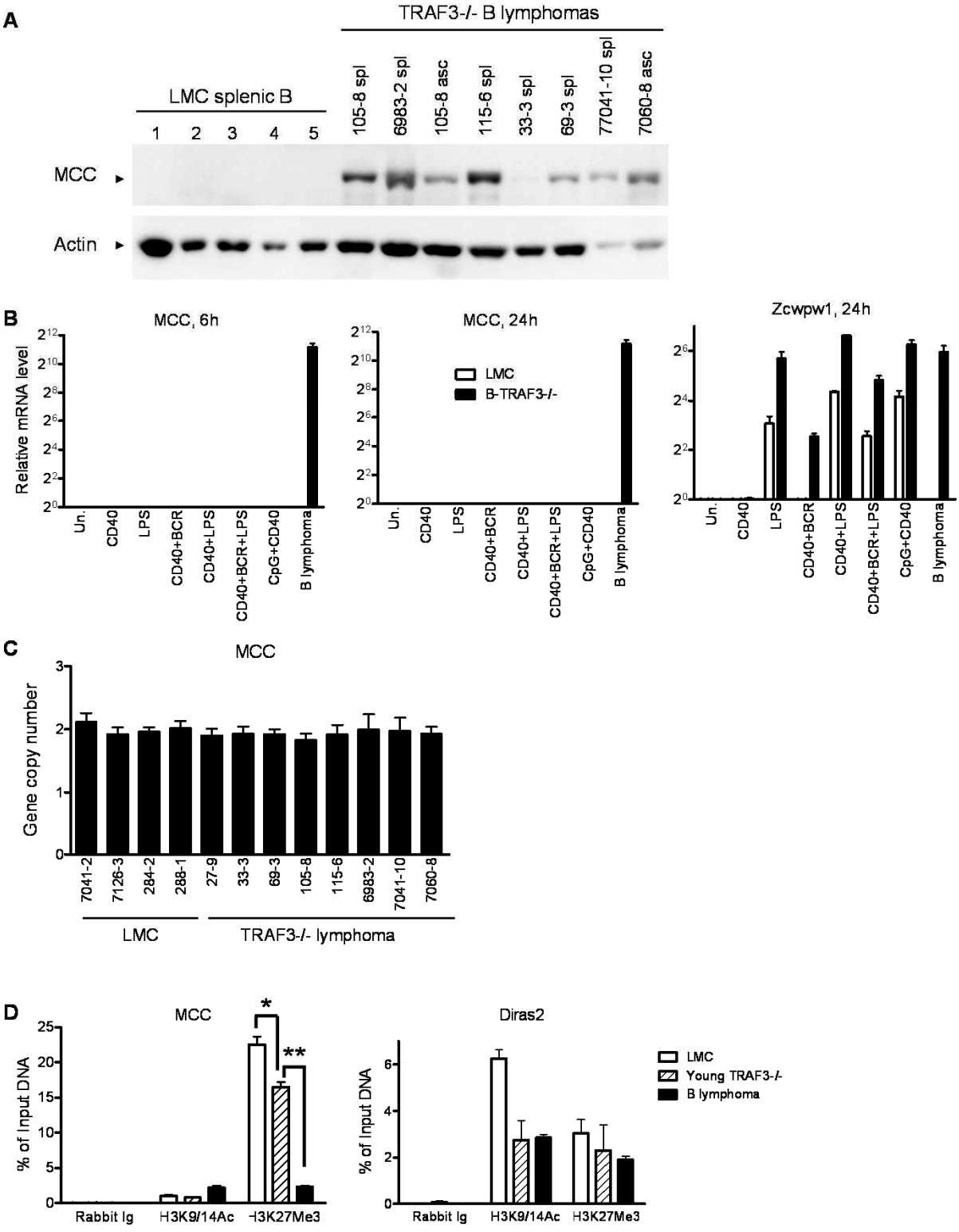
A
TRAF3-/- B lymphomas
LMC splenic B
1 2 3 4 5
105-8 spl
6983-2 spl
105-8 asc
115-6 spl
33-3 spl
69-3 spl
77041-10 spl
7060-8 asc
MCC
Actin
B
MCC, 6h
MCC, 24h
Zcwpw1, 24h
Relative mRNA level
LMC
B-TRAF3-/-
Un.
CD40
LPS
CD40+BCR
CD40+LPS
CD40+BCR+LPS
CpG+CD40
B lymphoma
C
MCC
Gene copy number
7041-2
7126-3
284-2
288-1
27-9
33-3
69-3
105-8
115-6
6983-2
7041-10
7060-8
LMC
TRAF3-/- lymphoma
D
MCC
Diras2
% of Input DNA
Rabbit Ig
H3K9/14Ac
H3K27Me3
LMC
Young TRAF3-/-
B lymphoma

Figure 3

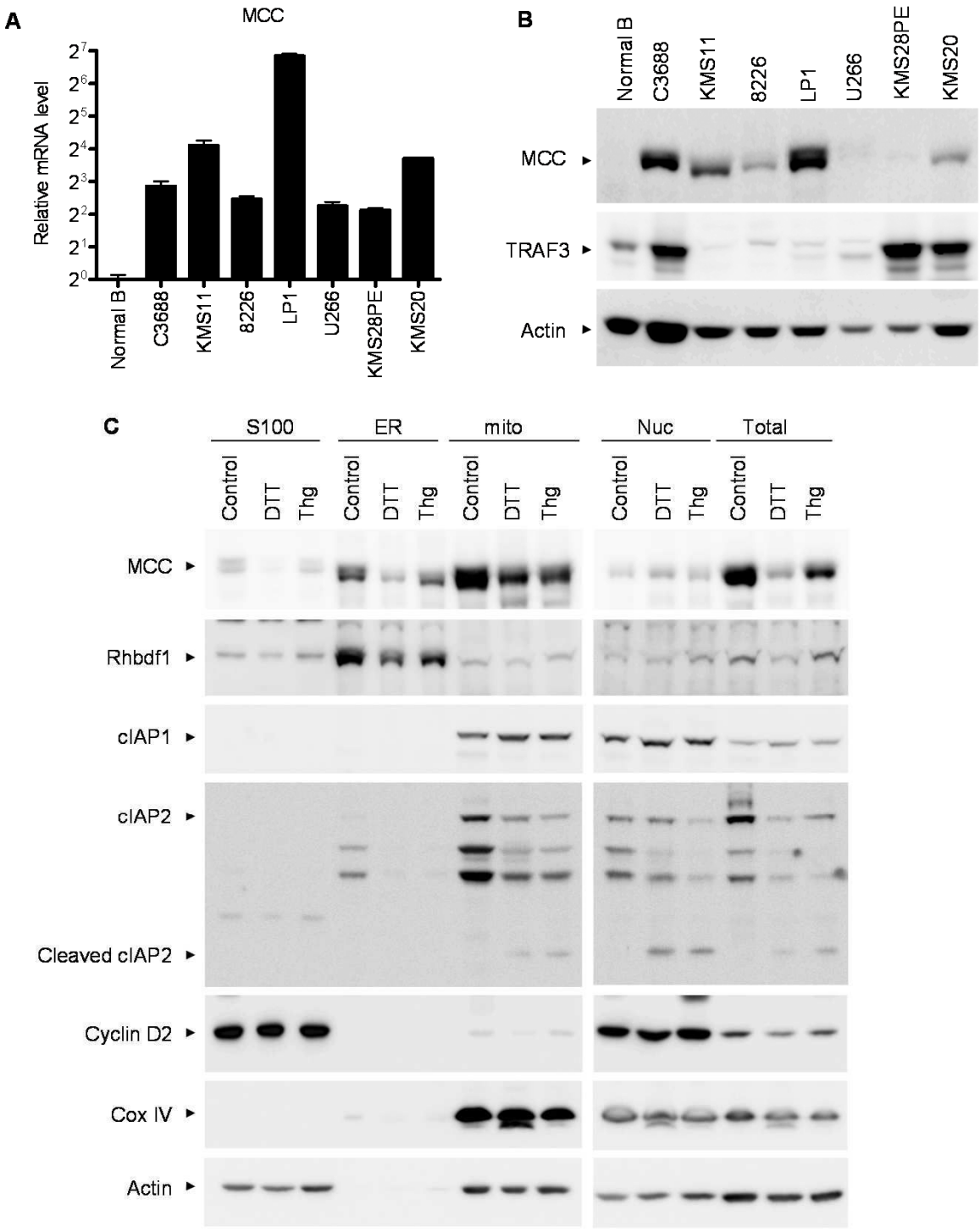
A
MCC
Relative mRNA level
Normal B
C3688
KMS11
8226
LP1
U266
KMS28PE
KMS20
B
Normal B
C3688
KMS11
8226
LP1
U266
KMS28PE
KMS20
MCC
TRAF3
Actin
C
S100
ER
mito
Nuc
Total
Control
DTT
Thg
MCC
Rhbdf1
cIAP1
cIAP2
Cleaved cIAP2
Cyclin D2
Cox IV
Actin

Figure 4

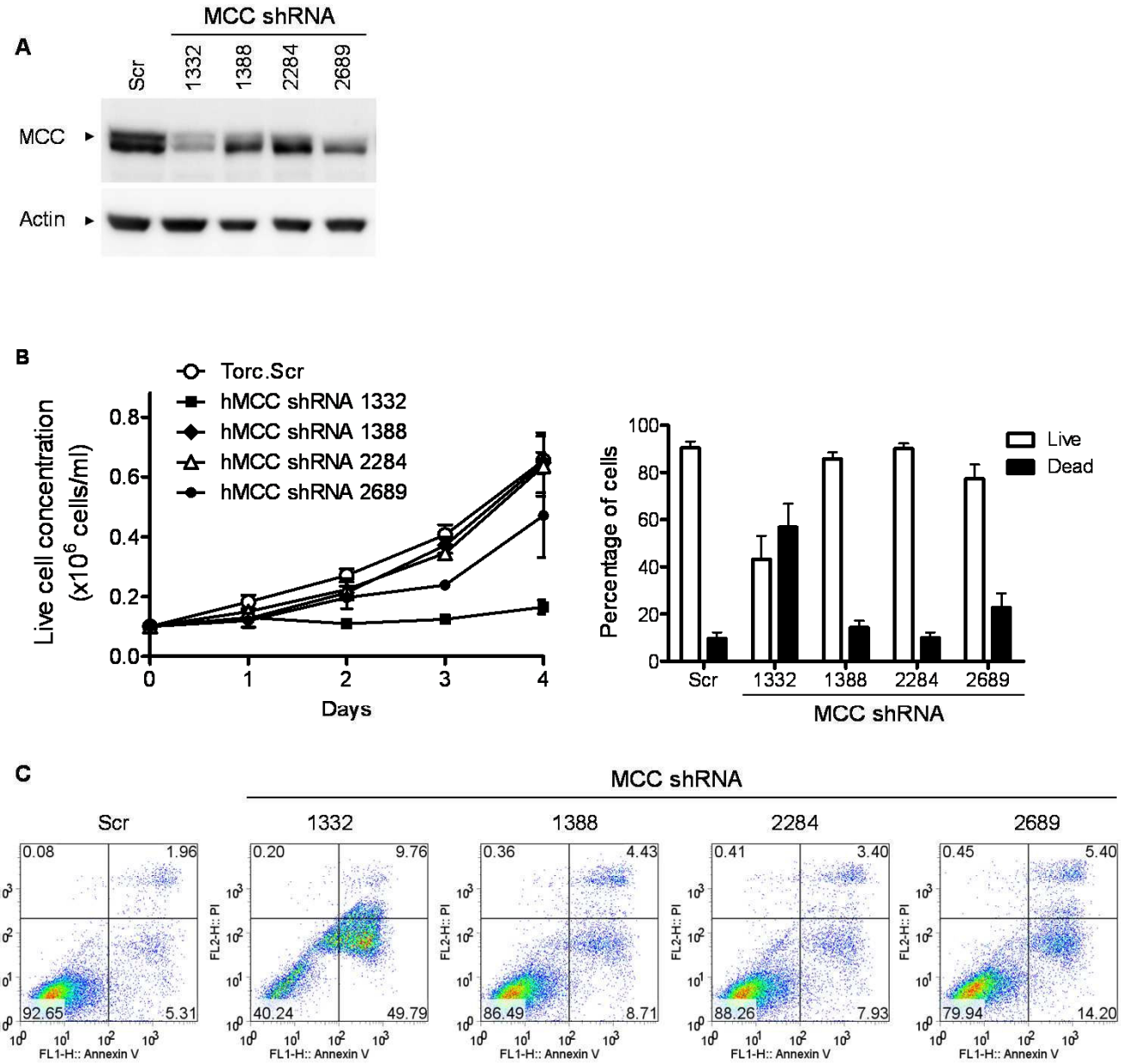
A
MCC shRNA
Scr
1332
1388
2284
2689
MCC
Actin
B
Torc.Scr
hMCC shRNA 1332
hMCC shRNA 1388
hMCC shRNA 2284
hMCC shRNA 2689
Live cell concentration (x10^6 cells/ml)
Days
Percentage of cells
Live
Dead
MCC shRNA
C
MCC shRNA
Scr
1332
1388
2284
2689
FL2-H:: PI
FL1-H:: Annexin V
0.08
1.96
92.65
5.31
0.20
9.76
40.24
49.79
0.36
4.43
86.49
8.71
0.41
3.40
88.26
7.93
0.45
5.40
79.94
14.20

Figure 5

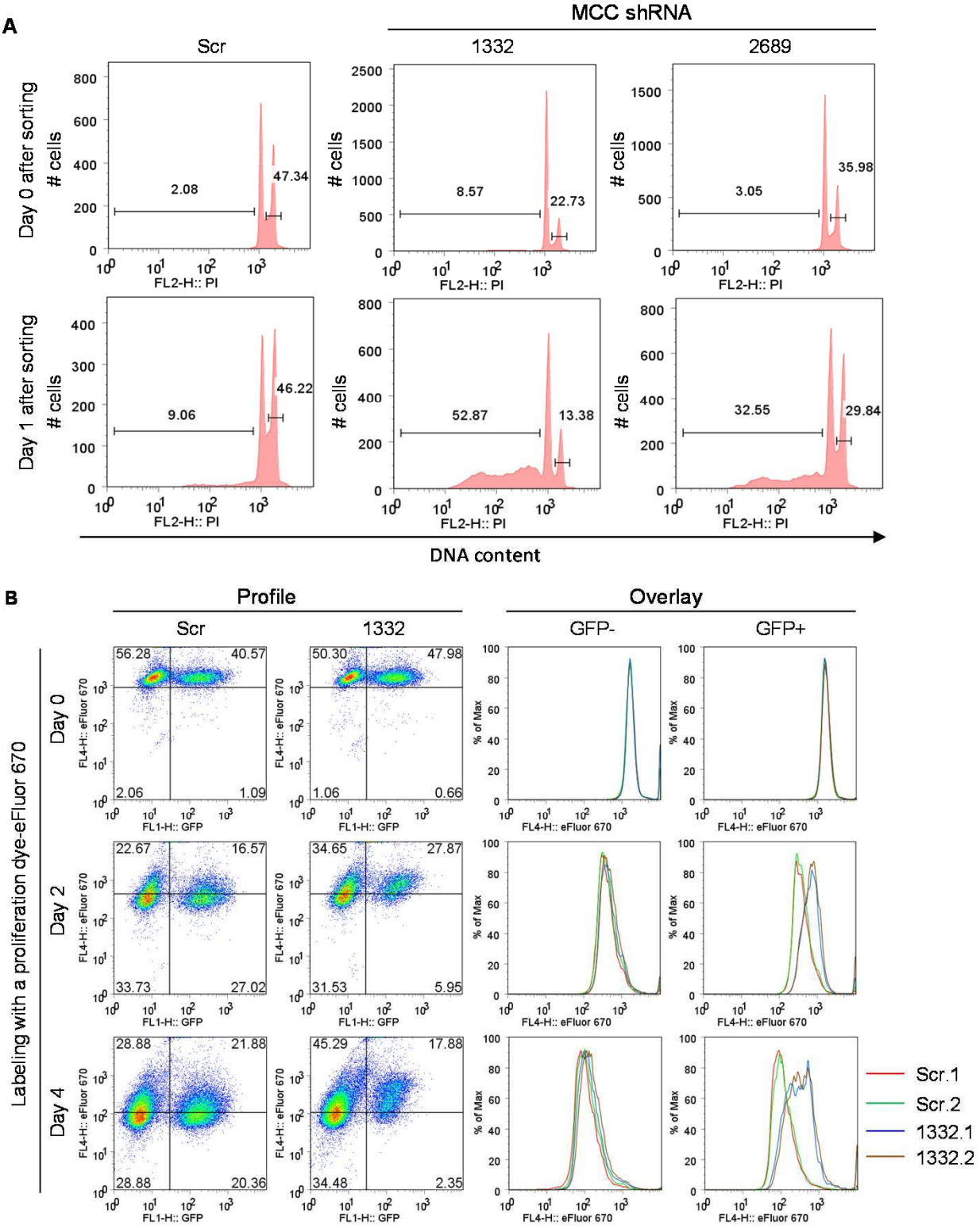
A
MCC shRNA
Scr
1332
2689
Day 0 after sorting
Day 1 after sorting
cells
FL2-H:: PI
2.08
47.34
8.57
22.73
3.05
35.98
9.06
46.22
52.87
13.38
32.55
29.84
DNA content
B
Profile
Overlay
Scr
1332
GFP-
GFP+
Labeling with a proliferation dye-eFluor 670
Day 0
Day 2
Day 4
FL4-H:: eFluor 670
FL1-H:: GFP
% of Max
56.28
40.57
2.06
1.09
50.30
47.98
1.06
0.66
22.67
16.57
33.73
27.02
34.65
27.87
31.53
5.95
28.88
21.88
28.88
20.36
45.29
17.88
34.48
2.35
Scr.1
Scr.2
1332.1
1332.2

Figure 6

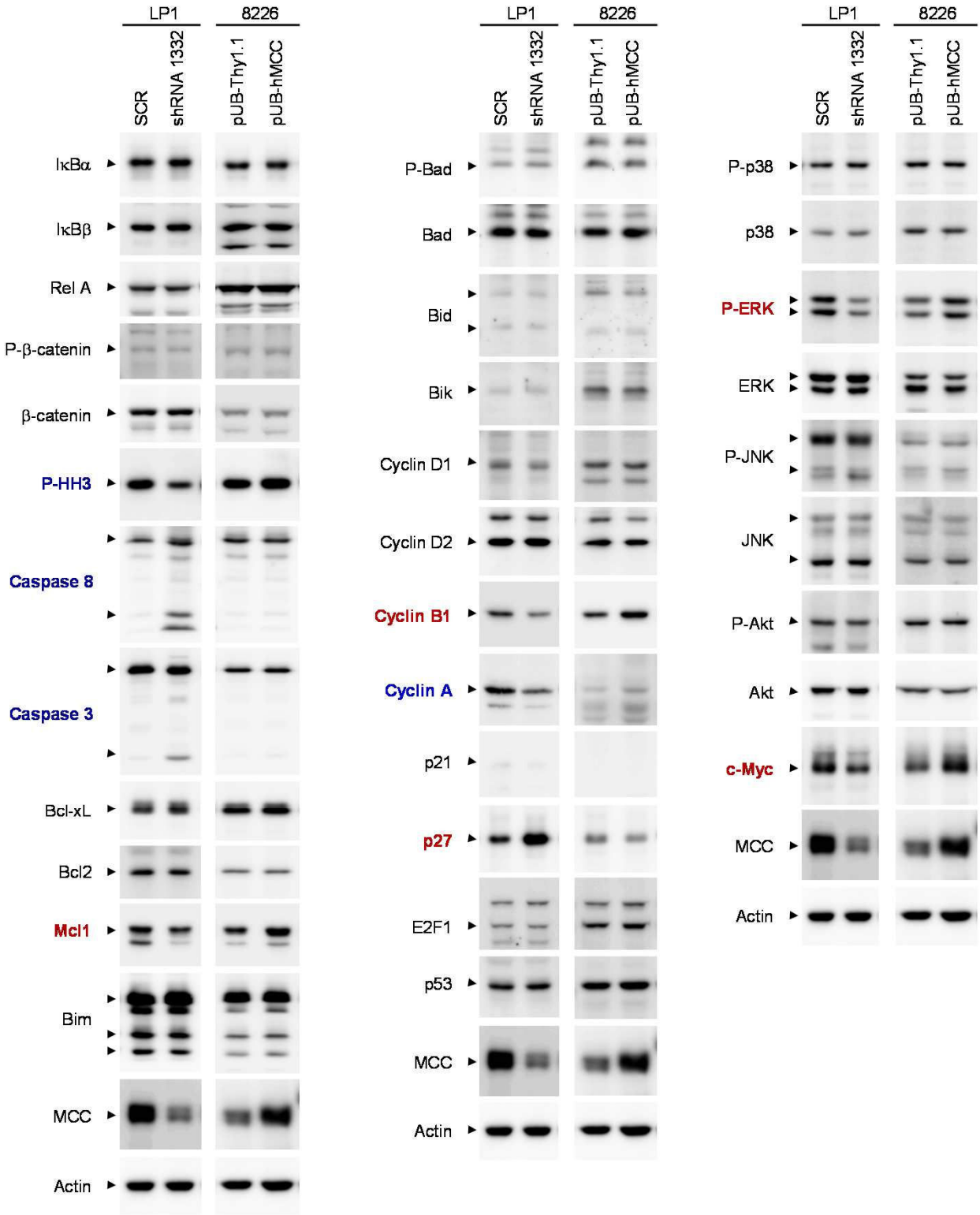
LP1
8226
SCR
shRNA 1332
pUB-Thy1.1
pUB-hMCC
IκBα
IκBβ
Rel A
P-β-catenin
β-catenin
P-HH3
Caspase 8
Caspase 3
Bcl-xL
Bcl2
Mcl1
Bim
MCC
Actin
P-Bad
Bad
Bid
Bik
Cyclin D1
Cyclin D2
Cyclin B1
Cyclin A
p21
p27
E2F1
p53
MCC
Actin
P-p38
p38
P-ERK
ERK
P-JNK
JNK
P-Akt
Akt
c-Myc
MCC
Actin

Figure 7

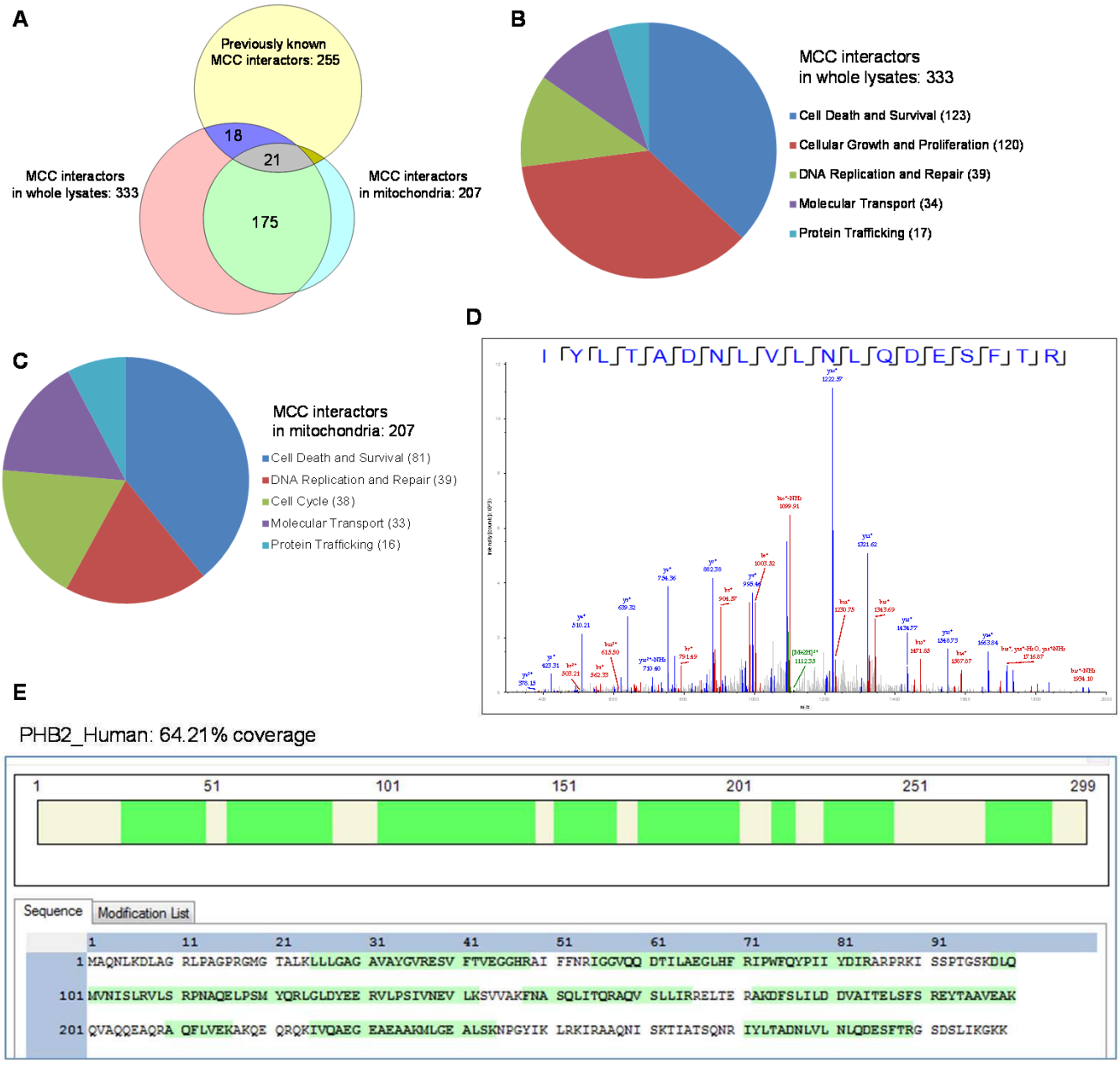
A
Previously known
MCC interactors: 255
18
21
175
MCC interactors
in whole lysates: 333
MCC interactors
in mitochondria: 207
B
MCC interactors
in whole lysates: 333
Cell Death and Survival (123)
Cellular Growth and Proliferation (120)
DNA Replication and Repair (39)
Molecular Transport (34)
Protein Trafficking (17)
C
MCC interactors
in mitochondria: 207
Cell Death and Survival (81)
DNA Replication and Repair (39)
Cell Cycle (38)
Molecular Transport (33)
Protein Trafficking (16)
D
I ⌈Y⌈L⌋T⌋A⌋D⌋N⌋L⌋V⌋L⌋N⌋L⌋Q⌋D⌋E⌋S⌋F⌋T⌋R⌋
E
PHB2_Human: 64.21% coverage
1
51
101
151
201
251
299
Sequence
Modification List
1 11 21 31 41 51 61 71 81 91
1 MAQNLKDLAG RLPAGPRGMG TALKLLLGAG AVAYGVRESV FTVEGGHRAI FFNRIGGVQQ DTILAEGLHF RIPWFQYPII YDIRARPRKI SSPTGSKDLQ
101 MVNISLRVLS RPNAQELPSM YQRLGLDYEE RVLPSIVNEV LKSVVAKFNA SQLITQRAQV SLLIRRELTE RAKDFSLILD DVAITELSFS REYTAAVEAK
201 QVAQQEAQRA QFLVEKAKQE QRQKIVQAEG EAEAAKMLGE ALSKNPGYIK LRKIRAAQNI SKTIATSQNR IYLTADNLVL NLQDESFTRG SDSLIKGKK

Figure 8

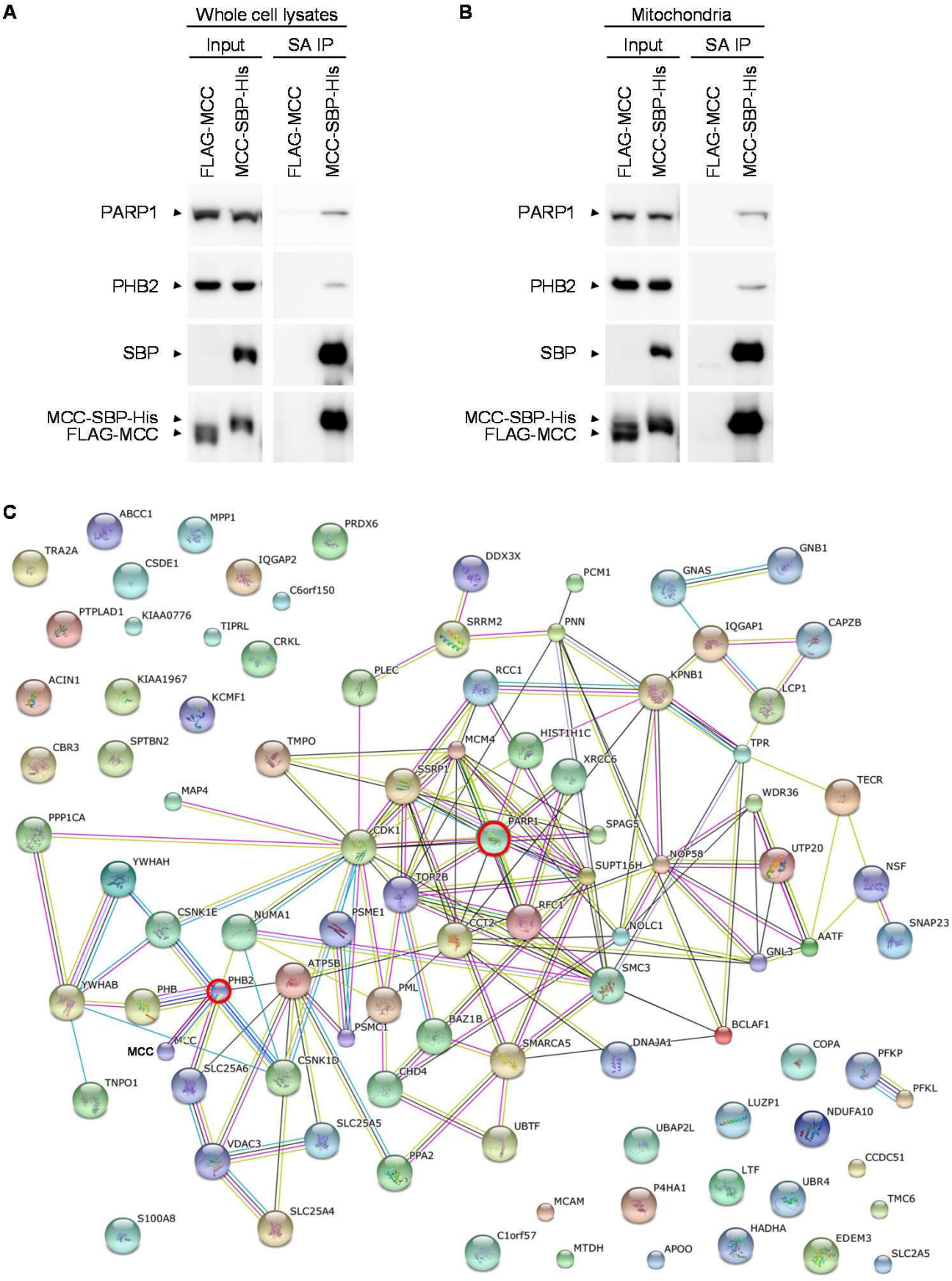
A
Whole cell lysates
Input
SA IP
FLAG-MCC
MCC-SBP-His
FLAG-MCC
MCC-SBP-His
PARP1
PHB2
SBP
MCC-SBP-His
FLAG-MCC
B
Mitochondria
Input
SA IP
FLAG-MCC
MCC-SBP-His
FLAG-MCC
MCC-SBP-His
PARP1
PHB2
SBP
MCC-SBP-His
FLAG-MCC
C
ABCC1
MPP1
PRDX6
TRA2A
CSDE1
IQGAP2
C6orf150
PTPLAD1
KIAA0776
TIPRL
CRKL
ACIN1
KIAA1967
KCMF1
CBR3
SPTBN2
TMPO
MAP4
PPP1CA
YWHAH
CSNK1E
NUMA1
PSME1
YWHAB
PHB
PHB2
ATP5B
MCC
SLC25A6
CSNK1D
TNPO1
VDAC3
SLC25A5
SLC25A4
S100A8
PPA2
PSMC1
PML
CHD4
UBTF
BAZ1B
SMARCA5
DNAJA1
BCLAF1
SMC3
GNL3
AATF
SNAP23
NSF
UTP20
NOP58
NOLC1
SUPT16H
RFC1
CCT2
TOP2B
CDK1
PARP1
SPAG5
SSRP1
MCM4
HIST1H1C
XRCC6
TPR
WDR36
TECR
LCP1
KPNB1
PLEC
RCC1
SRRM2
PNN
DDX3X
PCM1
IQGAP1
CAPZB
GNAS
GNB1
COPA
PFKP
PFKL
LUZP1
NDUFA10
CCDC51
UBAP2L
LTF
UBR4
TMC6
P4HA1
MCAM
C1orf57
MTDH
APOO
HADHA
EDEM3
SLC2A5

Additional files provided with this submission:

Additional file 1: Supplementary Figure MCC Edwards and Xie.pdf, 69K
http://www.jhoonline.org/imedia/1393176379132034/supp1.pdf
Additional file 2: Edwards and Xie MCC Supplementary Table 1.pdf, 107K
http://www.jhoonline.org/imedia/5407042571320349/supp2.pdf
Additional file 3: Edwards and Xie MCC Supplementary Table 2.pdf, 153K
http://www.jhoonline.org/imedia/2055421575132034/supp3.pdf

Supplementary Table 1. List of genes differentially expressed in TRAF3$^{-/-}$ mouse splenic B lymphomas identified by the microarray analysis

#	GeneSymbol	Gene Name	LogFC	AveExpr	t	P. Value	Adj. P. Val.
1	Zcwpw1	zinc finger, CW type with PWWP domain 1	3.36	9.50	14.20	4.07E-07	0.000126365
2	Diras2	DIRAS family, GTP-binding RAS-like 2	3.35	10.56	14.57	3.32E-07	0.000126365
3	Serpina3f	serine (or cysteine) peptidase inhibitor, clade A, member 3F	3.03	10.87	9.99	6.54E-06	0.000571
4	Sox5	SRY-box containing gene 5	2.93	9.48	13.97	4.65E-07	0.000130244
5	C130026I21Rik	RIKEN cDNA C130026I21 gene	2.87	9.95	5.58	0.000456113	0.008256021
6	Tnfrsf19	tumor necrosis factor receptor superfamily, member 19	2.87	9.00	13.59	5.78E-07	0.000148597
7	Mcc	mutated in colorectal cancers	2.76	8.68	31.01	6.98E-10	9.15E-06
8	Slamf9	SLAM family member 9	2.75	10.73	4.75	0.00131062	0.016097166
9	Fah	fumarylacetoacetate hydrolase	2.63	11.18	7.83	4.13E-05	0.00178595
10	Rdh12	retinol dehydrogenase 12	2.61	11.29	12.81	9.27E-07	0.000205961
11	Ahnak2	AHNAK nucleoprotein 2	2.54	8.93	12.49	1.13E-06	0.000226433
12	Chst7	carbohydrate (N-acetylglucosamino) sulfotransferase 7	2.42	9.23	7.85	4.05E-05	0.001759595
13	Vars	valyl-tRNA synthetase	2.30	11.46	16.48	1.23E-07	8.74E-05
14	Twsg1	twisted gastrulation homolog 1 (Drosophila)	2.30	10.96	10.51	4.41E-06	0.000441575
15	Tbc1d9	TBC1 domain family, member 9	2.29	9.53	17.05	9.34E-08	7.20E-05
16	Vars	valyl-tRNA synthetase	2.13	9.29	17.17	8.83E-08	7.20E-05
17	Cd59a	CD59a antigen	2.11	10.04	5.72	0.000385181	0.007336917
18	Gnb3	guanine nucleotide binding protein (G protein), beta 3	2.09	8.73	5.99	0.000283427	0.006099042
19	Sspn	sarcospan	2.08	10.14	4.98	0.000958982	0.013242851
20	Lacc1	laccase (multicopper oxidoreductase) domain containing 1	2.08	8.98	19.86	2.70E-08	5.06E-05
21	Gbp1	guanylate binding protein 1	2.06	9.78	4.19	0.00279695	0.02699119
22	Vars	valyl-tRNA synthetase	2.06	12.05	21.24	1.56E-08	3.41E-05
23	Ccbp2	chemokine binding protein 2	1.96	9.96	7.62	5.07E-05	0.002000536
24	Gng13	guanine nucleotide binding protein (G protein), gamma 13	1.94	8.60	7.33	6.70E-05	0.00236437
25	Plscr1	phospholipid scramblase 1	1.94	10.35	6.13	0.000239207	0.005519038
26	Clic4	chloride intracellular channel 4 (mitochondrial)	1.93	12.48	7.57	5.33E-05	0.002054453
27	Sema7a	sema domain, immunoglobulin domain (Ig), and GPI membrane anchor, (sema	1.91	9.22	9.70	8.22E-06	0.000643485
28	Chrnb1	cholinergic receptor, nicotinic, beta polypeptide 1 (muscle)	1.89	9.84	8.35	2.55E-05	0.001291342
29	Ppap2b	phosphatidic acid phosphatase type 2B	1.86	10.46	18.00	6.01E-08	7.20E-05
30	Ebi3	Epstein-Barr virus induced gene 3	1.82	9.85	10.82	3.51E-06	0.00039538
31	4930539E08Rik	RIKEN cDNA 4930539E08 gene	1.81	8.92	8.10	3.22E-05	0.001536721
32	Nacc2	nucleus accumbens associated 2, BEN and BTB (POZ) domain containing	1.79	9.23	12.76	9.57E-07	0.000209017
33	Fcrl5	Fc receptor-like 5	1.79	9.62	8.79	1.74E-05	0.001046831
34	Sel1l3	sel-1 suppressor of lin-12-like 3 (C. elegans)	1.76	8.30	7.70	4.70E-05	0.001893452
35	Dnajc7	DnaJ (Hsp40) homolog, subfamily C, member 7	1.76	10.73	6.73	0.000124642	0.003589973
36	Pdlim1	PDZ and LIM domain 1 (elfin)	1.74	11.75	6.79	0.000116482	0.003392213
37	Abca3	ATP-binding cassette, sub-family A (ABC1), member 3	1.71	10.86	11.21	2.66E-06	0.0003633
38	Rassf4	Ras association (RalGDS/AF-6) domain family member 4	1.66	11.54	10.68	3.89E-06	0.000397578
39	Kynu	kynureninase (L-kynurenine hydrolase)	1.65	10.56	14.43	3.57E-07	0.000126365
40	Cd274	CD274 antigen	1.64	11.38	16.17	1.43E-07	8.74E-05

41	Cd80	CD80 antigen	1.64	8.83	12.33	1.25E-06	0.00023571
42	Ccdc28b	coiled coil domain containing 28B	1.64	10.34	7.19	7.74E-05	0.002628686
43	Rassf4	Ras association (RalGDS/AF-6) domain family member 4	1.63	11.53	11.04	3.00E-06	0.000376611
44	Sp140	Sp140 nuclear body protein	1.63	9.80	11.51	2.15E-06	0.000322971
45	AF067061	cDNA sequence AF067061	1.63	8.54	4.77	0.001275097	0.015838995
46	Ero1lb	ERO1-like beta (S. cerevisiae)	1.63	11.22	12.45	1.16E-06	0.000226433
47	Nfatc1	nuclear factor of activated T cells, cytoplasmic, calcineurin dependent 1	1.61	9.89	8.27	2.76E-05	0.001378762
48	Hdac4	histone deacetylase 4	1.61	8.78	8.11	3.17E-05	0.001523759
49	Tubb2b	tubulin, beta 2B class IIB	1.60	10.65	5.22	0.000712545	0.010897018
50	Trim40	tripartite motif-containing 40	1.59	8.56	8.79	1.74E-05	0.001046831
51	Plscr1	phospholipid scramblase 1	1.57	9.33	6.70	0.000129091	0.003645988
52	Arhgap24	Rho GTPase activating protein 24	1.52	10.13	11.91	1.65E-06	0.000270244
53	D13Ertd608e	DNA segment, Chr 13, ERATO Doi 608, expressed	1.52	8.97	10.25	5.35E-06	0.0005051
54	Hn1l	hematological and neurological expressed 1-like	1.52	9.27	15.10	2.49E-07	0.000112734
55	Ccdc28b	coiled coil domain containing 28B	1.50	9.62	9.68	8.31E-06	0.000643485
56	Tcf4	transcription factor 4	1.50	12.04	9.19	1.24E-05	0.000847921
57	Zbtb32	zinc finger and BTB domain containing 32	1.49	8.54	9.39	1.05E-05	0.000754882
58	Gbp2	guanylate binding protein 2	1.48	11.56	7.68	4.79E-05	0.001904754
59	Caln1	calneuron 1	1.48	8.43	6.18	0.000228083	0.005366295
60	Gpr34	G protein-coupled receptor 34	1.48	8.77	6.37	0.000182843	0.004607992
61	Serpina3g	serine (or cysteine) peptidase inhibitor, clade A, member 3G	1.47	12.85	8.47	2.30E-05	0.001206517
62	Rbm47	RNA binding motif protein 47	1.45	9.83	11.02	3.04E-06	0.000376611
63	Fgd2	FYVE, RhoGEF and PH domain containing 2	1.45	11.91	5.76	0.000368771	0.007141322
64	Fgd6	FYVE, RhoGEF and PH domain containing 6	1.44	9.42	8.42	2.41E-05	0.001236456
65	Neurod4	neurogenic differentiation 4	1.43	8.19	7.07	8.74E-05	0.002845238
66	Rassf4	Ras association (RalGDS/AF-6) domain family member 4	1.42	10.14	7.45	5.94E-05	0.002191762
67	Rhbdf1	rhomboid family 1 (Drosophila)	1.42	10.30	8.74	1.81E-05	0.001056366
68	Gstt3	glutathione S-transferase, theta 3	1.40	9.14	6.47	0.000164429	0.004282628
69	Pafah1b3	platelet-activating factor acetylhydrolase, isoform 1b, subunit 3	1.40	10.94	5.50	0.000501117	0.00873186
70	Asph	aspartate-beta-hydroxylase	1.37	8.04	5.64	0.000426167	0.007789294
71	Nid1	nidogen 1	1.37	8.57	7.77	4.37E-05	0.001817842
72	Sgk3	serum/glucocorticoid regulated kinase 3	1.36	9.50	10.11	5.97E-06	0.000539159
73	Gas7	growth arrest specific 7	1.35	8.81	6.41	0.000176165	0.004524439
74	NA	NA	1.34	10.20	11.26	2.56E-06	0.000352915
75	Gm14137	predicted gene 14137	1.34	8.18	17.51	7.51E-08	7.20E-05
76	Prps2	phosphoribosyl pyrophosphate synthetase 2	1.33	9.69	8.55	2.13E-05	0.001175007
77	Sox5	SRY-box containing gene 5	1.32	8.42	11.10	2.87E-06	0.000365287
78	Hsp90ab1	heat shock protein 90 alpha (cytosolic), class B member 1	1.30	11.59	7.12	8.32E-05	0.002740232
79	Eps15	epidermal growth factor receptor pathway substrate 15	1.30	9.95	9.51	9.50E-06	0.000711445
80	Cybasc3	cytochrome b, ascorbate dependent 3	1.29	10.90	11.68	1.92E-06	0.000303211
81	Fbxw13	F-box and WD-40 domain protein 13	1.29	8.28	9.97	6.61E-06	0.000572834
82	Recql5	RecQ protein-like 5	1.28	9.46	7.40	6.26E-05	0.002267958
83	Kcnk5	potassium channel, subfamily K, member 5	1.28	10.16	10.71	3.81E-06	0.00039567
84	Ptpn22	protein tyrosine phosphatase, non-receptor type 22 (lymphoid)	1.27	11.57	8.75	1.80E-05	0.001056366

85	Pdia4	protein disulfide isomerase associated 4	1.27	12.33	7.50	5.68E-05	0.002143803
86	Ccnd2	cyclin D2	1.27	10.35	7.56	5.37E-05	0.002064785
87	Plac1l	placenta-specific 1-like	1.27	8.63	7.49	5.74E-05	0.002156914
88	Gpr137b	G protein-coupled receptor 137B	1.26	8.68	8.07	3.31E-05	0.001539334
89	R74862	expressed sequence R74862	1.26	8.57	8.55	2.13E-05	0.001175007
90	Cfp	complement factor properdin	1.25	13.35	8.51	2.22E-05	0.001185616
91	Plp2	proteolipid protein 2	1.24	10.88	5.00	0.000937488	0.013156142
92	Blm	Bloom syndrome, RecQ helicase-like	1.23	10.01	10.89	3.33E-06	0.000389533
93	Slc29a3	solute carrier family 29 (nucleoside transporters), member 3	1.23	9.84	11.50	2.17E-06	0.000322971
94	Neo1	neogenin	1.23	8.29	5.97	0.00028734	0.006114237
95	Gpr34	G protein-coupled receptor 34	1.23	8.84	3.81	0.004793627	0.038587517
96	Lysmd2	LysM, putative peptidoglycan-binding, domain containing 2	1.22	8.80	9.68	8.32E-06	0.000643485
97	Optn	optineurin	1.22	8.75	8.54	2.16E-05	0.001177646
98	D10Wsu102e	DNA segment, Chr 10, Wayne State University 102, expressed	1.22	9.14	10.67	3.91E-06	0.000397578
99	Igsf9	immunoglobulin superfamily, member 9	1.22	8.76	8.60	2.06E-05	0.001143744
100	Hmgn3	high mobility group nucleosomal binding domain 3	1.21	11.16	4.63	0.001537694	0.018154491
101	Man1a	mannosidase 1, alpha	1.21	9.81	7.55	5.42E-05	0.002069558
102	Robo1	roundabout homolog 1 (Drosophila)	1.21	8.23	5.95	0.000295706	0.006190469
103	Hmgn3	high mobility group nucleosomal binding domain 3	1.21	11.28	3.69	0.005709615	0.043452096
104	Apoe	apolipoprotein E	1.20	9.14	5.38	0.000582464	0.009505843
105	Oosp1	oocyte secreted protein 1	1.20	10.03	3.57	0.006900257	0.049987767
106	Nsf	N-ethylmaleimide sensitive fusion protein	1.20	10.71	10.25	5.36E-06	0.0005051
107	Rap1gap2	RAP1 GTPase activating protein 2	1.19	9.90	5.20	0.000724814	0.011044987
108	Camk2d	calcium/calmodulin-dependent protein kinase II, delta	1.19	9.22	8.84	1.66E-05	0.001025724
109	Il10	interleukin 10	1.19	8.19	11.29	2.51E-06	0.000352016
110	Ticam2	toll-like receptor adaptor molecule 2	1.19	8.59	14.17	4.14E-07	0.000126365
111	NA	NA	1.18	8.92	7.95	3.69E-05	0.001646747
112	Sgk3	serum/glucocorticoid regulated kinase 3	1.18	9.77	14.40	3.65E-07	0.000126365
113	Tcstv1	2-cell-stage, variable group, member 1	1.18	8.27	4.56	0.001684377	0.019177893
114	Rilpl2	Rab interacting lysosomal protein-like 2	1.18	10.26	4.87	0.001106368	0.014432138
115	Dnase1l3	deoxyribonuclease 1-like 3	1.17	9.18	7.37	6.46E-05	0.002318592
116	Suclg2	succinate-Coenzyme A ligase, GDP-forming, beta subunit	1.17	10.23	3.86	0.004475495	0.036934103
117	NA	NA	1.17	9.63	4.38	0.002134617	0.022487262
118	Ivns1abp	influenza virus NS1A binding protein	1.16	10.99	5.23	0.000701269	0.010805477
119	Rtn4ip1	reticulon 4 interacting protein 1	1.16	8.44	8.02	3.46E-05	0.001575493
120	Gpm6a	glycoprotein m6a	1.16	8.19	13.33	6.77E-07	0.000167465
121	Tmem154	transmembrane protein 154	1.15	10.03	16.07	1.50E-07	8.74E-05
122	Cd59b	CD59b antigen	1.15	8.70	5.23	0.0007025	0.010805477
123	NA	NA	1.14	8.20	11.11	2.86E-06	0.000365287
124	Tbc1d5	TBC1 domain family, member 5	1.13	10.54	7.82	4.17E-05	0.00179651
125	Lrrc8a	leucine rich repeat containing 8A	1.13	8.66	5.80	0.000350171	0.006880043
126	Optn	optineurin	1.12	8.65	7.60	5.16E-05	0.002011249
127	Timd2	T cell immunoglobulin and mucin domain containing 2	1.12	8.33	8.74	1.82E-05	0.001056366
128	Cobll1	Cobl-like 1	1.11	9.58	7.97	3.61E-05	0.001626306

129	Gbp3	guanylate binding protein 3	1.10	11.00	7.46	5.93E-05	0.002191762
130	Ftsjd2	FtsJ methyltransferase domain containing 2	1.10	12.78	7.16	7.94E-05	0.002664622
131	Kctd12	potassium channel tetramerisation domain containing 12	1.10	9.91	7.79	4.30E-05	0.00181213
132	Chrnb1	cholinergic receptor, nicotinic, beta polypeptide 1 (muscle)	1.09	8.73	7.03	9.11E-05	0.002946967
133	Psmd14	proteasome (prosome, macropain) 26S subunit, non-ATPase, 14	1.09	10.25	8.53	2.17E-05	0.001177646
134	Irak2	interleukin-1 receptor-associated kinase 2	1.09	10.08	12.03	1.52E-06	0.000258979
135	Fcho2	FCH domain only 2	1.08	11.25	9.05	1.40E-05	0.000906822
136	Tnfsf4	tumor necrosis factor (ligand) superfamily, member 4	1.07	8.38	5.71	0.000389426	0.007374903
137	Hsp90ab1	heat shock protein 90 alpha (cytosolic), class B member 1	1.07	11.52	6.39	0.000179522	0.004550005
138	Fut8	fucosyltransferase 8	1.06	8.78	7.94	3.74E-05	0.001653635
139	Ryk	receptor-like tyrosine kinase	1.06	9.24	7.63	5.01E-05	0.001984949
140	Myadm	myeloid-associated differentiation marker	1.05	10.34	6.12	0.000242092	0.005562299
141	Tgif1	TGFB-induced factor homeobox 1	1.05	9.59	7.81	4.20E-05	0.001800796
142	Cobll1	Cobl-like 1	1.05	9.11	10.81	3.53E-06	0.00039538
143	Il15	interleukin 15	1.05	8.97	3.89	0.004302602	0.036006133
144	Ints4	integrator complex subunit 4	1.04	11.45	13.91	4.82E-07	0.000130244
145	Camk2n1	calcium/calmodulin-dependent protein kinase II inhibitor 1	1.04	8.74	4.50	0.001832528	0.02028317
146	Fert2	fer (fms/fps related) protein kinase, testis specific 2	1.04	8.04	13.68	5.50E-07	0.000144109
147	Gbp2	guanylate binding protein 2	1.03	8.47	7.78	4.32E-05	0.00181213
148	Aifm2	apoptosis-inducing factor, mitochondrion-associated 2	1.03	8.85	8.25	2.80E-05	0.00138606
149	F9	coagulation factor IX	1.03	8.67	9.68	8.30E-06	0.000643485
150	Ppfibp2	PTPRF interacting protein, binding protein 2 (liprin beta 2)	1.03	8.92	7.87	3.98E-05	0.001737923
151	Marcks	myristoylated alanine rich protein kinase C substrate	1.03	11.22	6.39	0.000179412	0.004550005
152	Sh3bgrl2	SH3 domain binding glutamic acid-rich protein like 2	1.03	8.48	4.36	0.002212342	0.023065033
153	Rab31	RAB31, member RAS oncogene family	1.02	10.80	4.78	0.001244962	0.015627613
154	Unc119	unc-119 homolog (C. elegans)	1.02	9.44	5.65	0.000422166	0.007726939
155	Cbfa2t3	core-binding factor, runt domain, alpha subunit 2, translocated to, 3 (human)	1.01	9.74	6.72	0.000125996	0.003600003
156	Ly96	lymphocyte antigen 96	1.01	9.80	5.08	0.000853268	0.012383256
157	NA	NA	1.01	10.56	8.60	2.06E-05	0.001143744
158	Irak2	interleukin-1 receptor-associated kinase 2	1.01	9.42	12.27	1.30E-06	0.000236954
159	Cyp51	cytochrome P450, family 51	1.01	9.19	5.56	0.000465437	0.008365629
160	Cyb5r2	cytochrome b5 reductase 2	1.00	8.00	4.16	0.002895417	0.027587193
161	Tmem38b	transmembrane protein 38B	-1.00	8.78	-8.49	2.25E-05	0.001195989
162	Sit1	suppression inducing transmembrane adaptor 1	-1.01	8.65	-8.52	2.20E-05	0.001183798
163	Fam117a	family with sequence similarity 117, member A	-1.02	10.61	-4.07	0.003303844	0.030200374
164	Abhd8	abhydrolase domain containing 8	-1.02	8.87	-9.44	1.01E-05	0.00074318
165	Rgcc	regulator of cell cycle	-1.02	9.66	-4.43	0.001991212	0.021459569
166	P2ry6	pyrimidinergic receptor P2Y, G-protein coupled, 6	-1.03	8.68	-6.88	0.000106007	0.003202773
167	Cyp27a1	cytochrome P450, family 27, subfamily a, polypeptide 1	-1.03	8.45	-6.08	0.000253691	0.005670363
168	Fcgrt	Fc receptor, IgG, alpha chain transporter	-1.03	9.14	-4.21	0.002699974	0.026333605
169	Rnf144a	ring finger protein 144A	-1.03	8.65	-6.75	0.000121862	0.003541023
170	Gm5483	predicted gene 5483	-1.04	8.51	-4.12	0.003099077	0.028885777
171	Gata3	GATA binding protein 3	-1.04	8.38	-12.33	1.26E-06	0.00023571
172	Ddit4	DNA-damage-inducible transcript 4	-1.04	10.01	-5.42	0.000556829	0.009225337

173	Mgst1	microsomal glutathione S-transferase 1	-1.05	8.54	-3.57	0.006872263	0.049887542
174	Nrp1	neuropilin 1	-1.05	8.57	-6.12	0.000243368	0.005575765
175	Frat2	frequently rearranged in advanced T cell lymphomas 2	-1.05	8.43	-11.89	1.67E-06	0.000270244
176	Brwd1	bromodomain and WD repeat domain containing 1	-1.05	9.29	-3.86	0.004465454	0.036920991
177	P2ry14	purinergic receptor P2Y, G-protein coupled, 14	-1.05	8.76	-9.39	1.05E-05	0.000754882
178	Gmfg	glia maturation factor, gamma	-1.06	11.65	-4.91	0.001051831	0.013994156
179	Akap12	A kinase (PRKA) anchor protein (gravin) 12	-1.06	8.18	-7.97	3.64E-05	0.001633462
180	Gpr83	G protein-coupled receptor 83	-1.06	8.47	-9.72	8.06E-06	0.000643485
181	Cd27	CD27 antigen	-1.06	8.66	-12.95	8.50E-07	0.000191956
182	Apol7c	apolipoprotein L 7c	-1.06	8.64	-6.23	0.000214469	0.005176085
183	Socs3	suppressor of cytokine signaling 3	-1.06	10.41	-6.32	0.00019337	0.004772354
184	Serpinb6a	serine (or cysteine) peptidase inhibitor, clade B, member 6a	-1.07	9.46	-8.26	2.78E-05	0.00138606
185	Hpgd	hydroxyprostaglandin dehydrogenase 15 (NAD)	-1.07	8.13	-5.49	0.000510547	0.008795466
186	Xdh	xanthine dehydrogenase	-1.07	8.70	-9.00	1.45E-05	0.000923744
187	Xcl1	chemokine (C motif) ligand 1	-1.07	8.29	-13.93	4.75E-07	0.000130244
188	Zap70	zeta-chain (TCR) associated protein kinase	-1.08	8.76	-7.71	4.62E-05	0.001888593
189	Lrig1	leucine-rich repeats and immunoglobulin-like domains 1	-1.08	8.39	-10.76	3.66E-06	0.00039567
190	Klhl6	kelch-like 6	-1.08	12.72	-4.80	0.001218916	0.015444675
191	Pilrb1	paired immunoglobin-like type 2 receptor beta 1	-1.08	8.38	-9.71	8.15E-06	0.000643485
192	Klra7	killer cell lectin-like receptor, subfamily A, member 7	-1.09	8.24	-6.95	9.86E-05	0.003077668
193	Stat4	signal transducer and activator of transcription 4	-1.09	8.58	-7.78	4.35E-05	0.001817277
194	Nsg2	neuron specific gene family member 2	-1.09	8.21	-5.72	0.000388558	0.007374903
195	Sepp1	selenoprotein P, plasma, 1	-1.09	9.20	-7.46	5.92E-05	0.002191762
196	Prkcq	protein kinase C, theta	-1.09	8.51	-9.26	1.17E-05	0.000820031
197	Gstk1	glutathione S-transferase kappa 1	-1.09	8.52	-10.55	4.26E-06	0.000429447
198	Arrdc4	arrestin domain containing 4	-1.09	8.62	-9.97	6.64E-06	0.000572834
199	Stard10	START domain containing 10	-1.10	9.46	-5.06	0.000867359	0.012512813
200	Fam189b	family with sequence similarity 189, member B	-1.10	8.64	-5.67	0.000407926	0.007601808
201	Acss2	acyl-CoA synthetase short-chain family member 2	-1.10	9.26	-4.55	0.001709577	0.019280562
202	Tnfaip8l2	tumor necrosis factor, alpha-induced protein 8-like 2	-1.10	9.45	-14.09	4.34E-07	0.000126365
203	Rab3d	RAB3D, member RAS oncogene family	-1.10	9.20	-6.95	9.83E-05	0.003077254
204	Lpl	lipoprotein lipase	-1.10	8.47	-7.03	9.09E-05	0.002946967
205	Smad1	SMAD family member 1	-1.10	8.66	-6.20	0.000221278	0.005282699
206	Cdk5r1	cyclin-dependent kinase 5, regulatory subunit 1 (p35)	-1.11	9.32	-4.76	0.001283768	0.015886479
207	Apobr	apolipoprotein B receptor	-1.11	8.51	-6.82	0.00011301	0.003305794
208	Nrn1	neuritin 1	-1.11	8.48	-5.92	0.000306885	0.006333433
209	Cd14	CD14 antigen	-1.12	8.42	-7.59	5.21E-05	0.002014325
210	Clec4b1	C-type lectin domain family 4, member b1	-1.12	8.45	-7.25	7.28E-05	0.00250334
211	Smad1	SMAD family member 1	-1.13	8.63	-8.82	1.70E-05	0.001044514
212	Slc11a1	solute carrier family 11 (proton-coupled divalent metal ion transporters), membe	-1.13	8.94	-5.50	0.000504008	0.008759984
213	Prkd3	protein kinase D3	-1.13	8.79	-5.06	0.000872332	0.012548754
214	Krt10	keratin 10	-1.13	8.55	-14.30	3.85E-07	0.000126365
215	Vopp1	vesicular, overexpressed in cancer, prosurvival protein 1	-1.13	9.30	-5.65	0.000419539	0.007700368
216	Nkg7	natural killer cell group 7 sequence	-1.14	11.33	-4.16	0.002918159	0.027732032

217	Tcf7	transcription factor 7, T cell specific	-1.14	8.18	-5.88	0.000321124	0.00652455
218	Klk1	kallikrein 1	-1.14	8.12	-4.59	0.001608869	0.018579935
219	Hcst	hematopoietic cell signal transducer	-1.15	10.76	-5.30	0.00064044	0.010185633
220	Lck	lymphocyte protein tyrosine kinase	-1.15	11.14	-5.56	0.000467913	0.008365629
221	LOC547323	uncharacterized LOC547323	-1.15	8.57	-12.71	9.89E-07	0.000212413
222	NA	NA	-1.16	8.67	-10.00	6.49E-06	0.000571
223	Tmem66	transmembrane protein 66	-1.16	9.48	-7.35	6.56E-05	0.002342512
224	Pygl	liver glycogen phosphorylase	-1.17	9.54	-3.58	0.006723284	0.049085591
225	Cst3	cystatin C	-1.17	12.82	-6.51	0.000156878	0.004170149
226	Kmo	kynurenine 3-monooxygenase (kynurenine 3-hydroxylase)	-1.17	8.51	-7.15	8.07E-05	0.002684506
227	Ear10	eosinophil-associated, ribonuclease A family, member 10	-1.18	8.48	-7.67	4.80E-05	0.001904754
228	Hist1h1c	histone cluster 1, H1c	-1.18	10.21	-10.20	5.56E-06	0.000513086
229	Acpl2	acid phosphatase-like 2	-1.18	8.76	-7.89	3.91E-05	0.001713178
230	Pi16	peptidase inhibitor 16	-1.19	8.55	-6.92	0.000102002	0.003130533
231	NA	NA	-1.20	8.87	-15.10	2.49E-07	0.000112734
232	Prkd3	protein kinase D3	-1.21	9.48	-4.03	0.003499375	0.031290611
233	Nrp1	neuropilin 1	-1.21	8.85	-5.06	0.000867924	0.012512813
234	Anxa1	annexin A1	-1.21	8.46	-4.22	0.002662353	0.026134882
235	Il27ra	interleukin 27 receptor, alpha	-1.22	11.04	-9.74	7.94E-06	0.000643485
236	Selplg	selectin, platelet (p-selectin) ligand	-1.22	10.59	-7.42	6.13E-05	0.002226548
237	Lpar6	lysophosphatidic acid receptor 6	-1.22	10.65	-12.22	1.35E-06	0.000242138
238	Ppic	peptidylprolyl isomerase C	-1.23	8.33	-4.05	0.003389681	0.030741707
239	Sh2d2a	SH2 domain protein 2A	-1.23	10.75	-5.55	0.000476	0.008464011
240	Ear12	eosinophil-associated, ribonuclease A family, member 12	-1.23	8.60	-10.75	3.69E-06	0.00039567
241	Hvcn1	hydrogen voltage-gated channel 1	-1.24	12.02	-5.22	0.000712795	0.010897018
242	Sun2	Sad1 and UNC84 domain containing 2	-1.25	11.74	-10.93	3.24E-06	0.000384201
243	Fyb	FYN binding protein	-1.25	9.43	-9.69	8.24E-06	0.000643485
244	Fxyd5	FXYD domain-containing ion transport regulator 5	-1.25	10.04	-7.25	7.25E-05	0.00250152
245	Lrrk2	leucine-rich repeat kinase 2	-1.26	9.33	-3.86	0.004483801	0.036956105
246	Neurl3	neuralized homolog 3 homolog (Drosophila)	-1.27	8.57	-9.06	1.38E-05	0.000901477
247	NA	NA	-1.28	9.30	-14.09	4.34E-07	0.000126365
248	Sit1	suppression inducing transmembrane adaptor 1	-1.28	8.95	-10.25	5.34E-06	0.0005051
249	Foxp3	forkhead box P3	-1.28	8.88	-11.28	2.52E-06	0.000352016
250	Klf13	Kruppel-like factor 13	-1.29	10.80	-7.22	7.52E-05	0.002573373
251	Cd160	CD160 antigen	-1.29	8.72	-8.53	2.17E-05	0.001177646
252	Fas	Fas (TNF receptor superfamily member 6)	-1.29	8.97	-9.43	1.02E-05	0.00074318
253	Ifngr1	interferon gamma receptor 1	-1.29	9.89	-7.94	3.72E-05	0.001650647
254	Fam78a	family with sequence similarity 78, member A	-1.30	11.06	-6.07	0.000258382	0.005742531
255	Osm	oncostatin M	-1.30	9.04	-17.16	8.87E-08	7.20E-05
256	Asb2	ankyrin repeat and SOCS box-containing 2	-1.30	9.77	-7.78	4.33E-05	0.00181213
257	Tyrobp	TYRO protein tyrosine kinase binding protein	-1.31	9.68	-8.30	2.69E-05	0.001355341
258	Casp1	caspase 1	-1.32	11.79	-5.17	0.000758776	0.01139033
259	Bcl7a	B cell CLL/lymphoma 7A	-1.32	9.92	-9.88	7.12E-06	0.000602323
260	Cd247	CD247 antigen	-1.32	9.05	-12.17	1.39E-06	0.0002457

261	Zfp36	zinc finger protein 36	-1.33	11.52	-10.17	5.67E-06	0.000519334
262	Myo1f	myosin IF	-1.33	9.89	-6.64	0.000137512	0.003809939
263	Gpr68	G protein-coupled receptor 68	-1.34	8.89	-12.97	8.39E-07	0.000191956
264	Ephx1	epoxide hydrolase 1, microsomal	-1.34	10.81	-8.48	2.28E-05	0.001199946
265	Tacstd2	tumor-associated calcium signal transducer 2	-1.35	8.54	-15.12	2.46E-07	0.000112734
266	Itgad	integrin, alpha D	-1.35	8.45	-6.40	0.000178721	0.004550005
267	Tcf7	transcription factor 7, T cell specific	-1.36	8.57	-6.99	9.46E-05	0.003022162
268	Rgs10	regulator of G-protein signalling 10	-1.36	9.95	-13.03	8.11E-07	0.000189903
269	Sep9	septin 9	-1.37	8.95	-8.86	1.63E-05	0.001013828
270	Cd8b1	CD8 antigen, beta chain 1	-1.37	9.16	-3.66	0.005982465	0.045057589
271	Sema4a	sema domain, immunoglobulin domain (Ig), transmembrane domain (TM) and s	-1.37	10.37	-9.41	1.04E-05	0.000750419
272	Csf3r	colony stimulating factor 3 receptor (granulocyte)	-1.37	8.57	-10.39	4.81E-06	0.00047416
273	F13a1	coagulation factor XIII, A1 subunit	-1.37	8.55	-6.71	0.000126752	0.003600003
274	Tmem51	transmembrane protein 51	-1.38	9.54	-5.82	0.000341886	0.006791276
275	Gpr171	G protein-coupled receptor 171	-1.38	9.82	-17.78	6.65E-08	7.20E-05
276	Glipr2	GLI pathogenesis-related 2	-1.38	10.42	-8.98	1.48E-05	0.000927095
277	Csrp2	cysteine and glycine-rich protein 2	-1.39	8.74	-14.65	3.17E-07	0.000126365
278	Dusp2	dual specificity phosphatase 2	-1.39	9.31	-9.72	8.02E-06	0.000643485
279	Sostdc1	sclerostin domain containing 1	-1.41	8.64	-4.41	0.002053933	0.021870864
280	Ccr6	chemokine (C-C motif) receptor 6	-1.42	9.02	-6.59	0.000144894	0.003946706
281	Igfbp4	insulin-like growth factor binding protein 4	-1.42	8.50	-5.22	0.000711049	0.010897018
282	Sort1	sortilin 1	-1.42	9.14	-9.58	8.99E-06	0.000680709
283	Fpr2	formyl peptide receptor 2	-1.43	11.21	-4.16	0.002929021	0.027754753
284	Fxyd5	FXYD domain-containing ion transport regulator 5	-1.44	11.88	-7.42	6.12E-05	0.002226548
285	Klra4	killer cell lectin-like receptor, subfamily A, member 4	-1.45	8.77	-14.12	4.26E-07	0.000126365
286	Cmc1	COX assembly mitochondrial protein 1	-1.45	10.24	-8.41	2.43E-05	0.001241645
287	Myl4	myosin, light polypeptide 4	-1.45	10.47	-6.37	0.000183946	0.004612847
288	Dennd3	DENN/MADD domain containing 3	-1.46	10.21	-3.97	0.003801274	0.033188335
289	Hsd11b1	hydroxysteroid 11-beta dehydrogenase 1	-1.46	9.49	-14.72	3.06E-07	0.000126365
290	Csf3r	colony stimulating factor 3 receptor (granulocyte)	-1.47	8.43	-17.60	7.20E-08	7.20E-05
291	F2r	coagulation factor II (thrombin) receptor	-1.48	10.49	-7.14	8.10E-05	0.002688196
292	Fxyd5	FXYD domain-containing ion transport regulator 5	-1.48	10.46	-9.09	1.34E-05	0.000886427
293	Klre1	killer cell lectin-like receptor family E member 1	-1.48	8.64	-9.52	9.47E-06	0.000711445
294	Trib2	tribbles homolog 2 (Drosophila)	-1.50	9.82	-8.80	1.72E-05	0.001046831
295	Neurl3	neuralized homolog 3 homolog (Drosophila)	-1.50	8.63	-8.74	1.81E-05	0.001056366
296	Ctnna1	catenin (cadherin associated protein), alpha 1	-1.51	9.75	-15.87	1.67E-07	8.74E-05
297	Bcl11b	B cell leukemia/lymphoma 11B	-1.52	10.28	-5.81	0.000345715	0.006826447
298	Tmem108	transmembrane protein 108	-1.52	8.48	-10.23	5.44E-06	0.000509109
299	Cyp27a1	cytochrome P450, family 27, subfamily a, polypeptide 1	-1.52	9.00	-10.72	3.77E-06	0.00039567
300	Csf1r	colony stimulating factor 1 receptor	-1.52	9.68	-4.30	0.002397836	0.024405413
301	Gpc1	glypican 1	-1.52	9.28	-10.92	3.25E-06	0.000384201
302	Fcer2a	Fc receptor, IgE, low affinity II, alpha polypeptide	-1.55	8.61	-7.02	9.20E-05	0.002950886
303	Gcnt2	glucosaminyl (N-acetyl) transferase 2, I-branching enzyme	-1.55	9.28	-9.91	6.92E-06	0.000592709
304	Zap70	zeta-chain (TCR) associated protein kinase	-1.56	10.13	-12.46	1.15E-06	0.000226433

305	Chst1	carbohydrate (keratan sulfate Gal-6) sulfotransferase 1	-1.56	9.18	-4.94	0.001016143	0.013686077
306	Hvcn1	hydrogen voltage-gated channel 1	-1.56	11.55	-9.26	1.16E-05	0.000820031
307	Cdc42ep3	CDC42 effector protein (Rho GTPase binding) 3	-1.57	9.86	-10.46	4.57E-06	0.000453629
308	Cxcr3	chemokine (C-X-C motif) receptor 3	-1.59	9.84	-8.07	3.31E-05	0.001539334
309	Leprotl1	leptin receptor overlapping transcript-like 1	-1.61	10.19	-12.28	1.30E-06	0.000236954
310	Mmp9	matrix metallopeptidase 9	-1.61	9.03	-4.50	0.001814258	0.020131968
311	Gpr114	G protein-coupled receptor 114	-1.61	9.43	-7.29	6.97E-05	0.002424401
312	Ffar2	free fatty acid receptor 2	-1.61	9.67	-4.83	0.001168508	0.015027774
313	Pacsin1	protein kinase C and casein kinase substrate in neurons 1	-1.62	9.02	-7.53	5.52E-05	0.002097544
314	Lyz1	lysozyme 1	-1.62	14.55	-9.75	7.87E-06	0.000643485
315	Clec7a	C-type lectin domain family 7, member a	-1.62	8.95	-14.82	2.89E-07	0.000126365
316	Clec4d	C-type lectin domain family 4, member d	-1.64	8.80	-7.18	7.80E-05	0.002639989
317	Ngfrap1	nerve growth factor receptor (TNFRSF16) associated protein 1	-1.64	9.86	-8.08	3.27E-05	0.001539334
318	Rab32	RAB32, member RAS oncogene family	-1.64	9.66	-10.97	3.15E-06	0.000382174
319	Mt1	metallothionein 1	-1.65	10.74	-4.34	0.002276487	0.023602341
320	Cyp27a1	cytochrome P450, family 27, subfamily a, polypeptide 1	-1.65	8.74	-9.01	1.44E-05	0.00092333
321	Sgk1	serum/glucocorticoid regulated kinase 1	-1.65	10.28	-7.75	4.46E-05	0.001845096
322	Lgmn	legumain	-1.65	10.49	-7.38	6.39E-05	0.002306549
323	Itk	IL2 inducible T cell kinase	-1.66	9.64	-7.55	5.41E-05	0.002069558
324	Tmem66	transmembrane protein 66	-1.66	11.10	-6.92	0.000101909	0.003130533
325	Sort1	sortilin 1	-1.66	9.30	-10.09	6.06E-06	0.000540025
326	Tmem66	transmembrane protein 66	-1.67	11.01	-4.80	0.001212497	0.015397073
327	Arap3	ArfGAP with RhoGAP domain, ankyrin repeat and PH domain 3	-1.67	9.00	-8.54	2.17E-05	0.001177646
328	Ramp1	receptor (calcitonin) activity modifying protein 1	-1.69	8.75	-7.93	3.77E-05	0.001662267
329	St6galnac2	ST6 (alpha-N-acetyl-neuraminyl-2,3-beta-galactosyl-1,3)-N-acetylgalactosamini	-1.69	9.92	-13.38	6.54E-07	0.000164898
330	Pglyrp1	peptidoglycan recognition protein 1	-1.69	10.42	-4.91	0.001058114	0.014063476
331	Serpinb1a	serine (or cysteine) peptidase inhibitor, clade B, member 1a	-1.70	9.57	-9.08	1.35E-05	0.000886427
332	Ifitm3	interferon induced transmembrane protein 3	-1.72	11.17	-6.49	0.000160495	0.004214998
333	Hp	haptoglobin	-1.72	9.14	-4.28	0.002457471	0.024849662
334	Lmo2	LIM domain only 2	-1.72	11.85	-14.32	3.80E-07	0.000126365
335	Cd3e	CD3 antigen, epsilon polypeptide	-1.74	10.70	-10.78	3.61E-06	0.00039567
336	Tgfbi	transforming growth factor, beta induced	-1.74	9.71	-11.93	1.62E-06	0.000270244
337	Xlr4a	X-linked lymphocyte-regulated 4A	-1.74	11.46	-12.47	1.15E-06	0.000226433
338	Dok2	docking protein 2	-1.79	9.77	-7.16	7.95E-05	0.002664622
339	Zfp608	zinc finger protein 608	-1.79	8.70	-9.44	1.01E-05	0.00074318
340	Cd6	CD6 antigen	-1.80	9.99	-13.13	7.62E-07	0.00018156
341	NA	NA	-1.80	9.99	-8.21	2.90E-05	0.001422116
342	Tnfrsf4	tumor necrosis factor receptor superfamily, member 4	-1.81	10.02	-7.35	6.59E-05	0.002347302
343	Zyx	zyxin	-1.81	12.54	-12.12	1.44E-06	0.000248712
344	Hsd11b1	hydroxysteroid 11-beta dehydrogenase 1	-1.82	9.90	-18.01	5.98E-08	7.20E-05
345	Dusp2	dual specificity phosphatase 2	-1.82	10.38	-11.63	2.00E-06	0.000307633
346	Dgka	diacylglycerol kinase, alpha	-1.82	10.89	-7.18	7.82E-05	0.002642851
347	Lat	linker for activation of T cells	-1.83	10.61	-16.23	1.39E-07	8.74E-05
348	Tiam1	T cell lymphoma invasion and metastasis 1	-1.83	9.29	-10.33	5.03E-06	0.000491624

349	Trf	transferrin	-1.85	9.00	-6.84	0.000111008	0.003276496
350	NA	NA	-1.87	8.91	-8.06	3.35E-05	0.001544265
351	Gadd45g	growth arrest and DNA-damage-inducible 45 gamma	-1.90	10.08	-9.22	1.21E-05	0.000832985
352	Bcl6	B cell leukemia/lymphoma 6	-1.91	10.44	-8.08	3.29E-05	0.001539334
353	Dgka	diacylglycerol kinase, alpha	-1.91	11.54	-6.59	0.000144058	0.003943894
354	Il18r1	interleukin 18 receptor 1	-1.93	9.89	-17.37	8.04E-08	7.20E-05
355	C1qc	complement component 1, q subcomponent, C chain	-1.93	9.22	-11.44	2.27E-06	0.000333942
356	Fcgr3	Fc receptor, IgG, low affinity III	-1.93	9.07	-5.93	0.000302045	0.006253232
357	Cd6	CD6 antigen	-1.94	10.43	-11.40	2.32E-06	0.000338092
358	Hsd11b1	hydroxysteroid 11-beta dehydrogenase 1	-1.96	10.48	-23.34	7.23E-09	1.90E-05
359	Il7r	interleukin 7 receptor	-1.96	10.42	-9.99	6.53E-06	0.000571
360	Cd3g	CD3 antigen, gamma polypeptide	-1.98	11.13	-11.02	3.05E-06	0.000376611
361	Pxdc1	PX domain containing 1	-1.98	9.32	-9.14	1.29E-05	0.000864652
362	Tmem176b	transmembrane protein 176B	-2.00	9.68	-12.43	1.17E-06	0.000226433
363	Cd8b1	CD8 antigen, beta chain 1	-2.02	12.18	-5.97	0.000289485	0.006114237
364	Igfbp4	insulin-like growth factor binding protein 4	-2.04	8.88	-7.02	9.21E-05	0.002950886
365	Cd6	CD6 antigen	-2.05	10.96	-9.43	1.02E-05	0.00074318
366	Emb	embigin	-2.06	9.96	-15.10	2.49E-07	0.000112734
367	Ear4	eosinophil-associated, ribonuclease A family, member 4	-2.07	9.25	-8.97	1.48E-05	0.000927095
368	Fcer2a	Fc receptor, IgE, low affinity II, alpha polypeptide	-2.07	9.04	-9.09	1.35E-05	0.000886427
369	Cd27	CD27 antigen	-2.08	11.11	-17.27	8.41E-08	7.20E-05
370	Klk8	kallikrein related-peptidase 8	-2.09	9.80	-8.60	2.05E-05	0.001143744
371	Ifitm6	interferon induced transmembrane protein 6	-2.10	9.77	-5.07	0.000859724	0.012443619
372	C1qb	complement component 1, q subcomponent, beta polypeptide	-2.10	9.58	-11.12	2.82E-06	0.000365287
373	Lyz2	lysozyme 2	-2.12	12.10	-15.93	1.62E-07	8.74E-05
374	Ly6c1	lymphocyte antigen 6 complex, locus C1	-2.14	10.49	-6.17	0.000228945	0.005376928
375	Lgals3	lectin, galactose binding, soluble 3	-2.15	11.95	-11.17	2.73E-06	0.000364587
376	Stat4	signal transducer and activator of transcription 4	-2.17	10.16	-10.82	3.52E-06	0.00039538
377	B3gnt8	UDP-GlcNAc:betaGal beta-1,3-N-acetylglucosaminyltransferase 8	-2.17	10.18	-14.13	4.23E-07	0.000126365
378	Cd3d	CD3 antigen, delta polypeptide	-2.18	10.96	-13.89	4.87E-07	0.000130244
379	Sirpb1a	signal-regulatory protein beta 1A	-2.19	9.88	-16.08	1.50E-07	8.74E-05
380	Ccr6	chemokine (C-C motif) receptor 6	-2.19	10.34	-5.75	0.000374546	0.007176066
381	Il4i1	interleukin 4 induced 1	-2.22	11.72	-7.69	4.75E-05	0.00190209
382	Thy1	thymus cell antigen 1, theta	-2.24	10.76	-10.21	5.49E-06	0.000510469
383	Ifitm2	interferon induced transmembrane protein 2	-2.25	10.80	-10.10	6.01E-06	0.000539159
384	Ccl9	chemokine (C-C motif) ligand 9	-2.27	9.39	-13.17	7.42E-07	0.000180048
385	Dpp4	dipeptidylpeptidase 4	-2.28	10.18	-11.69	1.91E-06	0.000303211
386	Ctsw	cathepsin W	-2.28	10.26	-14.53	3.40E-07	0.000126365
387	Klrd1	killer cell lectin-like receptor, subfamily D, member 1	-2.29	9.84	-10.70	3.83E-06	0.00039567
388	Il1b	interleukin 1 beta	-2.31	9.62	-12.15	1.41E-06	0.000246908
389	Axl	AXL receptor tyrosine kinase	-2.33	9.65	-9.10	1.33E-05	0.000885286
390	Lyz2	lysozyme 2	-2.33	13.02	-10.27	5.28E-06	0.0005051
391	Hp	haptoglobin	-2.34	9.83	-5.82	0.000344727	0.006824249
392	S100a9	S100 calcium binding protein A9 (calgranulin B)	-2.35	12.85	-4.01	0.003592089	0.031897675

393	Ear2	eosinophil-associated, ribonuclease A family, member 2	-2.44	9.87	-10.97	3.14E-06	0.000382174
394	Prg2	proteoglycan 2, bone marrow	-2.50	9.43	-26.42	2.61E-09	1.14E-05
395	Vcam1	vascular cell adhesion molecule 1	-2.53	9.44	-10.93	3.24E-06	0.000384201
396	Alox5ap	arachidonate 5-lipoxygenase activating protein	-2.53	10.63	-12.50	1.12E-06	0.000226433
397	Chchd10	coiled-coil-helix-coiled-coil-helix domain containing 10	-2.60	11.67	-23.74	6.28E-09	1.90E-05
398	Chi3l3	chitinase 3-like 3	-2.63	10.46	-3.92	0.004099802	0.034940263
399	Fcna	ficolin A	-2.74	9.51	-14.52	3.40E-07	0.000126365
400	Fcer2a	Fc receptor, IgE, low affinity II, alpha polypeptide	-2.90	9.99	-9.64	8.61E-06	0.000659489
401	Satb1	special AT-rich sequence binding protein 1	-2.92	11.26	-9.26	1.17E-05	0.000820031
402	Slc40a1	solute carrier family 40 (iron-regulated transporter), member 1	-2.98	10.90	-16.03	1.54E-07	8.74E-05
403	Vpreb3	pre-B lymphocyte gene 3	-3.59	10.07	-26.45	2.58E-09	1.14E-05
404	Slpi	secretory leukocyte peptidase inhibitor	-3.67	11.58	-6.89	0.000105045	0.003186622

Column headings:

LogFC: Log2-fold of change between TRAF3-/- B lymphomas and LMC spleens

AveExpr: average expression level for both conditions (LMC and TRAF3-/-)

t: the t-statistic

P. Value: the p value based on the t-statistic

Adj. P. Val.: the p value adjusted for multiple measurements (essentially the false discovery rate)

The mRNA expression profiles of splenocytes from LMC and tumor-bearing B-TRAF3-/- mice (mouse ID: 6983-2, 7041-10, and 7060-8) were analyzed by a microarray analysis. cRNA was hybridized to Illumina Sentrix Mouse Whole Genome 24K Microarray (Illumina). We determined two group comparisons of the normalized data for triplicate samples using paired t tests and false discovery rate. Genes listed include 160 up-regulated and 244 down-regulated genes (fold of change: >2).

Supplementary Table 2. The MCC-interactome in human MM cells identified by affinity purification followed by LC-MS/MS

#	Accession	Description	SwissProt ID	Average spectral count difference (hMCC-SBP-6xHis - FLAG-hMCC)		Previously known MCC-interactor
				Mitochondria	Whole lysates	
NA	P23508	Colorectal mutant cancer protein	CRCM_HUMAN	415	1223	Not applicable
1	P23508-2	Isoform 2 of Colorectal mutant cancer protein	CRCM_HUMAN	395.5	1172.5	No
2	P09874	Poly [ADP-ribose] polymerase 1	PARP1_HUMAN	72	43.5	No
3	O15020-2	Isoform 2 of Spectrin beta chain, non-erythrocytic 2	SPTN2_HUMAN	34	3	No
4	P40939	Trifunctional enzyme subunit alpha, mitochondrial	ECHA_HUMAN	31	24	No
5	P05141	ADP/ATP translocase 2	ADT2_HUMAN	24	33.5	No
6	P12236	ADP/ATP translocase 3	ADT3_HUMAN	20.5	27.5	No
7	P06576	ATP synthase subunit beta, mitochondrial	ATPB_HUMAN	18.5	19.5	No
8	Q99623	Prohibitin-2	PHB2_HUMAN	17	23.5	Yes (Ewing, 2007)
9	Q13576	Ras GTPase-activating-like protein IQGAP2	IQGA2_HUMAN	16	50	No
10	P12235	ADP/ATP translocase 1	ADT1_HUMAN	15.5	24	No
11	Q9Y277	Voltage-dependent anion-selective channel protein 3	VDAC3_HUMAN	15.5	2.5	No
12	Q02880-2	Isoform Beta-1 of DNA topoisomerase 2-beta	TOP2B_HUMAN	14.5	12.5	No
13	O60264	SWI/SNF-related matrix-associated actin-dependent regulator	SMCA5_HUMAN	13.5	2	No
14	P35232	Prohibitin	PHB_HUMAN	13	3.5	No
15	O00571	ATP-dependent RNA helicase DDX3X	DDX3X_HUMAN	12	17.5	No
16	P13674	Prolyl 4-hydroxylase subunit alpha-1	P4HA1_HUMAN	12	9	No
17	Q9Y2X3	Nucleolar protein 58	NOP58_HUMAN	11.5	10.5	No
18	P13674-2	Isoform 2 of Prolyl 4-hydroxylase subunit alpha-1	P4HA1_HUMAN	11	8.5	No
19	P16403	Histone H1.2	H12_HUMAN	9.5	8.5	Yes (Sigglekow, 2012)
20	P13796	Plastin-2	PLSL_HUMAN	9.5	7.5	No
21	P42166	Lamina-associated polypeptide 2, isoform alpha	LAP2A_HUMAN	9	19.5	No
22	P46940	Ras GTPase-activating-like protein IQGAP1	IQGA1_HUMAN	8	31	No
23	P47756-2	Isoform 2 of F-actin-capping protein subunit beta	CAPZB_HUMAN	7.5	6.5	Yes (Ewing, 2007)
24	P06493	Cyclin-dependent kinase 1	CDK1_HUMAN	7	8	No
25	P12956	X-ray repair cross-complementing protein 6	XRCC6_HUMAN	7	6.5	No
26	P35251-2	Isoform 2 of Replication factor C subunit 1	RFC1_HUMAN	7	3.5	No
27	Q14974	Importin subunit beta-1	IMB1_HUMAN	6.5	18	No
28	P78371	T-complex protein 1 subunit beta	TCPB_HUMAN	6.5	12	No
29	Q9Y5B9	FACT complex subunit SPT16	SP16H_HUMAN	6.5	6	Yes (Ewing, 2007)
30	Q86UE4	Protein LYRIC	LYRIC_HUMAN	6.5	3.5	No
31	Q9BVP2-2	Isoform 2 of Guanine nucleotide-binding protein-like 3	GNL3_HUMAN	6.5	1	No
32	Q5T4S7-3	Isoform 3 of E3 ubiquitin-protein ligase UBR4	UBR4_HUMAN	6	69	No
33	Q96ER9	Coiled-coil domain-containing protein 51	CCD51_HUMAN	6	17	No
34	P31689	DnaJ homolog subfamily A member 1	DNJA1_HUMAN	6	14.5	No
35	P63092	Guanine nucleotide-binding protein G(s) subunit alpha isoforms	GNAS2_HUMAN	6	5.5	No
36	P53621	Coatomer subunit alpha	COPA_HUMAN	6	5	No
37	P22732	Solute carrier family 2, facilitated glucose transporter member 5	GTR5_HUMAN	6	4	No

38	P63092-2	Isoform Gnas-2 of Guanine nucleotide-binding protein G(s) sub	GNAS2_HUMAN	5.5	5.5	No
39	P63092-3	Isoform 3 of Guanine nucleotide-binding protein G(s) subunit al	GNAS2_HUMAN	5.5	5	No
40	Q14839	Chromodomain-helicase-DNA-binding protein 4	CHD4_HUMAN	5.5	4.5	No
41	Q8NI36	WD repeat-containing protein 36	WDR36_HUMAN	5.5	4	No
42	P17858	6-phosphofructokinase, liver type	K6PL_HUMAN	5	6.5	No
43	P30041	Peroxiredoxin-6	PRDX6_HUMAN	5	6	No
44	Q9P035	Very-long-chain (3R)-3-hydroxyacyl-[acyl-carrier protein] dehydı	HACD3_HUMAN	5	6	No
45	P18754	Regulator of chromosome condensation	RCC1_HUMAN	5	4.5	No
46	Q9BSD7	Cancer-related nucleoside-triphosphatase	NTPCR_HUMAN	5	4	No
47	P62873	Guanine nucleotide-binding protein G(I)/G(S)/G(T) subunit beta	GBB1_HUMAN	5	3.5	Yes (Ewing, 2007)
48	O94874	E3 UFM1-protein ligase 1	UFL1_HUMAN	5	3	No
49	O95299	NADH dehydrogenase [ubiquinone] 1 alpha subcomplex subun	NDUAA_HUMAN	5	3	No
50	Q9UQE7	Structural maintenance of chromosomes protein 3	SMC3_HUMAN	4.5	24	Yes (Ewing, 2007)
51	P62136	Serine/threonine-protein phosphatase PP1-alpha catalytic subu	PP1A_HUMAN	4.5	8.5	No
52	Q14157	Ubiquitin-associated protein 2-like	UBP2L_HUMAN	4.5	7	No
53	O75534-2	Isoform Short of Cold shock domain-containing protein E1	CSDE1_HUMAN	4.5	5	Yes (Ewing, 2007)
54	Q00013	55 kDa erythrocyte membrane protein	EM55_HUMAN	4.5	2.5	No
55	P17480-2	Isoform UBF2 of Nucleolar transcription factor 1	UBF1_HUMAN	4.5	2.5	No
56	Q01813	6-phosphofructokinase type C	K6PP_HUMAN	4.5	2	Yes (Ewing, 2007)
57	Q9UIG0-2	Isoform 2 of Tyrosine-protein kinase BAZ1B	BAZ1B_HUMAN	4.5	2	No
58	P33991	DNA replication licensing factor MCM4	MCM4_HUMAN	4	27	Yes (Ewing, 2007)
59	Q92973-2	Isoform 2 of Transportin-1	TNPO1_HUMAN	4	15.5	No
60	Q08945	FACT complex subunit SSRP1	SSRP1_HUMAN	4	9.5	Yes (Ewing, 2007)
61	Q13242	Serine/arginine-rich splicing factor 9	SRSF9_HUMAN	4	5	No
62	P23528	Cofilin-1	COF1_HUMAN	4	4	No
63	Q92922	SWI/SNF complex subunit SMARCC1	SMRC1_HUMAN	4	3.5	No
64	Q14699	Raftlin	RFTN1_HUMAN	4	3	No
65	O94826	Mitochondrial import receptor subunit TOM70	TOM70_HUMAN	4	2.5	No
66	P51531-2	Isoform Short of Probable global transcription activator SNF2L2	SMCA2_HUMAN	4	2.5	No
67	Q9UQ80	Proliferation-associated protein 2G4	PA2G4_HUMAN	4	2	No
68	O43396	Thioredoxin-like protein 1	TXNL1_HUMAN	3.5	15.5	No
69	O60884	DnaJ homolog subfamily A member 2	DNJA2_HUMAN	3.5	10	No
70	P36873	Serine/threonine-protein phosphatase PP1-gamma catalytic sul	PP1G_HUMAN	3.5	8.5	No
71	P53985	Monocarboxylate transporter 1	MOT1_HUMAN	3.5	8.5	No
72	P40938	Replication factor C subunit 3	RFC3_HUMAN	3.5	4.5	No
73	Q53HL2	Borealin	BOREA_HUMAN	3.5	4	No
74	P21912	Succinate dehydrogenase [ubiquinone] iron-sulfur subunit, mito	DHSB_HUMAN	3.5	3.5	Yes (Ewing, 2007)
75	Q86WU2-2	Isoform 2 of Probable D-lactate dehydrogenase, mitochondrial	LDHD_HUMAN	3.5	3.5	No
76	Q96JB5	CDK5 regulatory subunit-associated protein 3	CK5P3_HUMAN	3.5	3	No
77	O95563	Mitochondrial pyruvate carrier 2	MPC2_HUMAN	3.5	2.5	No
78	Q96QK1	Vacuolar protein sorting-associated protein 35	VPS35_HUMAN	3.5	2.5	Yes (Ewing, 2007)
79	Q9BZQ8	Protein Niban	NIBAN_HUMAN	3.5	1.5	No
80	O14773-2	Isoform 2 of Tripeptidyl-peptidase 1	TPP1_HUMAN	3.5	1.5	No
81	Q92945	Far upstream element-binding protein 2	FUBP2_HUMAN	3	7.5	No

82	Q9P0L0	Vesicle-associated membrane protein-associated protein A	VAPA_HUMAN	3	6	No
83	Q15181	Inorganic pyrophosphatase	IPYR_HUMAN	3	5.5	No
84	Q12788	Transducin beta-like protein 3	TBL3_HUMAN	3	5	No
85	O95573	Long-chain-fatty-acid--CoA ligase 3	ACSL3_HUMAN	3	4.5	No
86	Q02978	Mitochondrial 2-oxoglutarate/malate carrier protein	M2OM_HUMAN	3	3	No
87	Q9UKM7	Endoplasmic reticulum mannosyl-oligosaccharide 1,2-alpha-ma	MA1B1_HUMAN	3	3	No
88	Q7Z3B4	Nucleoporin p54	NUP54_HUMAN	3	2	No
89	P42224	Signal transducer and activator of transcription 1-alpha/beta	STAT1_HUMAN	3	2	No
90	Q99733	Nucleosome assembly protein 1-like 4	NP1L4_HUMAN	3	2	No
91	P35998	26S protease regulatory subunit 7	PRS7_HUMAN	2.5	10	No
92	P12004	Proliferating cell nuclear antigen	PCNA_HUMAN	2.5	8.5	Yes (Ewing, 2007)
93	O00299	Chloride intracellular channel protein 1	CLIC1_HUMAN	2.5	8.5	Yes (Ewing, 2007)
94	O75083	WD repeat-containing protein 1	WDR1_HUMAN	2.5	5.5	No
95	Q9Y3F4	Serine-threonine kinase receptor-associated protein	STRAP_HUMAN	2.5	5	No
96	P43358	Melanoma-associated antigen 4	MAGA4_HUMAN	2.5	5	No
97	Q08752	Peptidyl-prolyl cis-trans isomerase D	PPID_HUMAN	2.5	5	No
98	O43175	D-3-phosphoglycerate dehydrogenase	SERA_HUMAN	2.5	4.5	No
99	Q9GZS3	WD repeat-containing protein 61	WDR61_HUMAN	2.5	4	No
100	P53701	Cytochrome c-type heme lyase	CCHL_HUMAN	2.5	4	No
101	Q14258	E3 ubiquitin/ISG15 ligase TRIM25	TRI25_HUMAN	2.5	3.5	No
102	P35249	Replication factor C subunit 4	RFC4_HUMAN	2.5	3	No
103	P51159	Ras-related protein Rab-27A	RB27A_HUMAN	2.5	3	No
104	P07741	Adenine phosphoribosyltransferase]	APT_HUMAN	2.5	2.5	Yes (Ewing, 2007)
105	Q96HE7	ERO1-like protein alpha	ERO1A_HUMAN	2.5	2.5	No
106	Q8WYP5	Protein ELYS	ELYS_HUMAN	2.5	2.5	No
107	Q9H0U3	Magnesium transporter protein 1	MAGT1_HUMAN	2.5	1.5	No
108	O15400-2	Isoform 2 of Syntaxin-7	STX7_HUMAN	2.5	1	No
109	Q9Y5X1	Sorting nexin-9	SNX9_HUMAN	2.5	1	No
110	Q969V3-2	Isoform 2 of Nicalin	NCLN_HUMAN	2.5	1	No
111	Q9BQG0	Myb-binding protein 1A	MBB1A_HUMAN	2.5	1	No
112	P38117	Electron transfer flavoprotein subunit beta	ETFB_HUMAN	2	14	No
113	Q9BYG3	MKI67 FHA domain-interacting nucleolar phosphoprotein	MK67I_HUMAN	2	9	No
114	Q9NX58	Cell growth-regulating nucleolar protein	LYAR_HUMAN	2	9	No
115	Q9BPW8	Protein NipSnap homolog 1	NIPS1_HUMAN	2	8	No
116	Q8IYB3	Serine/arginine repetitive matrix protein 1	SRRM1_HUMAN	2	8	No
117	P69849	Nodal modulator 3	NOMO3_HUMAN	2	7.5	No
118	Q14203-5	Isoform 5 of Dynactin subunit 1	DCTN1_HUMAN	2	6.5	No
119	Q6DD88	Atlastin-3	ATLA3_HUMAN	2	6.5	No
120	P53004	Biliverdin reductase A	BIEA_HUMAN	2	6.5	No
121	O60763	General vesicular transport factor p115	USO1_HUMAN	2	5	No
122	P13010	X-ray repair cross-complementing protein 5	XRCC5_HUMAN	2	5	No
123	Q16836	Hydroxyacyl-coenzyme A dehydrogenase, mitochondrial	HCDH_HUMAN	2	4.5	Yes (Ewing, 2007)
124	Q09028-3	Isoform 3 of Histone-binding protein RBBP4	RBBP4_HUMAN	2	4	No
125	Q15126	Phosphomevalonate kinase	PMVK_HUMAN	2	3.5	No

126	P18669	Phosphoglycerate mutase 1	PGAM1_HUMAN	2	3.5	No
127	P23258	Tubulin gamma-1 chain	TBG1_HUMAN	2	3.5	No
128	Q9HC21	Mitochondrial thiamine pyrophosphate carrier	TPC_HUMAN	2	3.5	No
129	P61160	Actin-related protein 2	ARP2_HUMAN	2	3	No
130	Q12769	Nuclear pore complex protein Nup160	NU160_HUMAN	2	2.5	No
131	Q96HY6	DDRGK domain-containing protein 1	DDRGK_HUMAN	2	2	No
132	P48960-2	Isoform 2 of CD97 antigen	CD97_HUMAN	2	2	No
133	Q13610	Periodic tryptophan protein 1 homolog	PWP1_HUMAN	2	1.5	No
134	Q9H7Z7	Prostaglandin E synthase 2	PGES2_HUMAN	2	1.5	No
135	Q14008-2	Isoform 2 of Cytoskeleton-associated protein 5	CKAP5_HUMAN	2	1	No
136	Q14C86-4	Isoform 4 of GTPase-activating protein and VPS9 domain-cont	GAPD1_HUMAN	1.5	29.5	No
137	P62937	Peptidyl-prolyl cis-trans isomerase A	PPIA_HUMAN	1.5	14.5	No
138	Q99798	Aconitate hydratase, mitochondrial	ACON_HUMAN	1.5	8.5	No
139	O43291	Kunitz-type protease inhibitor 2	SPIT2_HUMAN	1.5	6	No
140	Q02790	Peptidyl-prolyl cis-trans isomerase FKBP4	FKBP4_HUMAN	1.5	5	No
141	Q15397	Pumilio domain-containing protein KIAA0020	K0020_HUMAN	1.5	5	No
142	Q96SB4	SRSF protein kinase 1	SRPK1_HUMAN	1.5	5	No
143	P46977	Dolichyl-diphosphooligosaccharide--protein glycosyltransferase	STT3A_HUMAN	1.5	4.5	No
144	P07686	Beta-hexosaminidase subunit beta	HEXB_HUMAN	1.5	4	No
145	Q6P1M0	Long-chain fatty acid transport protein 4	S27A4_HUMAN	1.5	3.5	No
146	P11532-3	Isoform 2 of Dystrophin	DMD_HUMAN	1.5	2.5	No
147	Q9NQS7-2	Isoform 2 of Inner centromere protein	INCE_HUMAN	1.5	2.5	No
148	O96008	Mitochondrial import receptor subunit TOM40 homolog	TOM40_HUMAN	1.5	2	No
149	O60488-2	Isoform Short of Long-chain-fatty-acid--CoA ligase 4	ACSL4_HUMAN	1.5	2	No
150	Q9UL25	Ras-related protein Rab-21	RAB21_HUMAN	1.5	2	Yes (Ewing, 2007)
151	Q9Y2W1	Thyroid hormone receptor-associated protein 3	TR150_HUMAN	1	25	No
152	Q9Y3T9	Nucleolar complex protein 2 homolog	NOC2L_HUMAN	1	7	No
153	P07195	L-lactate dehydrogenase B chain	LDHB_HUMAN	1	6.5	No
154	Q13243	Serine/arginine-rich splicing factor 5	SRSF5_HUMAN	1	6.5	No
155	P22061	Protein-L-isoaspartate(D-aspartate) O-methyltransferase	PIMT_HUMAN	1	5.5	Yes (Ewing, 2007)
156	Q5JTV8	Torsin-1A-interacting protein 1 OS=Homo sapiens GN=TOR1A	TOIP1_HUMAN	1	5.5	No
157	O75494-5	Isoform 5 of Serine/arginine-rich splicing factor 10	SRS10_HUMAN	1	5.5	No
158	P35914	Hydroxymethylglutaryl-CoA lyase, mitochondrial	HMGCL_HUMAN	1	5	No
159	Q9H9B4	Sideroflexin-1	SFXN1_HUMAN	1	4.5	Yes (Ewing, 2007)
160	O00487	26S proteasome non-ATPase regulatory subunit 14	PSDE_HUMAN	1	4.5	Yes (Ewing, 2007)
161	O43684-2	Isoform 2 of Mitotic checkpoint protein BUB3	BUB3_HUMAN	1	4	No
162	Q9UNQ2	Probable dimethyladenosine transferase	DIM1_HUMAN	1	4	No
163	Q8ND30	Liprin-beta-2	LIPB2_HUMAN	1	4	No
164	Q96F07-2	Isoform 2 of Cytoplasmic FMR1-interacting protein 2	CYFP2_HUMAN	1	4	No
165	Q9NTK5	Obg-like ATPase 1	OLA1_HUMAN	1	4	No
166	P62879	Guanine nucleotide-binding protein G(I)/G(S)/G(T) subunit beta	GBB2_HUMAN	1	3.5	No
167	Q9UKG1	DCC-interacting protein 13-alpha	DP13A_HUMAN	1	3.5	No
168	Q9Y5K5-2	Isoform 2 of Ubiquitin carboxyl-terminal hydrolase isozyme L5	UCHL5_HUMAN	1	3	No
169	P61964	WD repeat-containing protein 5	WDR5_HUMAN	1	3	Yes (Ewing, 2007)

170	Q8NE71-2	Isoform 2 of ATP-binding cassette sub-family F member 1	ABCF1_HUMAN	1	3	No
171	Q9BQ75-2	Isoform 2 of Protein CMSS1	CMS1_HUMAN	1	2.5	No
172	Q14764	Major vault protein	MVP_HUMAN	1	2.5	No
173	Q96N66-2	Isoform 2 of Lysophospholipid acyltransferase 7	MBOA7_HUMAN	1	2.5	No
174	O75477	Erlin-1	ERLN1_HUMAN	1	2.5	No
175	Q9Y679-2	Isoform Short of Ancient ubiquitous protein 1	AUP1_HUMAN	1	2	No
176	Q15149-4	Isoform 4 of Plectin	PLEC_HUMAN	61.5	0	No
177	P33527-4	Isoform 4 of Multidrug resistance-associated protein 1	MRP1_HUMAN	9.5	0	No
178	Q8N884	Cyclic GMP-AMP synthase	CGAS_HUMAN	9	0.5	No
179	P43121	Cell surface glycoprotein MUC18	MUC18_HUMAN	6.5	0	No
180	P31946-2	Isoform Short of 14-3-3 protein beta/alpha	1433B_HUMAN	6	0	No
181	O00161-2	Isoform SNAP-23b of Synaptosomal-associated protein 23	SNP23_HUMAN	5.5	0.5	No
182	Q9BUR5	Apolipoprotein O	APOO_HUMAN	5.5	0.5	No
183	P46459	Vesicle-fusing ATPase	NSF_HUMAN	5	0	No
184	Q04917	14-3-3 protein eta	1433F_HUMAN	4.5	0.5	No
185	Q7Z403	Transmembrane channel-like protein 6	TMC6_HUMAN	4.5	0	No
186	Q92508	Piezo-type mechanosensitive ion channel component 1	PIEZ1_HUMAN	4.5	0	No
187	Q8NC56	LEM domain-containing protein 2	LEMD2_HUMAN	4	0.5	No
188	P31947-2	Isoform 2 of 14-3-3 protein sigma	1433S_HUMAN	4	0	No
189	Q9C0B5-2	Isoform 2 of Palmitoyltransferase ZDHHC5	ZDHC5_HUMAN	3.5	0	No
190	Q8IV63-3	Isoform 3 of Inactive serine/threonine-protein kinase VRK3	VRK3_HUMAN	3.5	0	No
191	Q8NBJ5	Procollagen galactosyltransferase 1	GT251_HUMAN	3.5	0	No
192	O96000	NADH dehydrogenase [ubiquinone] 1 beta subcomplex subunit	NDUBA_HUMAN	3	0.5	No
193	Q9Y5Y6	Suppressor of tumorigenicity 14 protein	ST14_HUMAN	3	0	No
194	Q96S97	Myeloid-associated differentiation marker	MYADM_HUMAN	3	0	No
195	Q92485	Acid sphingomyelinase-like phosphodiesterase 3b	ASM3B_HUMAN	3	0	No
196	Q13185	Chromobox protein homolog 3	CBX3_HUMAN	3	0	No
197	Q9H078-2	Isoform 2 of Caseinolytic peptidase B protein homolog	CLPB_HUMAN	2.5	0.5	No
198	Q8NBI5	Solute carrier family 43 member 3	S43A3_HUMAN	2.5	0	No
199	O94776	Metastasis-associated protein MTA2	MTA2_HUMAN	2.5	0	No
200	Q13425-2	Isoform 2 of Beta-2-syntrophin	SNTB2_HUMAN	2.5	0	No
201	Q13951-2	Isoform 2 of Core-binding factor subunit beta	PEBB_HUMAN	2.5	0	No
202	Q99595	Mitochondrial import inner membrane translocase subunit Tim1	TI17A_HUMAN	2.5	0	No
203	Q8TB52	F-box only protein 30	FBX30_HUMAN	2	0	No
204	Q6PJF5-2	Isoform 2 of Inactive rhomboid protein 2	RHDF2_HUMAN	2	0	No
205	Q9H4I3	TraB domain-containing protein	TRABD_HUMAN	2	0	No
206	Q15599-2	Isoform 2 of Na(+)/H(+) exchange regulatory cofactor NHE-RF2	NHRF2_HUMAN	2	0	No
207	Q9H061	Transmembrane protein 126A	T126A_HUMAN	2	0	No
208	P12270	Nucleoprotein TPR	TPR_HUMAN	0	22	No
209	Q9H307	Pinin	PININ_HUMAN	0	18.5	No
210	Q9NYF8-2	Isoform 2 of Bcl-2-associated transcription factor 1	BCLF1_HUMAN	0	18	No
211	P49674	Casein kinase I isoform epsilon	KC1E_HUMAN	0	15.5	Yes (Ewing, 2007)
212	Q9UQ35	Serine/arginine repetitive matrix protein 2	SRRM2_HUMAN	0	15.5	No
213	Q14980-2	Isoform 2 of Nuclear mitotic apparatus protein 1	NUMA1_HUMAN	0.5	14.5	No

214	Q86V48-2	Isoform 2 of Leucine zipper protein 1	LUZP1_HUMAN	0	14.5	No
215	P48730-2	Isoform 2 of Casein kinase I isoform delta	KC1D_HUMAN	0	14.5	Yes (Ewing, 2007)
216	Q9UKV3	Apoptotic chromatin condensation inducer in the nucleus	ACINU_HUMAN	0.5	14	No
217	Q14978-3	Isoform 3 of Nucleolar and coiled-body phosphoprotein 1	NOLC1_HUMAN	0	13	No
218	Q14978	Nucleolar and coiled-body phosphoprotein 1	NOLC1_HUMAN	0	13	No
219	P02788-2	Isoform DeltaLf of Lactotransferrin	TRFL_HUMAN	0	11.5	No
220	P27816-6	Isoform 6 of Microtubule-associated protein 4	MAP4_HUMAN	0.5	10	No
221	Q8N163	DBIRD complex subunit KIAA1967	K1967_HUMAN	0	10	No
222	O75828	Carbonyl reductase [NADPH] 3	CBR3_HUMAN	0	9.5	No
223	P05109	Protein S100-A8	S10A8_HUMAN	0.5	9	No
224	Q9H2U2	Inorganic pyrophosphatase 2, mitochondrial	IPYR2_HUMAN	0.5	8.5	No
225	O75691	Small subunit processome component 20 homolog	UTP20_HUMAN	0	8.5	No
226	P62191	26S protease regulatory subunit 4	PRS4_HUMAN	0	8	No
227	Q96R06	Sperm-associated antigen 5	SPAG5_HUMAN	0	8	No
228	Q15154	Pericentriolar material 1 protein	PCM1_HUMAN	0	8	No
229	Q9BZQ6	ER degradation-enhancing alpha-mannosidase-like protein 3	EDEM3_HUMAN	0.5	7.5	No
230	Q13595	Transformer-2 protein homolog alpha	TRA2A_HUMAN	0.5	7	No
231	Q9NZ01	Very-long-chain enoyl-CoA reductase	TECR_HUMAN	0	7	No
232	Q9NY61	Protein AATF	AATF_HUMAN	0	7	No
233	P46109	Crk-like protein	CRKL_HUMAN	0	6.5	No
234	O75663	TIP41-like protein	TIPRL_HUMAN	0	6.5	No
235	Q06323	Proteasome activator complex subunit 1	PSME1_HUMAN	0	6.5	No
236	P29590-14	Isoform PML-14 of Protein PML	PML_HUMAN	0	6.5	No
237	Q9P0J7	E3 ubiquitin-protein ligase KCMF1	KCMF1_HUMAN	0	6.5	No
238	Q8IZT6-2	Isoform 2 of Abnormal spindle-like microcephaly-associated pr	ASPM_HUMAN	0	6.5	No
239	P49821-2	Isoform 2 of NADH dehydrogenase [ubiquinone] flavoprotein 1,	NDUV1_HUMAN	0.5	6	No
240	P45974-2	Isoform Short of Ubiquitin carboxyl-terminal hydrolase 5	UBP5_HUMAN	0.5	6	No
241	Q5SRE5-2	Isoform 2 of Nucleoporin NUP188 homolog	NU188_HUMAN	0.5	6	No
242	P51114	Fragile X mental retardation syndrome-related protein 1	FXR1_HUMAN	0	6	No
243	Q9H9E3	Conserved oligomeric Golgi complex subunit 4	COG4_HUMAN	0	6	No
244	P29353-2	Isoform p52Shc of SHC-transforming protein 1	SHC1_HUMAN	-0.5	6	No
245	Q92597	Protein NDRG1	NDRG1_HUMAN	-0.5	6	No
246	Q9BRK5	45 kDa calcium-binding protein	CAB45_HUMAN	0.5	5.5	No
247	P50897	Palmitoyl-protein thioesterase 1	PPT1_HUMAN	0.5	5.5	No
248	Q6NVY1	3-hydroxyisobutyryl-CoA hydrolase, mitochondrial	HIBCH_HUMAN	0.5	5.5	No
249	O00170	AH receptor-interacting protein	AIP_HUMAN	0	5.5	No
250	Q9NVN8	Guanine nucleotide-binding protein-like 3-like protein	GNL3L_HUMAN	0	5.5	No
251	Q00534	Cyclin-dependent kinase 6	CDK6_HUMAN	0	5.5	No
252	Q96FW1	Ubiquitin thioesterase OTUB1	OTUB1_HUMAN	0	5	Yes (Ewing, 2007)
253	Q7LBC6	Lysine-specific demethylase 3B	KDM3B_HUMAN	0	5	No
254	Q5VT06	Centrosome-associated protein 350	CE350_HUMAN	0	5	No
255	Q8TC07-2	Isoform 2 of TBC1 domain family member 15	TBC15_HUMAN	0	5	Yes (Ewing, 2007)
256	P54819-5	Isoform 5 of Adenylate kinase 2, mitochondrial	KAD2_HUMAN	0.5	4.5	Yes (Ewing, 2007)
257	Q6FI81-3	Isoform 3 of Anamorsin	CPIN1_HUMAN	0.5	4.5	No

258	Q8WUM0	Nuclear pore complex protein Nup133	NU133_HUMAN	0.5	4.5	No
259	O75832	26S proteasome non-ATPase regulatory subunit 10	PSD10_HUMAN	0	4.5	No
260	O00233	26S proteasome non-ATPase regulatory subunit 9	PSMD9_HUMAN	0	4.5	No
261	O60711	Leupaxin	LPXN_HUMAN	0	4.5	No
262	P61289	Proteasome activator complex subunit 3	PSME3_HUMAN	0	4.5	Yes (Ewing, 2007)
263	P55735-2	Isoform 2 of Protein SEC13 homolog	SEC13_HUMAN	0	4.5	Yes (Ewing, 2007)
264	Q8IYS1	Peptidase M20 domain-containing protein 2	P20D2_HUMAN	0	4.5	No
265	Q8IUF8-4	Isoform 4 of Bifunctional lysine-specific demethylase and histid	MINA_HUMAN	0	4.5	No
266	Q9UHD8-7	Isoform 7 of Septin-9	SEPT9_HUMAN	0	4.5	No
267	Q9ULX6	A-kinase anchor protein 8-like	AKP8L_HUMAN	0	4.5	No
268	Q8N3U4	Cohesin subunit SA-2	STAG2_HUMAN	0	4.5	No
269	P59045-3	Isoform 3 of NACHT, LRR and PYD domains-containing protein	NAL11_HUMAN	0	4.5	No
270	O75330-4	Isoform 4 of Hyaluronan mediated motility receptor	HMMR_HUMAN	0	4.5	No
271	Q6RFH5	WD repeat-containing protein 74	WDR74_HUMAN	0.5	4	No
272	O75569-3	Isoform 3 of Interferon-inducible double stranded RNA-depende	PRKRA_HUMAN	0.5	4	No
273	Q9Y5Y2	Cytosolic Fe-S cluster assembly factor NUBP2	NUBP2_HUMAN	0.5	4	No
274	Q9Y3C1	Nucleolar protein 16	NOP16_HUMAN	0.5	4	No
275	Q8NEJ9-2	Isoform 2 of Neuroguidin	NGDN_HUMAN	0.5	4	No
276	Q92785	Zinc finger protein ubi-d4	REQU_HUMAN	0.5	4	No
277	Q9GZP4-2	Isoform 2 of PITH domain-containing protein 1	PITH1_HUMAN	0	4	No
278	P61758	Prefoldin subunit 3	PFD3_HUMAN	0	4	No
279	Q9UBV8	Peflin	PEF1_HUMAN	0	4	No
280	P68400	Casein kinase II subunit alpha	CSK21_HUMAN	0	4	No
281	Q9H501	ESF1 homolog	ESF1_HUMAN	0	4	No
282	Q7Z2W4	Zinc finger CCCH-type antiviral protein 1	ZCCHV_HUMAN	0	4	No
283	Q15628	Tumor necrosis factor receptor type 1-associated DEATH dom	TRADD_HUMAN	0.5	3.5	No
284	Q86YT6	E3 ubiquitin-protein ligase MIB1	MIB1_HUMAN	0.5	3.5	No
285	P25787	Proteasome subunit alpha type-2	PSA2_HUMAN	0	3.5	No
286	P09525	Annexin A4	ANXA4_HUMAN	0	3.5	No
287	P40925	Malate dehydrogenase, cytoplasmic	MDHC_HUMAN	0	3.5	No
288	Q16740	Putative ATP-dependent Clp protease proteolytic subunit, mitoc	CLPP_HUMAN	0	3.5	No
289	O95861	3'(2'),5'-bisphosphate nucleotidase 1	BPNT1_HUMAN	0	3.5	No
290	P23526-2	Isoform 2 of Adenosylhomocysteinase	SAHH_HUMAN	0	3.5	Yes (Ewing, 2007)
291	Q15054	DNA polymerase delta subunit 3	DPOD3_HUMAN	0	3.5	No
292	O15355	Protein phosphatase 1G	PPM1G_HUMAN	0	3.5	No
293	Q9UJU6	Drebrin-like protein	DBNL_HUMAN	0	3.5	No
294	Q8IWC1-2	Isoform 2 of MAP7 domain-containing protein 3	MA7D3_HUMAN	0	3.5	No
295	Q9H3P7	Golgi resident protein GCP60	GCP60_HUMAN	0	3.5	No
296	O00267-2	Isoform 2 of Transcription elongation factor SPT5	SPT5H_HUMAN	0	3.5	No
297	Q6ZU80	Centrosomal protein of 128 kDa	CE128_HUMAN	0	3.5	No
298	Q8IWJ2	GRIP and coiled-coil domain-containing protein 2	GCC2_HUMAN	0	3.5	No
299	Q9H9E3-3	Isoform 3 of Conserved oligomeric Golgi complex subunit 4	COG4_HUMAN	0	3.5	No
300	P36957	Dihydrolipoyllysine-residue succinyltransferase component of 2	ODO2_HUMAN	0.5	3	No
301	P41227-2	Isoform 2 of N-alpha-acetyltransferase 10	NAA10_HUMAN	0	3	Yes (Ewing, 2007)

302	Q96J01	THO complex subunit 3	THOC3_HUMAN	0	3	No
303	Q96P16	Regulation of nuclear pre-mRNA domain-containing protein 1A	RPR1A_HUMAN	0	3	No
304	P35520	Cystathionine beta-synthase	CBS_HUMAN	0	3	No
305	Q9UJU6-2	Isoform 2 of Drebrin-like protein	DBNL_HUMAN	0	3	No
306	P23458	Tyrosine-protein kinase JAK1	JAK1_HUMAN	0	3	No
307	Q9HA64	Ketosamine-3-kinase	KT3K_HUMAN	0	3	No
308	Q6PJT7-4	Isoform 4 of Zinc finger CCCH domain-containing protein 14	ZC3HE_HUMAN	0	3	No
309	Q86VM9	Zinc finger CCCH domain-containing protein 18	ZCH18_HUMAN	0	3	No
310	Q9Y2X9	Zinc finger protein 281	ZN281_HUMAN	0	3	No
311	Q9BUQ8	Probable ATP-dependent RNA helicase DDX23	DDX23_HUMAN	0	3	No
312	O14976	Cyclin-G-associated kinase	GAK_HUMAN	0	3	No
313	Q53H96	Pyrroline-5-carboxylate reductase 3	P5CR3_HUMAN	0	3	No
314	P52732	Kinesin-like protein KIF11	KIF11_HUMAN	0	3	No
315	Q96KA5-2	Isoform 2 of Cleft lip and palate transmembrane protein 1-like p	CLP1L_HUMAN	0	3	No
316	P55769	NHP2-like protein 1	NH2L1_HUMAN	0.5	2.5	No
317	Q15691	Microtubule-associated protein RP/EB family member 1	MARE1_HUMAN	0.5	2.5	Yes (Ewing, 2007)
318	Q15653-2	Isoform 2 of NF-kappa-B inhibitor beta	IKBB_HUMAN	0	2.5	Yes (Bouwmeester, 2004
319	Q9NUQ9	Protein FAM49B	FA49B_HUMAN	0	2.5	No
320	P62993	Growth factor receptor-bound protein 2	GRB2_HUMAN	0	2.5	Yes (Ewing, 2007)
321	Q96EY8	Cob(I)yrinic acid a,c-diamide adenosyltransferase, mitochondria	MMAB_HUMAN	0	2.5	No
322	P51553-2	Isoform 2 of Isocitrate dehydrogenase [NAD] subunit gamma, n	IDH3G_HUMAN	0	2.5	No
323	Q9BTE7	DCN1-like protein 5	DCNL5_HUMAN	0	2.5	No
324	Q16637-4	Isoform SMN-delta57 of Survival motor neuron protein	SMN_HUMAN	0	2.5	No
325	Q9H8H0	Nucleolar protein 11	NOL11_HUMAN	0	2.5	No
326	Q9BV38	WD repeat-containing protein 18	WDR18_HUMAN	0	2.5	No
327	P08758	Annexin A5	ANXA5_HUMAN	0	2.5	No
328	Q6JBY9	CapZ-interacting protein	CPZIP_HUMAN	0	2.5	No
329	Q9Y4R8	Telomere length regulation protein TEL2 homolog	TELO2_HUMAN	0	2.5	No
330	Q92540-2	Isoform 2 of Protein SMG7	SMG7_HUMAN	0	2.5	No
331	Q76FK4-4	Isoform 4 of Nucleolar protein 8	NOL8_HUMAN	0	2.5	No
332	Q9UJC3	Protein Hook homolog 1	HOOK1_HUMAN	0	2.5	No
333	P11802	Cyclin-dependent kinase 4	CDK4_HUMAN	0	2.5	Yes (Ewing, 2007)
334	Q00535-2	Isoform 2 of Cyclin-dependent kinase 5	CDK5_HUMAN	0	2.5	No
335	P04083	Annexin A1	ANXA1_HUMAN	0	2.5	Yes (Sigglekow, 2012)
336	P43487	Ran-specific GTPase-activating protein	RANG_HUMAN	0.5	2	Yes (Ewing, 2007)
337	P54920	Alpha-soluble NSF attachment protein	SNAA_HUMAN	0.5	2	No
338	Q6UXN9	WD repeat-containing protein 82	WDR82_HUMAN	0.5	2	No
339	Q14790-8	Isoform 8 of Caspase-8	CASP8_HUMAN	0.5	2	No
340	Q96T51	RUN and FYVE domain-containing protein 1	RUFY1_HUMAN	0.5	2	No
341	Q86Y82	Syntaxin-12	STX12_HUMAN	0.5	2	No
342	Q9NXW2	DnaJ homolog subfamily B member 12	DJB12_HUMAN	0.5	2	No
343	P16591-3	Isoform 3 of Tyrosine-protein kinase Fer	FER_HUMAN	0.5	2	No
344	Q9BVC4	Target of rapamycin complex subunit LST8	LST8_HUMAN	0.5	2	No
345	Q8IZP0-10	Isoform 10 of Abl interactor 1	ABI1_HUMAN	0	2	No

346	P48556	26S proteasome non-ATPase regulatory subunit 8	PSMD8_HUMAN	0	2	Yes (Ewing, 2007)
347	Q9H6Y2	WD repeat-containing protein 55	WDR55_HUMAN	0	2	No
348	Q9NQT4	Exosome complex component RRP46	EXOS5_HUMAN	0	2	No
349	Q15003	Condensin complex subunit 2	CND2_HUMAN	0	2	No
350	P38432	Coilin	COIL_HUMAN	0	2	No
351	Q86X83	COMM domain-containing protein 2	COMD2_HUMAN	0	2	No
352	Q6IQ49-2	Isoform 2 of Protein SDE2 homolog	SDE2_HUMAN	0	2	No
353	P42574	Caspase-3	CASP3_HUMAN	0	2	No
354	Q3KQU3-2	Isoform 2 of MAP7 domain-containing protein 1	MA7D1_HUMAN	0	2	No
355	P39687	Acidic leucine-rich nuclear phosphoprotein 32 family member A	AN32A_HUMAN	0	2	No
356	P78417-3	Isoform 3 of Glutathione S-transferase omega-1	GSTO1_HUMAN	0	2	No
357	O00273	DNA fragmentation factor subunit alpha	DFFA_HUMAN	0	2	Yes (Ewing, 2007)
358	Q7Z460-2	Isoform 2 of CLIP-associating protein 1	CLAP1_HUMAN	0	2	No
359	Q5JSZ5	Protein PRRC2B	PRC2B_HUMAN	0	2	No
360	O15118	Niemann-Pick C1 protein	NPC1_HUMAN	0	2	No
361	Q9NWH9	SAFB-like transcription modulator	SLTM_HUMAN	0	2	No
362	Q9Y263	Phospholipase A-2-activating protein	PLAP_HUMAN	0	2	No
363	P15927	Replication protein A 32 kDa subunit	RFA2_HUMAN	0	2	No
364	Q9Y697-2	Isoform Cytoplasmic of Cysteine desulfurase, mitochondrial	NFS1_HUMAN	0	2	No
365	Q9H3N1	Thioredoxin-related transmembrane protein 1	TMX1_HUMAN	0	2	Yes (Ewing, 2007)

The human MM cell line 8226 cells were transduced with pUB-hMCC-SBP-6xHis or pUB-FLAG-hMCC. Immunoprecipitates of hMCC-SBP-6xHis by streptavidin-sepharose beads from whole cell lysates and purified mitochondria of 8226 cells were analyzed by high resolution LC-MS/MS, respectively. Immunoprecipitates of FLAG-hMCC by streptavidin-sepharose beads were used as negative control in these experiments. LC-MS/MS data were searched against the human IPI and UniProt databases using the Mascot and Proteome Discoverer search engines. Protein assignments were considered highly confident using a stringent false discovery rate threshold of <1%, as estimated by reversed database searching, and requiring that ≥2 peptides per protein be unambiguously identified. Rough relative protein amounts were estimated using spectra counting values, and requiring that ≥2 of average spectra count difference between hMCC-SBP-6xHis and FLAG-hMCC (negative control) of two experiments. Proteins that were previously identified as MCC-interactors in CRCs or 293T cells are indicated. SBP: streptavidin binding peptide tag

References:

Ewing RM, Chu P, Elisma F, Li H, Taylor P, Climie S et al. Large-scale mapping of human protein-protein interactions by mass spectrometry. *Mol Syst Biol* 2007; **3**: 89.

Sigglekow ND, Pangon L, Brummer T, Molloy M, Hawkins NJ, Ward RL et al. Mutated in colorectal cancer protein modulates the NF-κB pathway. *Anticancer Res* 2012; **32**: 73-79.

Bouwmeester T, Bauch A, Ruffner H, Angrand PO, Bergamini G, Croughton K et al. A physical and functional map of the human TNF-α/NF-κB signal transduction pathway. *Nat Cell Biol* 2004; **6**: 97-105.

Supplementary Figure 1

A MCC isoform 1: 82.63% coverage

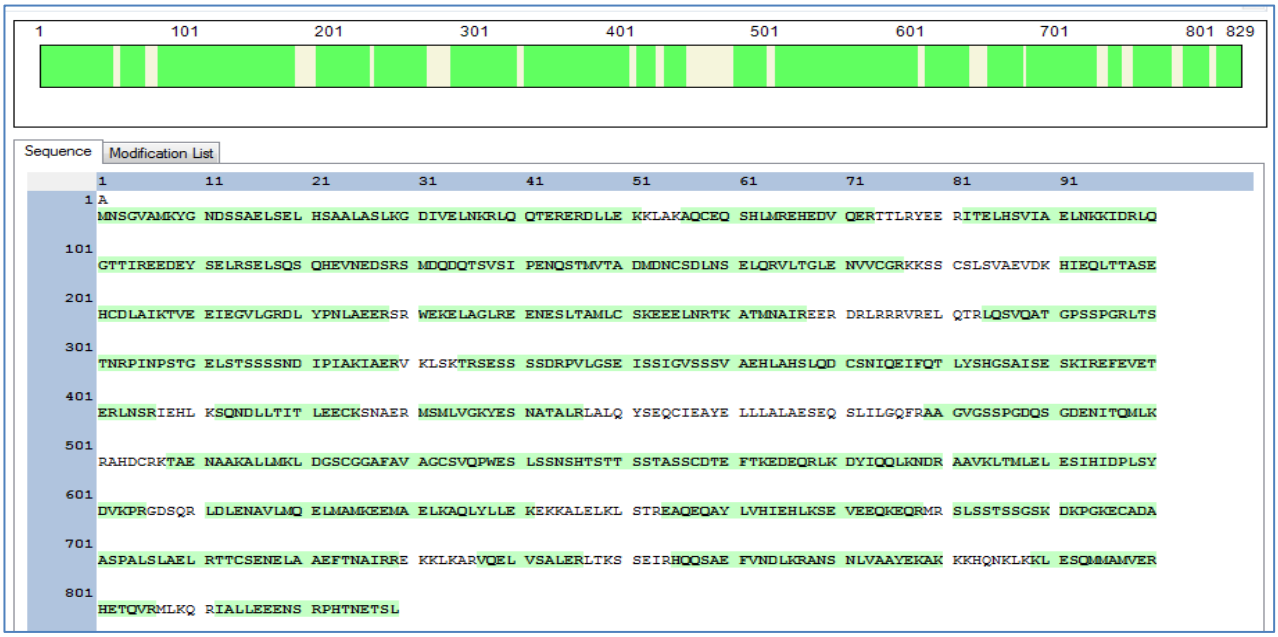

B MCC isoform 2: 74.29% coverage

Supplementary Figure 1. The MCC isoform 2 was identified as an MCC-interacting protein by affinity purification and LC-MS/MS. The two isoforms of MCC proteins differ at their extreme N-terminus due to alternative promoter usage. Both pUB-FLAG-hMCC and pUB-hMCC-SBP-6xHis are cloned from MCC isoform 1 (829 aa). (**A**) Schematic diagram of peptide sequences of MCC isoform 1 identified by LC-MS/MS. (**B**) Schematic diagram of peptide sequences of MCC isoform 2 (1019 aa) identified by LC-MS/MS. The peptide sequences detected by LC-MS/MS are highlighted in green color. The unique region of MCC isofrom 2 is marked with a dashed black box.